Visible-light-driven Photocatalytic Disinfection of Bacteria by the Natural Sphalerite

CHEN, Yanmin

A Thesis Submitted in Partial Fulfillment
of the Requirements for the Degree of
Doctor of Philosophy
in
Biology

The Chinese University of Hong Kong
July 2011

ProQuest LLC.
789 East Eisenhower Parkway
P.O. Box 1346
Ann Arbor, MI 48106 - 1346

Thesis Committee

Professor J. C. Yu (Chair)

Professor P. K. Wong (Thesis Supervisor)

Professor N. Y. S. WOO (Committee Member)

Professor L.Z. Zhang (External Examiner)

Professor H. Chua (Alternate External Examiner)

Acknowledgements

I am extremely grateful to my supervisor, Prof. P.K. Wong, whose patience and kindness, as well as his academic experience, has been invaluable to me. Throughout my project, he has guided me to be analytical and critical as well as given me a lot of precious ideas and comments.

I would like to express my sincere thanks to my internal examiners, Profs. J.C. Yu and N.Y.S. WOO, the external examiner, Prof. L.Z. Zhang and the additional examiner, Prof. H. Chua for their valuable comments and suggestions on my project.

In addition, I would like to express my deep gratitude to Prof. A.H. Lu and Dr. Y. Li, for their supporting the photocatalysts and valuable suggestions for my project. I am also very grateful to Profs. T.C. An and G.Y. Li, for precious comments on my manuscripts.

I would like to use this opportunity to truly thank Mr. Freddie C.H. Kwok for the procedural guiding me to conduct the TEM technique, and Ms. Jessie P.K. Lee and Mr. Thomas C.O. Tang for coaching me various instrumental techniques.

Besides, I have been indebted to Mr. H.Y. Yip and Dr. Alex K.H. Wong, for their technical assistance and practical suggestion during these three years' research study. In addition, the informal support and encouragement of other colleagues has been

indispensable, and I would like particularly to acknowledge the contribution of Mr. T.W. Ng, Mr. W.J. Wang, Ms. M.H. Gao, Ms. L.S. Zhang and Ms. Q.H. Cai.

My mother and all relatives have been a constant source of support – emotional and moral. Finally, my friend Mr. J.B. Zhang has been, always my joy and my guiding light, and I thank him very much.

Part of the work in this dissertation has been published in *Environmental Science & Technology* **and** *Chemosphere*.

Abstract

Wastewater disinfection is practiced with the goal of reducing risks of human exposure to pathogenic microorganisms. In 1985, Matsunaga *et al.* first successfully reported that titanium dioxide (TiO_2) photocatalyst could disinfect bacterial cells in water. Since then, photocatalytic technology was extensively studied and proved to be a cost-effective, safe and promising alternative for wastewater treatment. However, TiO_2 can only be excited by light with wavelengths in the near ultraviolet (UV) region which is only 4% of the solar spectrum. Therefore, it is a crucial issue to develop new photocatalysts which can be excited by sunlight. Although synthetic photocatalysts show good disinfection efficiency under visible light (VL), however, the amounts of those synthetic visible-light-driven (VLD) photocatalysts are very limited so that they cannot satisfy with the large-scale application in the practical wastewater treatment. Obviously, a large quantity and low-cost VLD photocatalysts must be more popular than artificial semiconductors.

In this study, the photocatalytic disinfection capability of a natural semiconducting mineral, sphalerite, is studied for the first time. Natural sphalerite (NS), a ZnS containing metal ions such as Fe^{2+} and Cd^{2+}, exhibits good photoactivity under VL. Firstly, NS can inactivate *Escherichia coli* K-12 irradiated by fluorescent tubes (FTs). Moreover, it is the first time to experimentally prove that the photogenerated electron (e^-) and hydrogen peroxide (H_2O_2) play important roles in the bacterial disinfection of *E. coli* K-12 using multiple scavengers coupled with a partition system.

Secondly, the effect of different parameters of VL on photocatalytic disinfection efficiency of NS is explored. The "discreted peak spectrum" of FTs is much more effective than the "continuous spectrum" of white light emitting diode (LED) lamps and Xenon lamp to inactivate bacterial cells. Bacterial inactivation efficiency depends on the wavelength of VL. At equivalent intensity, blue and yellow LED lamps show the more disinfection efficiency than green and red LED lamps. Photocatalytic disinfection is also related to the VL intensity.

Finally, NS shows high photocatalytic activity to disinfect wastewater bacteria such as the Gram –ve bacterium, *E. coli,* and the Gram +ve bacterium, *Microbacterium barkeri*, under VL irradiation. The photocatalytic disinfection efficiencies at different pH are strongly influenced by the amount of H_2O_2. Moreover, different reactive species are involved in the photocatalytic disinfection of *E. coli* and *M. barkeri*. A possible cell damage mechanism by the photogenerated e^- produced by NS is tentatively proposed.

In this study, NS is explored as a novel, cost-effective VLD photocatalyst. Due to its natural abundance and ease of procurement, NS can be used economically for the large-scale photocatalytic disinfection of bacterial cells.

摘要

废水处理的目的是要降低污水中致病微生物对人类健康的影响。在过去几十年中，环境污染问题，特别是污水中有机物及有害微生物造成的环境污染问题已成为国内外迫切需要解决的问题。由于二氧化钛能够在水环境中成功灭菌，使得光催化技术已经成为一种有效的，安全的污水处理技术，引起了人们的广泛关注。但是，以二氧化钛为催化剂的传统光催化技术对光的吸收主要在紫外区，太阳能利用率低，极大地限制了光催化技术在污水处理中的应用。因此，开发利用新型高效的可见光光催化剂成为解决问题的有效途径。目前，尽管大多数合成半导体能够高效的利用可见光灭菌，但是，其低产量无法满足污水处理中的要求。很明显，大量廉价的天然可见光光催化剂显示出了在实际污水处理中的优势。

值得关注的是，以硫化锌为主要成分的天然闪锌矿在自然界具有相当规模的储量。与合成硫化锌相比，天然闪锌矿有着更复杂的化学组成和缺陷结构,特别是其晶格内所含有的丰富的类质同像替代杂质离子使其具有良好的可见光催化活性，在处理重金属和有机染料等方面均表现出一定的应用前景。

在我的研究中，闪锌矿作为天然半导体矿物被首次应用于光催化灭菌。日光灯作为一种可见光光源，在实验中被采用。在日光灯的激发下，天然闪锌矿对大肠杆菌具有高效的灭菌和去除性能。更为重要的是，在捕获剂和分离装置的使用中，我对天然闪锌矿的杀菌机理做了研究。结果发现日光灯激发天然闪锌矿产生的活性成分，如电子和过氧化氢，对灭菌起了主要作用。电子的杀菌作用首次被提出，并与过氧化氢对细菌的氧化作用进行了比较。

其次，我研究了光谱，波长以及光强等几个可见光参数对杀菌效率的影响。结果显示，日光灯的多波峰光谱在杀菌效率上明显高于发光二极管和氙灯的连续光谱。另外，在同等光强下，蓝光和黄光所在波长比绿光和红光所在波长有更好的杀菌效果。灭菌效率同样依赖于可见光光强，光强越高，杀菌效率也越好。

最后，天然闪锌矿被应用于灭菌废水中的革兰氏阳性巴氏微杆菌，并与革兰氏阴性大肠杆菌进行了比较。结果显示，天然闪锌矿光激发产生的电子对两种不同革兰氏细菌的作用不同。由于革兰氏阴性菌的细胞壁较薄，电子更容易穿过细菌的细胞壁攻击细胞膜；而对于革兰氏阳性菌的较厚细胞壁，电子的穿过性很差。因此，天然闪锌矿更易于灭菌较薄细胞壁的大肠杆菌。

本研究结果预示着天然半导体矿物闪锌矿作为一种新的低成本,高效率的可见光催化材料将在环境污染治理领域具有一定的应用前景。

Table of Contents

List of Figures

List of Plates

List of Tables

List of Equations

Abbreviations

AAS	Atomic absorption spectrophotometry
AOPs	Advanced oxidation processes
Ar	Argon
BOM	Biodegradable organic matter
Br^-	Bromide ion
CAT	Catalase
CB	Conduction band
CDC	Centers for Disease Control and Prevention
cfu	Colony forming unit
Cl_2	Chlorine
ClO_2	Chlorine dioxide
CO_2	Carbon dioxide
CoA	Coenzyme A
DBPs	Disinfection byproducts
DMPO	5,5-Dimethyl-1-pyrroline-*N*-oxide
DNA	Deoxyribonucleic acid
DO	Dissolved oxygen
DPD	N,N-diethyl-*p*-phenylenediamine
e^-	Electron
ESR	Electron spin resonance
F^-	Fluorine

$FeSO_4$	Iron sulfate
FTs	Fluorescent tubes
H^+	Hydrogen ion
h^+	Hole
H_2O	Water
H_2O_2	Hydrogen peroxide
HCl	Hydrochloric acid
HOBr	Hypobromous acid
HOCl	Hypochlorous acid
$HOO^{\bullet}$	Perhydroxyl radical
HSP	Huangshaping
IC	Inorganic carbon
K^+	Potassium ion
LED	Light emitting diode
MnO_4^-	Permanganate
MO	Methyl Orange
MWCO	Molecular weight cut-off
Na_2EDTA	Ethylenediaminetetraacetic disodium salt
NB	Nutrient broth
NH_2Cl	Chloramines
NS	Natural sphalerite
O	Atomic oxygen

O_2	Oxygen molecule
O_3	Ozone
$^{\bullet}O_2^-$	Superoxide radical
$^{\bullet}OH$	Hydroxyl radical
$^{\bullet}OH_{ads}$	Hydroxyl radical adsorption on the surface of the photocatalyst
$^{\bullet}OH_{free}$	Free hydroxyl radical
P25	Titanium dioxide from Degussa Corporation (Frankfurt, Germany)
POD	Peroxidase
Purpald	4-amino-3-hydrazino-5-mercapto-1,2,4-triazole
PZC	Point of zero charge
RNA	Ribonucleic acid
ROSs	Reactive oxidative species
saline	0.9% NaCl solution
SCE	Saturated calomel electrode
SOD	Superoxide dismutase
TC	Total carbon
TEM	Transmission electron microscopy
TEMPOL	4-hydroxy-2,2,6,6-tetramethylpiperidinyloxy
THMs	Trihalomethanes
TiO_2	Titanium dioxide
TOC	Total organic carbon

UNICEF	United Nations Children's Fund
USEPA	United States Environmental Protection Agency
UV	Ultraviolet
VB	Valence band
VBNC	Viable but non-culturable
VL	Visible light
VLD	Visible-light-driven
VUV	Vacuum UV
WHO	World Health Organization

1. Introduction

1.1 Water crisis

Water crisis is now one of the glaring environmental problems throughout the world that is becoming more and more piercing day by day. Today, scarcity of water is the most excruciating problem in the face of the earth after global warming (United States Environmental Protection Agency (USEPA), 2009). Already there is more wastewater produced and dispersed today than at any other time in the history of our world: more than one out of six people lack access to safe drinking water, namely 1.1 billion people, and more than two out of six lack adequate sanitation, namely 2.6 billion people (World Health Organization (WHO)/United Nations Children's Fund (UNICEF)/Joint Monitoring Program for Water Supply and Sanitation, 2005). Problems with water are expected to grow worse in future, both in the developing and developed countries.

The major aspects of the water crisis are water-borne diseases and absence of sanitary domestic water (Shannon *et al.*, 2008). With an estimate 80% of illness and deaths in the developing world are the results of water-borne diseases. The studies reveal that 2.1 million people die every year from diarrhea and cholera (Centers for Disease Control and Prevention (CDC), 2005). For children under age five, water-borne diseases are the leading cause of death. According to the World Bank, 88 percent of all diseases are caused by unsafe drinking water, inadequate sanitation and poor hygiene (CDC, 2005).

Common water-related pathogenic microbes include bacteria, viruses, protozoa and other organisms (USEPA, 2009). Among them, pathogenic bacteria can occur on surface water in large numbers, either being excreted in faeces or occurring naturally in the environment. Disease-causing bacteria that can be transmitted by water include the genera of *Escherichia*, *Shigella*, *Salmonella*, *Legionella* and *Campylobacter*, etc. (CDC, 2005). These pathogenic bacteria can lead to severe or fatal diseases, such as tuberculosis, pneumonia and typhoid fever, etc. (WHO, 2004).

Increasingly, bacterial contamination issues are commanding the attention of water and wastewater treatments (WHO, 2003). There are many treatment methods to eliminate pathogenic bacteria (LeChevallier and Au, 2004). Therefore, finding efficient disinfection methods are essential to achieving safe water and protecting the human health.

1.2 Traditional disinfection methods

Disinfection is the antimicrobial reduction of the number of viable microorganisms on or in a product or surface to a level previously specified as appropriate for its intended further handling or use (McDonnell, 2007). Various physical and chemical disinfection methods are used to remove bacterial cells from water. Physical methods include ultrasound (Dehghani, 2005), freezing (Marazza, 1960), heating (Ayliffe *et al.*, 1974), ionizing radiation (Kubin *et al.*, 1982) and solar radiation (Davies *et al.*, 2009). Chemical methods depend mostly on selected chemicals with oxidizing and biocidal

properties. In the following section, chlorine (Cl_2), ozonation, ultraviolet (UV) irradiation and some latest disinfection methods are introduced.

1.2.1 Chlorine

Cl_2 is one of the most commonly used disinfectants for water disinfection and can be applied for the deactivation of most microorganisms (USEPA, 1999a). According to Community Water System Survey, majority of surface water and ground water systems in United States adopt chlorine for disinfection (USEPA, 1999b).

Cl_2 gas and water react to form hypochlorous acid (HOCl) and hydrochloric acid (HCl). Then, HOCl will dissociate into the hypochlorite ion (OCl^-) and the hydrogen ion (H^+), according to the following equations (Equations 1.1 and 1.2):

$$Cl_2 + H_2O \rightarrow HOCl + HCl \qquad \text{(Equation 1.1)}$$

$$HOCl \rightarrow H^+ + OCl^- \qquad \text{(Equation 1.2)}$$

The OCl^- and HOCl species are commonly considered as the free Cl_2, which serves as effective disinfectants to react with the bacterial cells. HOCl can react with numerous bacterial components to produce oxidation, hydrolysis and deamination reactions, and eventually affect cellular processes through producing physiological lesions. It is reported that Cl_2 destroys bacterial cells by combing with proteins to produce N-chloro compounds (Baker, 1926). Others report that Cl_2 plays an important role in

the formation of sulfhydryl groups of proteins (Knox *et al.*, 1948; Venkobachar *et al.*, 1977) and oxidizes several α-amino acids into a mixture of corresponding nitriles and aldehydes (Patton *et al.*, 1972). Recently study shows Cl_2 has high power to oxidize the structural and functional proteins, lipids and carbohydrates on membrane surface or in intracellular compartment, causing disruption of cell membrane and cell wall, as well as the leakage through the membrane (McDonnell, 2007).

Cl_2 and its compounds have some attractive advantages for their wide application on the water purification and wastewater treatment. Firstly, Cl_2 disinfection is reliable and effective against a wide spectrum of pathogenic organisms, such as *Escherichia* O157:H7 (Lisle *et al.*, 1998) and *Pseudomonas aeruginosa* (Xu *et al.*, 1996). Secondly, the Cl_2 residual can prolong disinfection even after initial treatment and can be measured to evaluate the effectiveness. Thirdly, Cl_2 is cost effective and can be used for preventing algal growth (White, 1992). However, there are still a number of potential problems with Cl_2 disinfection. On one hand, the process of Cl_2 disinfection can produce oxidation by-products, such as trihalomethanes (THMs), haloacetic acids and bromated, which can cause human carcinogen and mutagen (Watts *et al.*, 1995; Hua and Reckhowa, 2007; Ranieri and Świetlik, 2010). On the other hand, some parasitic species show resistance to low doses of Cl_2 (USEPA, 1999a).

1.2.2 Ozonation

Ozonation is another widely used disinfection method in water purification and

wastewater treatment since the 1970s (Wert el al., 2007). Ozone (O_3) is produced when oxygen molecules (O_2) are dissociated by an energy source into oxygen atoms (O) and subsequently collide with an O_2 to form an unstable gas, O_3, which is used to disinfect bacteria, such as *Escherichia coli* (Zuma *et al.*, 2009), *Salmonella* mutagenicity (Claxton *et al.*, 2008) and *Shigella sonnei* (Selma *et al.*, 2007) in the wastewater. O_3 is a very strong oxidant, which can oxidize components of the bacterial cell wall, followed by oxidizing all essential components including enzymes, proteins, DNA and RNA. When the cellular membrane is damaged during this process, the bacterial cells will fall apart (Doroszkiewicz *et al.*, 1994; Young and Setlow, 2004).

Ozonation is more effective than Cl_2 in destroying bacterial cells and viruses (USEPA, 1991, 2003). In addition, there is no regrowth of microorganisms after ozonation (Bancroft *et al.*, 1984). Furthermore, ozonation increases the dissolved oxygen (DO) concentration of the discharged wastewater (USEPA, 1999c). However, ozonation will lead to the formation of organic disinfection byproducts (DBPs), such as aldehydes, carboxylic acids and ketones in the presence of dissolved organic matter (Richardson *et al.*, 1999; Huang *et al.*, 2005). On the other hand, in the presence of bromide ion (Br^-), inorganic DBPs will be generated, which is classified as a probable human carcinogen (Haag and Hoigne, 1983; USEPA, 2001). In addition, ozonation is a more complex technology than Cl_2 disinfection, requiring complicated equipment and efficient contacting systems (Metcalf, 2005; Sichel *et al.*, 2007).

1.2.3 Ultraviolet irradiation

UV composes of electromagnetic radiation with a wavelength in the range from 100 to 400 nm, which is longer than X-rays, but shorter than visible light (VL). It can be further divided into UVA (315-400 nm), UVB (280-315 nm), UVC (200-280 nm) and vacuum UV (VUV) (100-200 nm). The optimum wavelength of effectively inactivate microorganisms is in the range of 250 to 270 nm, which is belong to UVC (USEPA, 1999d).

In recent years, the use of UVC light for the disinfection of microorganisms in water purification and wastewater treatment has become more and more popular. The mechanism of UVC disinfection is primarily related to the absorption of UVC by bacterial deoxyribonucleic acid (DNA) and subsequent photoreactions in microorganisms. Thyminedimers formed between adjacent thymines in the polynucleotide chains of DNA are the primary photoproducts of UVC exposed DNA (Jagger, 1967; Wolfe, 1990; Snider *et al.*, 1991; Wang *et al.*, 2010).

UV irradiation is a powerful disinfection method which can be accomplished in the order of seconds. Because of no additional chemicals are required for UV irradiation, there are almost no DBPs produced (Yamagiwa *et al.*, 2002). However, for UV irradiation, due to the weak penetration power, disinfection can only inactivate bacterial cells on the surface of the wastewater (Kühn *et al.*, 2003). In addition, UVC irradiation is mutagenic and carcinogenic which can cause skin cancer on human

(Parsons, 2004) and the treated cells can regrowth after removal of UV irradiation (Hancock and Davis, 1999). Furthermore, UV irradiation is not suitable for water with high levels of suspended solids, turbidity, color, or soluble organic matter. These materials can react with UV irradiation (USEPA, 1999d).

All three disinfection methods described above can effectively meet the discharge permit requirements for treated water and wastewater. However, the advantages and disadvantages of each must be weighed when selecting a method of disinfection.

1.2.4 Multiple disinfectants

Multiple disinfectants, the sequential or simultaneous use of two or more disinfectants, have been used in the real wastewater disinfection treatment recent years, such as O_3/hydrogen peroxide (H_2O_2), O_3/Cl_2, UV/Cl_2, $UV/O_3/H_2O_2$ and chlorine dioxide (ClO_2)/Cl_2. The aim of multiple disinfectants is to increase the disinfection efficiency towards a widely range of pathogens and reduction hazardous DBPs production (Cho *et al.*, 2003; Huang *et al.*, 2003; He *et al.*, 2008).

The amounts and types of DBPs formed in the water depend on water quality and the multiple disinfectants used in the primary and secondary disinfections. For instance, under some water quality conditions, O_3/chloramines (NH_2Cl) disinfectants can produce less amounts of THMs than Cl_2/NH_2Cl disinfectants. However, O_3/NH_2Cl disinfectants can enhance the concentrations of other DBPs such as aldehydes and

biodegradable organic matter (BOM). Although multiple disinfectants can achieve good disinfection efficiency, they may pose additional expenses and complexity for the system set-up.

1.3 Advanced oxidation processes

Advanced oxidation processes (AOPs) refer to a set of chemical treatment procedures used to remove organic or inorganic compounds in environment by oxidation. AOPs are based on the generation of powerful reactive oxidative species (ROSs), such as hydroxyl radical ($^{\bullet}OH$), H_2O_2, superoxide radical ($^{\bullet}O_2^-$), and perhydroxyl radical ($HOO^{\bullet}$). Among these ROSs, $^{\bullet}OH$ is considered the most powerful ROSs to remove organic, inorganic and microbial pollutants (Watts *et al.*, 1995; Cho *et al.*, 2005). AOPs usually refer to photocatalysis, Fenton's reaction and E-beam irradiation, etc. Table 1.1 shows the oxidation potential of common ROSs.

1.4 Photocatalysis

Photocatalysis is defined as the acceleration of a photoreaction in the presence of a photocatalyst. It is a photo-induced AOPs, which based on the generation of powerful reactive species, commonly $^{\bullet}OH$ and H_2O_2, to decompose hazardous pollutants and destroy the bacterial cells in the water environment (Saito *et al.*, 1992; Hoffmann *et al.*, 1995; Maness *et al.*, 1999; Kim *et al.*, 2003). Photocatalytic disinfection was firstly reported to successfully inactivate *E. coli* in 1985 (Matsunaga *et al.*, 1985). Since then, photocatalysis was extensively studied and proved to be a cost-effective,

safe and promising alternative for water purification and wastewater treatment during the past three decades.

Table 1.1 Oxidation potential of common oxidative species (Sies, 1985; Docampo, 1995; Rice-Evans and Gopinathan, 1995).

Species	Oxidation potential (V vs NHE)
Fluorine (F_2)	3.03
$^{\bullet}OH$	2.80
O	2.42
O_3	2.07
H_2O_2	1.78
$HOO^{\bullet}$	1.70
Permanganate (MnO_4^-)	1.68
Hypobromous acid (HOBr)	1.59
ClO_2	1.57
HOCl	1.49
Cl_2	1.36

1.4.1 Fundamentals and mechanism of photocatalysis

The basic mechanism of photocatalysis is well established and briefly summarized by the example of titanium dioxide (TiO_2) photocatalyst coupled with UV light (Ollis, 1985; Rincón and Pulgarin, 2003; Cho *et al.*, 2004). Upon the shining of UV

irradiation onto the TiO_2 photocatalyst, because absorption of photon energy greater than the bandgap energy of the photocatalyst, electron (e^-) in TiO_2 will be photoexcited from the valence band (VB) to the conduction band (CB) and form an e^-/hole (h^+) pair on the TiO_2 surface (Equation 1.3):

$$TiO_2 + UV\ (\lambda < 380\ nm) \rightarrow TiO_2\ (e^-_{(CB)} + h^+_{(VB)}) \qquad \text{(Equation 1.3)}$$

The h^+ on the VB reacts with water (H_2O) or hydroxyl ion (OH^-) to generate $^{\bullet}OH$ (Equations 1.4 and 1.5):

$$h^+_{(VB)} + H_2O \rightarrow {}^{\bullet}OH + H^+ \qquad \text{(Equation 1.4)}$$

$$h^+_{(VB)} + OH^- \rightarrow {}^{\bullet}OH \qquad \text{(Equation 1.5)}$$

On the CB, the excited e^- will react with O_2 to form $^{\bullet}O_2^-$ (Equation 1.6). Then $^{\bullet}O_2^-$ will react with H^+ and e^- and through a series of reaction to form H_2O_2 (Equation 1.7) (Cho *et al.*, 2004). Finally, H_2O_2 will then further react with e^- or $^{\bullet}O_2^-$ to form $^{\bullet}OH$ (Equations 1.8 and 1.9) (Wolfrum *et al.*, 1994; Pichat *et al.*, 1995; Rincón and Pulgarin, 2003).

$$O_2 + e^-_{(CB)} \rightarrow {}^{\bullet}O_2^- \qquad \text{(Equation 1.6)}$$

$$^{\bullet}O_2^- + H^+ + e^-_{(CB)} \rightarrow H_2O_2 \qquad \text{(Equation 1.7)}$$

$$H_2O_2 + e^- \rightarrow {}^{\bullet}OH + OH^- \qquad \text{(Equation 1.8)}$$

$H_2O_2 + {}^{\bullet}O_2^- \rightarrow {}^{\bullet}OH + OH^- + O_2$ (Equation 1.9)

However, due to the unstable nature of the excited e^-, some excited e^- returns to the VB and recombines with the positive h^+. This recombination process releases energy as heat (Carp *et al.*, 2004). A schematic diagram showing the mechanism of photocatalysis with TiO_2 coupled with UV light is shown in Plate 1.1

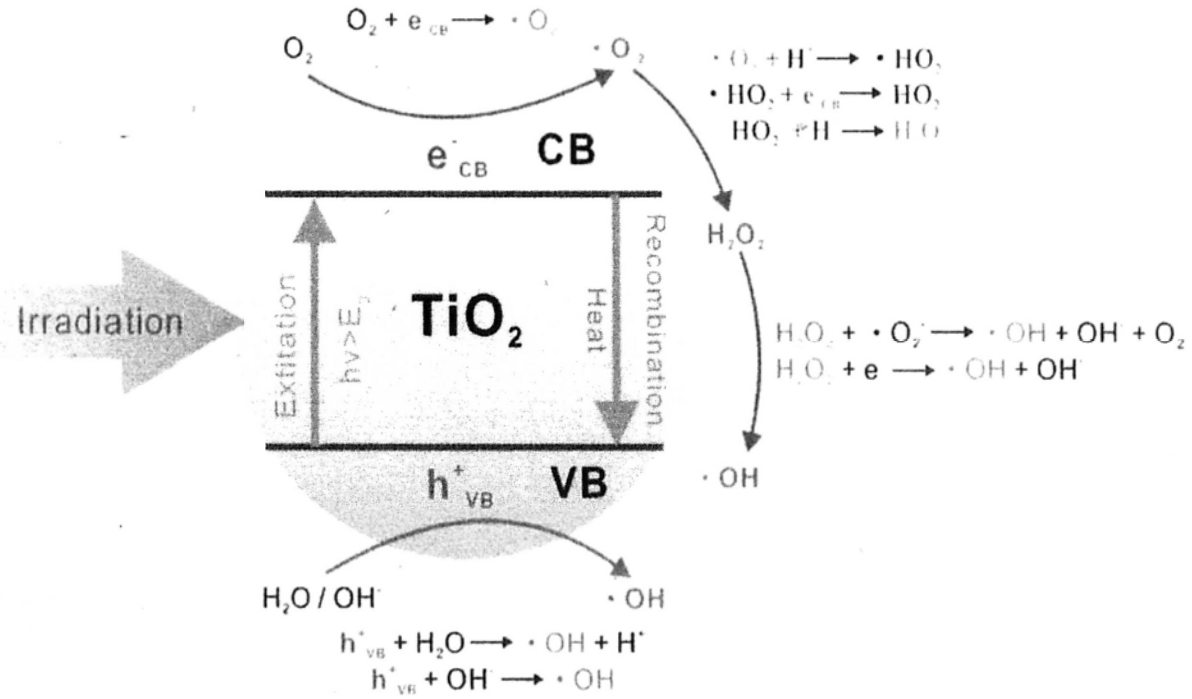

Plate 1.1 A schematic diagram showing the mechanism of photocatalysis with TiO_2 coupled with UV light (Hoffmann *et al.*, 1995).

According to the reactions described above, ${}^{\bullet}OH$, H_2O_2, ${}^{\bullet}O_2^-$, h^+ and e^- potentially play important roles in the photocatalytic disinfection.

1.4.2 Proposed mechanism of photocatalytic disinfection

Until now, several photocatalytic disinfection mechanisms have been proposed. In the late 19th century, Matsunaga *et al.* (1985, 1988) first proposed that disinfection mechanism was related to the dimerization of intracellular coenzyme A (CoA). Microbial cells were inactivated photoelectrochemically with semiconductor TiO_2 power. During oxidative attack, h^+ in the VB received electron from intracellular CoA leading to the formation of dimeric CoA, resulting in the inhibition of the respiration activity that caused cell death.

Later, Saito *et al.* (1992) accounted the complete destruction of mutants *Streptococci* by photocatalytic oxidation for the lipid peroxidation of polyunsaturated phospholipids components, resulting in the significant disorder in permeability of cell membranes, followed by rapid leakage of potassium ion (K^+), and slow leakage of protein and ribonucleic acid (RNA). Moreover, the photographs of transmission electron microscopy (TEM) revealed that the cell wall destruction was a secondary phenomenon of photocatalysis followed by oxidative damage of cytoplasmic membrane.

Afterwards, Sunada *et al.* (1998) found the photocatalytic degradation of endotoxin, which is a pyrogenic constituent of *E. coli* by the TiO_2 film. In a following study, they suggested the photoinactivating mechanism involved two steps, with the first step disordering of the outer membrane and a partial decomposition of the outer membrane,

and the second step disordering the inner membrane (the cytoplasmic membrane) (Sunada *et al.*, 2003). The cell wall of *E. coli* acted as a barrier to the photoinactivating process, while peptidoglycan layer did not have a barrier function.

Maness *et al.* (1999) elucidated lipid peroxidation reaction was the underlying mechanism of death of *E. coli* K-12. In their study, TiO_2 promoted peroxidation of the polyunsaturated phospholipid component of the lipid membrane and induced major disorder in the cell membrane leading respiration loss and cell death.

Huang *et al.* (2000) investigated the cellular damage sites and their contribution to cell death using *o*-nitrophenol-D-galactopyranoside (ONPG) as the probe and *E. coli* as model cells. The results showed that cell wall damage took place first due to the directly contact with the TiO_2 photocatalytic surface. After eliminating the protection of the cell wall, the oxidative species produced by photocatalysis attacked cytoplasmic membrane, increased the cell permeability and followed by progressive damage of intracellular components that eventually lead to cell death.

Koimumi *et al.* (2002) established a relationship between the intracellular superoxide dismutase (SOD) activity and the cell death. The photoreaction of *E. coli* with TiO_2 photocatalyst lethally attacked bacterial cells by decreasing the intracellular activity of SOD.

Photocatalysis inducing an abnormal cell division was a new point of view. Amezaga-Madrid *et al.* (2003) observed that during cell division, the irradiated bacteria did not form a septum, but developed an incomplete cell separation with a "bridge" between the daughter cells. They proposed that abnormal bacteria cell division was responsible for cell death.

Cheng *et al.* (2007) elucidated unsaturated fatty acid was more susceptible to peroxidation, and outer membrane and cytoplasmic membrane with tightly packed saturated fatty acid formed a barrier for ROSs to enter the cell. As an essential mechanism in living organisms, SOD and catalase (CAT), which are common enzymes, contributed to the protection of living organisms from excess oxidative stress by decomposition of harmful $^{\bullet}O_2^-$ and H_2O_2. Consequently, it was expected that the living organisms expressing different activities of SOD and CAT would display different deactivation profiles against superoxide and hydrogen peroxide stress arising from photoirradiated TiO_2.

Leung *et al.* (2008) utilized fluorescent tubes (FTs) to photocatalytically disinfect marine bacterial cells and studied the mechanism. They found that SOD and CAT levels affected the photocatalytic disinfection efficiency. Higher SOD and CAT levels implied bacterial cells could defend against ROSs attack from disinfection to a greater extent.

Recently, Kambala *et al.* (2009) demonstrated that sol-gel TiO_2 thin film could decompose the lipopolysaccharide layer and peptidoglycan layer, leading to a change in the cell permeability and resultant leakage of intracellular substances.

1.4.3 Titanium dioxide

At present, TiO_2, the most commonly used and commercially available photocatalyst has been widely investigated for the degradation of organic pollutants (Muszkat *et al.*, 1992; Depero, 1993) and disinfection of bacterial cells (Pal *et al.*, 2007; Leung *et al.*, 2008). Powered TiO_2, with brand name Degussa P25, is manufactured by Degussa, Frankfurt in Germany. P25 consists of 70% anatase and 30% rutile (Dunlop *et al.*, 2002). There are several advantages of TiO_2 as a photocatalyst. Firstly, TiO_2 exerts strong oxidability, thus it can completely mineralize most of organic and inorganic compounds, even effective at very low concentration of contaminants (Saito *et al.*, 1992). Secondly, TiO_2 itself is non-toxic and the oxidation products are carbon dioxide (CO_2), H_2O or other harmless inorganic acids (Hu *et al.*, 2001). Thirdly, TiO_2 itself is unchanged during the process so it is photostability (Saito *et al.*, 1992). All these advantages thus contribute to its popularity for the wastewater treatment process.

However, with a bandgap of 3.2 eV, TiO_2 can only be excited by light with wavelengths in the near UV region which is only 4% of the solar spectrum. Strong recombination of photo-generated e^-/h^+ pairs also limits photocatalysis of pure

photocatalysts. Therefore, it is a crucial issue to develop new synthetic photocatalysts which can be excited by VL.

1.4.4 The development of synthetic visible-light-driven photocatalysts

At present, two main synthesis strategies have been explored for the preparation of visible-light-drive (VLD) photocatalysts. One strategy is to extend the photoresponse of TiO_2 to the VL region, which is called TiO_2 based VLD photocatalysts (Zhang *et al.*, 2003; Yu *et al.*, 2005). The other strategy involves exploiting new type VLD photocatalysts such as $BiVO_4$ (Kudo *et al.*, 1999) and AgBr-Ag-Bi_2WO_6 (Zhang *et al.*, 2009a). Doping transition metal ions, coating noble metals on the surface, material sensitizing and synthesizing hybrid semiconductors are the common methods to develop VLD photocatalysts.

1.4.4.1 TiO_2 based visible-light-driven photocatalysts

To improve the photocatalytic efficiency under VL, great efforts have been undertaken to broaden the photoresponse of TiO_2. Various strategies have been pursued including doping with nonmetallic elements or metal ions. Asahi *et al.* (2001) reported the VL photocatalytic degradation of acetaldehyde and methylene blue with nitrogen-doped TiO_2. Sakthivel *et al.* (2003) investigated the daylight photocatalysis by carbon-modified TiO_2. Yu *et al.* (2005) reported that sulfur-doped TiO_2 exhibited a strong visible-light-induced bactericidal effect. Ma *et al.* (2009) investigated the photocatalytic activity of Fe-doped TiO_2 through the degradation of methylene blue

under VL irradiation. The photocatalytic activity of VLD Ru-doped TiO_2 was investigated to remove metsulfuron-methyl in aqueous phase (Senthilnanthan *et al.*, 2010).

1.4.4.2 The new type of visible-light-driven photocatalysts

In the 1980s, new type of VLD photocatalysts, other than TiO_2 based VLD photocatalysts, have been developed (Kudo *et al.*, 1989). The novel VLD photocatalysts include simple oxides and sulfides, such as Cu_2O (Hara *et al.*, 1998) and CdS (Shangguan *et al.*, 2002), complex oxides, such as $BiVO_4$ (Kudo *et al.*, 1999) and $In_{1-x}Ni_xTaO_4$ (Zou *et al.*, 2001), and complex nanostructure, such as AgBr-Ag-Bi_2WO_6 (Zhang *et al.*, 2009a) and Zn:$In(OH)_yS_z$ (Zhang *et al.*, 2009b).

Although these synthetic photocatalysts show high photocatalytic efficiency under VL, the amounts of these synthetic photocatalysts produced are too small, and the modification techniques are still complicated and make the prices of them to be very high. These drawbacks of synthetic VLD photocatalysts cannot satisfy with the large-scale application in the practical wastewater treatment. Obviously, a large quantity and low-cost VLD photocatalysts must be more popular than artificial semiconductors.

1.4.5 Natural visible-light-driven photocatalysts

TiO_2 can only be excited by light with wavelengths less than 380 nm which is only 4%

of the sunlight. It is interesting to note that the natural V-bearing TiO_2 contains minor elements of both V and Fe and exhibits effective photoactivity under VL irradiation (Lu *et al.*, 2004a,b, 2007). Unlike pure synthetic TiO_2 which lacks VL photoactivity, because the substitution of V for Ti caused distortion of coordination polyhedral, increased structural microstain and created structural vacancies, natural V-bearing TiO_2 showed high photoactivity to degrade halohydrocarbons (Lu *et al.*, 2004a,b) and Methyl Orange (MO) (Lu *et al.*, 2007) under VL irradiation.

Sphalerite (ZnS) has its conduction band at a much negative potential (-1.4 V vs. a saturated calomel electrode (SCE)) (Zang *et al.*, 1995), which is thermodynamically amenable for photoreduction of many organic pollutants, such as photoreductive dehalogenation of polyhalogenated benzenes (Yin *et al.*, 2001) and photoreductive decoloration of azo dyes (Zang *et al.*, 1995). However, with a bandgap of 3.6 eV, the application of pure sphalerite in photocatalysis is limited due to the low photocatalytic efficiency under VL. Fortunately, the natural sphalerite (NS) collected from Huangshaping (HSP) deposit contains some foreign metal ions (such as Fe^{2+} and Cd^{2+}) which makes its band structure different from the pure ZnS (Figure 1.1) (Li *et al.*, 2008). The bandgap of NS is only 2.95 eV (Figure 1.2) (Li *et al.*, 2009a). At present, there are several reports on the applying of NS to photocatalytcially reduce metal ions and degrade azo dyes under VL (Li *et al.*, 2006, 2008, 2009a,b). The results showed that 91.95% of the Cr^{6+} was reduced under 9 h VL irradiation (Li *et al.*, 2006) and 98.74% of MO was decolorized after 2 h VL irradiation (Li *et al.*, 2008) by NS.

Spectral analysis indicated an initial adsorption of MO to NS via its sulfonate group. Further reduction of the adsorbed MO by NS under VL irradiation led to the destruction of the azo structure (Li *et al.*, 2009a). In addition, NS as a VLD photocatalyst was investigated in terms of substituting ions, impurity phases and surface defects (Li *et al.*, 2009b). The substitution of metal ions for Zn^{2+} altered the band structure and resulted in the VL response. The coexistence of impurity semiconductors helped to prolong the lifetime of e^-/ h^+ pairs. The cleavage planes and fracture surfaces improved the photocatalytic activity of NS by providing more active sites than perfect faces (Li *et al.*, 2009b).

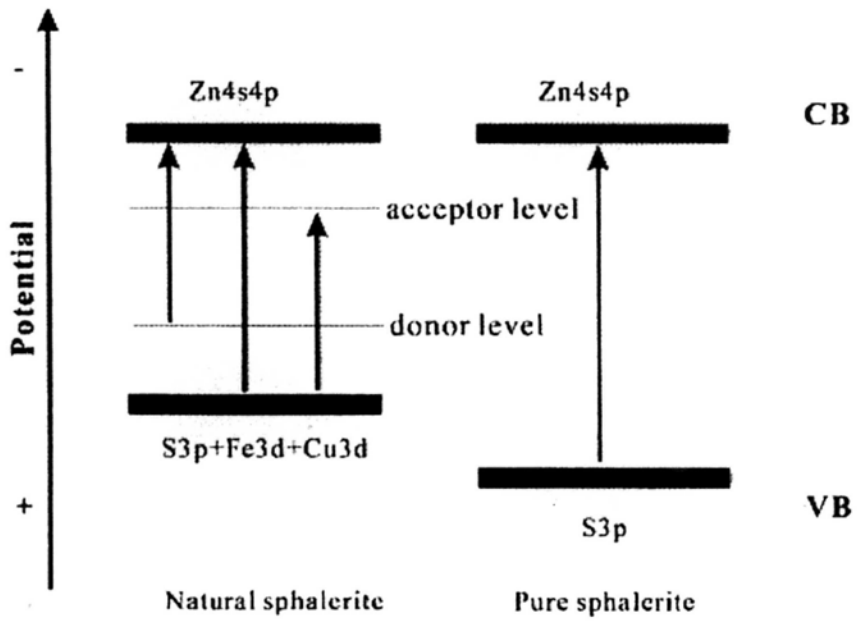

Figure 1.1 The proposed band structure of sphalerite (Li *et al.*, 2008).

Most importantly, the natural photocatalysts show their outstanding advantages over other synthetic VLD photocatalysts such as a large amount can be obtained from a mining site with a comparatively low cost. It is believed that the natural

photocatalysts are destined to have a promising future in the wastewater treatment.

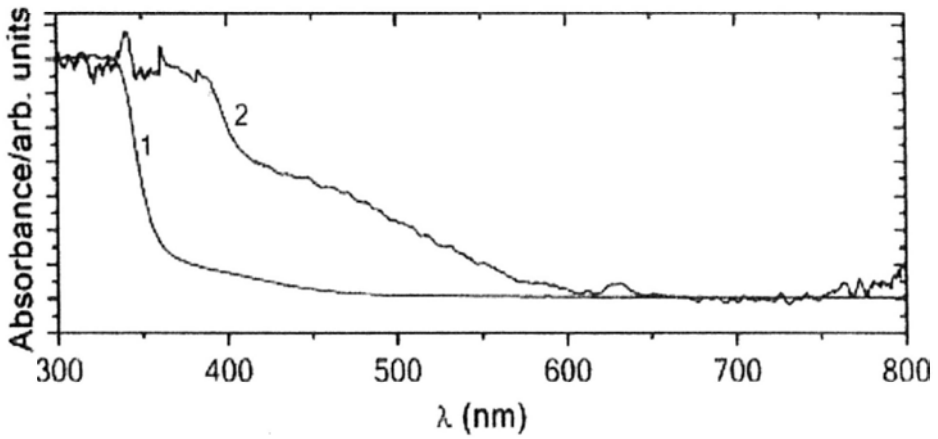

Figure 1.2 UV-vis diffuse reflectance spectra of (1) Pure sphalerite, and (2) NS (Li *et al.*, 2009a).

1.4.6 Irradiation light sources

The two most popular UV light sources for disinfection are UV fluorescent light tube and black light UV tube. UV fluorescent light tube has no phosphor coating on the wall of the tube. When an electrical discharge passes through the low-pressure vapor of mercury in a vaccum tube, it will emit the maximum wavelength at 254 nm in the range of UVC, which has a strong germicidal effect. For black light UV tube, due to no black-blue phosphor coating on the wall of the tube, it emits the maximum wavelength at 365 nm, which are referred to as UVA. Because UVC is difficult to handle and can cause skin cancer or blindness, UVA is commonly used as the UV light source in the photocatalysis.

The common VL sources are Xenon lamp, halogen lamp, FT and light emitting diode (LED) lamp. Xenon lamp is an artificial light source, which can use ionized xenon gas to produce a bright white light that closely natural daylight. Halogen lamp is an incandescent lamp with a filament contained with inert gas and a small amount of halogen such as iodine or bromine (Excelitas Technologies' Cermax®). For the basic study in the photocatalysis, the most common VL sources are Xenon lamp and halogen lamp due to their high light intensity (Hu *et al.*, 2006; Whang *et al.*, 2009; Zhang *et al.*, 2010). However, they cannot be practically used in the wastewater treatment because of their high cost and higher energy consumption.

FT is the common used household lightening source because of its low cost. It can emit not only the VL ($\lambda \geq 400$ nm), but also trace amounts of UV ($\lambda \leq 400$ nm). The effectiveness of photocatalysis using FTs to disinfect different bacterial cells was demonstrated (Pal *et al.*, 2007; Leung *et al.*, 2008). Because FT is cheap, safe and easy available, it has a good potential application in the water purification and wastewater treatment.

LED lamp, which is a new developing technical product, is another VL source. Compared with traditional VL sources, such as FT, Xenon lamp and halogen lamp, the advantages claimed for LED lamp are that they have the traits of long life expectancy and relatively low energy use. Most importantly, LED lamp can emit strongly single colored light in a very small range of wavelengths. These single colored LED lamps

can be used to study the light wavelength effect on the photocatalytic disinfection. Thus, with diode technology developing, LED lamp is making it possible to replace other lamps as the VL source.

1.4.7 Bacteria

1.4.7.1 *Escherichia coli* K-12

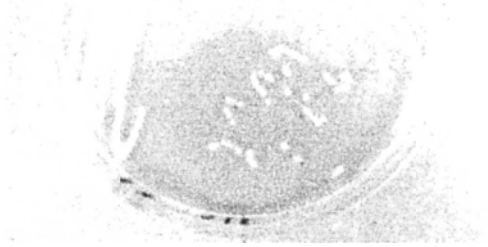

Plate 1.2 Colonies of *E. coli* K-12.

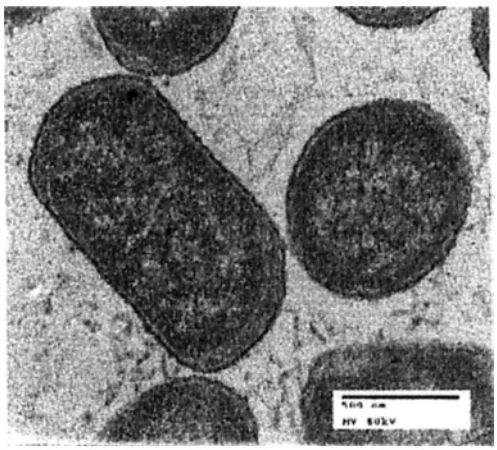

Figure 1.3 TEM image of *E. coli* K-12.

E. coli K-12 is a Gram-negative, non-spore forming and facultative anaerobic bacterium of the family *Enterobacteriaceae*. *E. coli* is a rod-shaped bacterium that is commonly found in the lower intestine of warm-blooded organism. Most *E. coli* stains are nonpathogenic, but some, such as *E. coli* O157:H7, are pathogenic and they can cause serious food poisoning in human (Scheutz and Strockbine, 2005). The morphology of bacterial cells is a straight cylindrical rod with the diameter of 1.1-1.5 μm and the length of 2.0-6.0 μm (Kubitschek, 1990). The growth pH condition for *E. coli* K-12 is from 5-9 and the optimal growth temperature occurs at 37°C. Colonies grows on nutrient agar as the appearance of convex, moist and pale gray colonies

(Plate 1.2). Figure 1.3 shows the TEM image of *E. coli* K-12.

1.4.7.2 *Microbacterium barkeri*

Members of the genus *Microbacterium* are small, slender, irregular rods with 0.4-0.8 μm in diameter by 1-4 μm or more in length. *Microbacterium barkeri* is a Gram-positive and non-spore forming bacterium (Collins *et al.*, 1983). They can grow under aerobic and facultative anaerobic conditions, and the optimal growth temperature occurs at 30°C. Colonies of *M. barkeri* grow on nutrient agar as the appearance of circular, opaque, glistening colonies with yellowish pigmentation (Plate 1.3). Figure 1.4 shows the TEM image of *M. barkeri*.

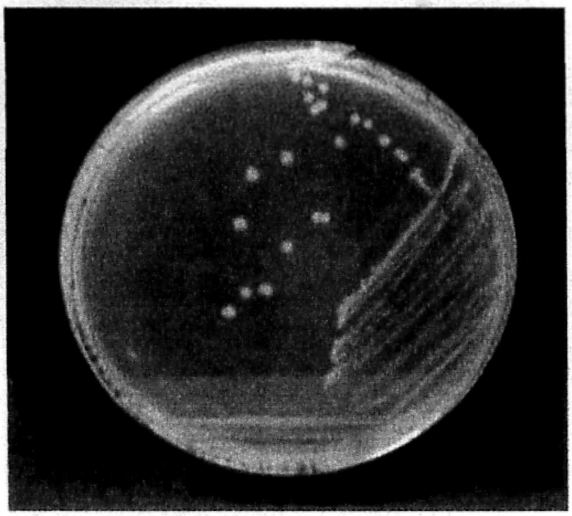

Plate 1.3 Colonies of *M. barkeri.*

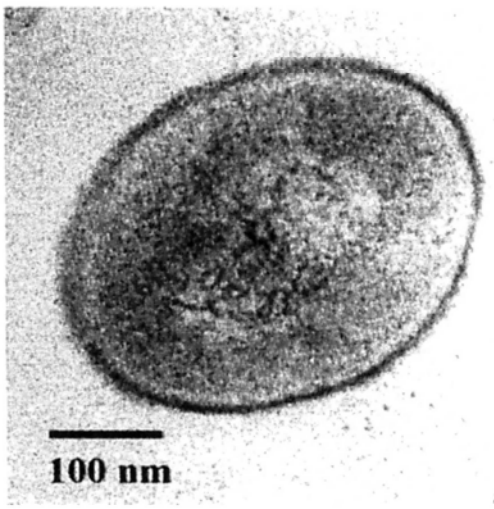

Figure 1.4 TEM image of *M. barkeri.*

1.4.8 The application of photocatalytic disinfection

Photocatalysis practically being used in the environmental applications thus far has been provided with decomposition of pollutants and detoxification of wastewater. It is important to note that photocatalysis is obtained without using any toxic chemicals,

but with only sunlight outdoor or light source indoor. Therefore, these photocatalyst-coated materials can be classified as being environmentally friendly.

Environmental pollution, including water, soil and air has become a serious problem today. There have been many studies focus on applying TiO_2 photocatalysis to degrade pollutions. Watanabe *et al.* (1992) first reported photocatalytic cleaning TiO_2-coated material with a ceramic tile. One of the first commercialized products using photocatalysis was the self-cleaning cover glass for tunnel light. TiO_2 photocatalyst coated on the cover glass coupled with tunnel light was sufficient to keep the surface clean (Honda *et al.*, 1998). The light cleaning based on the photocatalytic degradation effect is also used now in other various commercial products, for example, window blinds.

Another example of photocatalysis applying in the real environmental treatment is detoxification chemicals in the agriculture. To stop the spread of plant diseases, various classes of pesticides have been used in agriculture. Such problem becomes much more serious in developing countries. To solve the chemical problem, Hashimoto *et al.* (2007) developed a glass wool mat with a large surface area coated with TiO_2 nanoparticles. They used the photocatalytic mat under sunlight to detoxify the chemicals in the agriculture. The results showed that the agricultural chemicals were completely decomposed under sunlight in a few days.

2. Objectives

Most of the photocatalysts can only be excited by UV irradiation, which is only 4% of the sunlight. It is necessary to develop new photocatalysts, which have high photocatalytic activity under VL to degrade the pollutants and disinfect bacterial cells. Actually, there are large quantities of semiconducting minerals on the surface of the earth. They are in good coherence with the modified synthetic photocatalysts. However, there have been relatively few reports on the application of the natural minerals to environmental treatment. NS sample used in this study contains small amount of transition metal ions, such as Fe^{2+} and Cd^{2+}. According to the band structure of NS, it is reasonable to infer that these transition metal ions change the band gap of pure sphalerite, and probably lead to VLD activity. Based on these results, the present study will investigate on the use of NS in VLD photocatalytic disinfection of bacterial cells. The objectives involved in this study will investigate in several aspects to further support that NS is a novel, cost-effective VLD photocatalyst in the applications of environmental protection. This study is included three parts.

(1) To investigate the VLD photocatalytic disinfection efficiency with NS under VL. *E. coli* K-12 is selected as a model bacterium. Although there are some studies on the VLD photocatalytic degradation of organic pollutants by NS, there is no study focusing on photocatalytic disinfection of bacterial cells by NS under VL. Then, the mechanisms of VLD photocatalytic disinfection of bacterial cells by NS is elucidated using scavenger study and a partition system. The corresponding inactivation

mechanism is illustrated and compared by observing the morphological changes during the disinfection process by TEM.

(2) To study the most appropriate light source (with specific spectrum, wavelength and light intensity) for VLD photocatalytic disinfection of *E. coli* K-12 by NS. The spectral effect of VL is investigated the photocatalytic disinfection efficiency with NS under LED lamps, Xenon lamp and FTs. Then, compare the disinfection efficiency of different wavelengths (400, 500, 600 and 700 nm) of LED at the same intensity and suggest the influence of the disinfection by the different wavelength of VL. Finally, study the relationship between the disinfection efficiency and the VL intensity.

(3) To study the VLD photocatalytic disinfection by NS for two selected wastewater bacteria (Gram +ve bacterium, *M. barkeri*, and Gram -ve bacterium, *E. coli*) irradiated by FTs. Their susceptibility towards VLD photocatalytic disinfection with NS under FTs is determined. The optimal conditions for the VLD photocatalytic disinfection of these two wastewater bacteria are investigated. Various scavengers are used to identify the major oxidative species for VLD photocatalytic disinfection of two classes of bacteria. TEM and leakage of K^+ during the photocatalysis process are also determined to see whether the bacterial inactivation is in line with the leakage of intracellular components.

3. Natural sphalerite as a novel cost-effective photocatalyst for bacterial disinfection under visible light

3.1 Introduction

In last few years, a growing awareness of inadequate access to clean drinking water and sanitation has been witnessed (Shannon *et al.*, 2008). The conventional water treatment technologies, such as chlorination, ozonation and UV irradiation (Hass and Engelbrecht, 1980; Sobotka, 1993; Rakness, 2005), are powerful to degrade the pollutants and disinfect water-borne pathogens, while they also have obvious drawbacks. Chlorination and ozonation can form high levels of unregulated harmful DBPs, such as THMs and brominated haloacetic acids (Richardson *et al.*, 2002; Richardson *et al.*, 2003; Plewa *et al.*, 2004). For UV irradiation, it has weak penetration power and can cause skin cancer on human (Parsons *et al.*, 2004). In the coming decades, problems with water are expected to grow worse. Hence, an effective, non-toxic and low-cost method is urgently needed in the water treatment.

Photocatalysis is defined as the acceleration of photoreaction in the presence of a semiconductor catalyst. So there are two necessary components: they are photocatalyst and light source. It is a photo-induced AOPs which based on the generation of a powerful oxidizing species, such as $^{\bullet}OH$, H_2O_2, $^{\bullet}O_2^-$, e^-, and h^+ (Hoffmann *et al.*, 1995). Compared with other AOPs, photocatalysis shows several advantages in the application of the environment treatment. Firstly, photocatalysis saves energy because it can utilize sunlight, a kind of renewable and natural energy, as

energy input. Secondly, photocatalytic process can completely mineralize the pollutants. Thirdly, photocatalysis can non-selectively degrade a variety of pollutants by ROSs produced by photocatalyst. Lastly, the photocatalytic reaction occurs at room temperature without any complex apparatus and toxic chemicals so that it is simple and mild.

At present, TiO_2, which is a widely available commercial photocatalyst, is commonly used to degrade organic pollutants and disinfect bacterial cells (Muszkat *et al.*, 1992; Pal *et al.*, 2007). However, with a bandgap of 3.2 eV, TiO_2 can only be excited by UV, and thus much effort has been devoted to synthesize new VLD photocatalysts. Although synthetic photocatalysts show promising disinfection performance under VL, the massive production of such synthetic photocatalysts at low cost has been a major limitation to its large-scale application. In this study, the natural photocatalyst, sphalerite, which possesses VL photocatalytic activity and can be readily supplied in large quantities at low cost, is introduced. It is envisaged that developing a natural photocatalyst based disinfection technique will be an economically viable solution for large-scale wastewater treatment.

More recently, it has been found that several active species, such as h^+, $^{\bullet}O_2^-$, H_2O_2, and $^{\bullet}OH$ generated from the TiO_2-UV system, can inactivate bacterial cells. However, the fundamental mechanism of VLD photocatalytic disinfection has not been well-established. To date, no study has investigated the photocatalytic disinfection of

bacterial cells by NS under VL irradiation, or reported which reactive species are mainly involved in the NS-VL disinfection system.

To study the bactericidal effect of NS, a set of parallel experiments is designed to investigate (1) whether photocatalytic reaction occurs on the surface of photocatalysts, and (2) which reactive species are the bactericidal agents in VLD photocatalytic disinfection. The suggested mechanism and reactive species involved in the photocatalytic disinfection of *E. coli* K-12 by NS under VL irradiation are also discussed using scavenger study and a partition system.

3.2 Materials and methods

3.2.1 Materials

NS used in this work was collected from the HSP deposit in Hunan Province, China. The sample showed a grey color (Plate 3.1) and a compact-grain structure in hydrothermal veins. NS sample was mechanically crushed and milled at the mine. The resultant sphalerite particles were passed through a 340-mesh sieve pore to obtain sphalerite powder with particle sizes < 40 μm (Figure 3.1). The crystal structure of NS was cubic, with a calculated lattice constant of a = 0.54264 nm. The bandgap energy of NS was 2.95 eV. The chemical compositions of the HSP sphalerite sample studied by electron microprobe analysis were listed in Table 3.1 (Li *et al.*, 2009a).

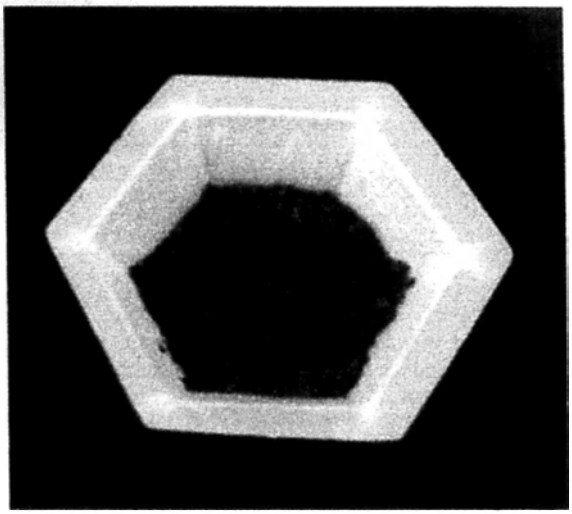

Plate 3.1 NS sample.

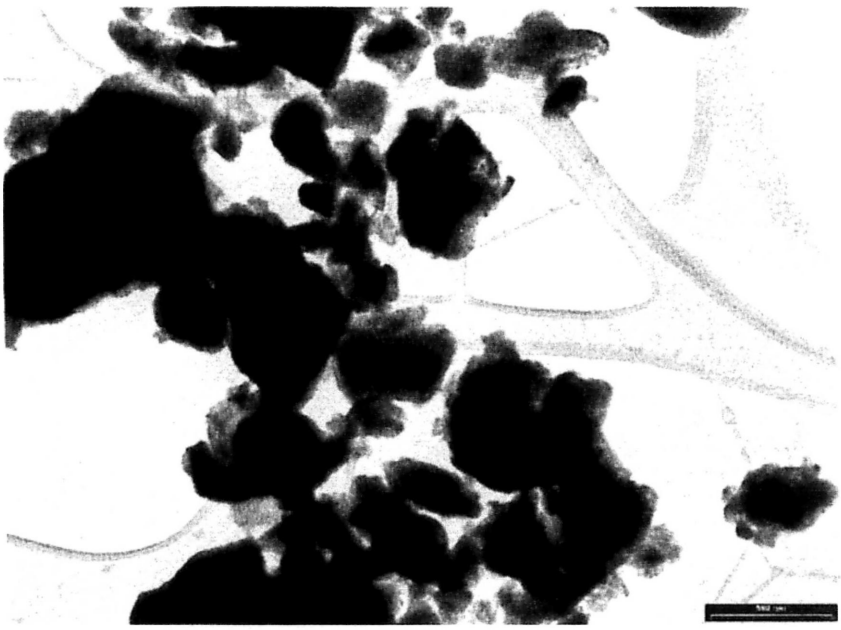

Figure 3.1 TEM image of NS sample.

3.2.2 Bacterial culture preparation

E. coli K-12 was used as a testing organism for photocatalytic disinfection because it was safe to use and easy to grow. The bacterial cells were cultured in nutrient broth (NB) (BioLife, Milano, Italy) solution at 37°C and agitated at 200 rpm for 16 h. The cultures were then washed twice with saline (0.9% NaCl) solution by centrifugation at

24,000 *g* for 5 min using a Hermle Z323 centrifuge (Hermle Labortechnik, Germany) (Plate 3.2), and the cell pellet was resuspended in saline solution. The cell density was analyzed by measuring the absorbance at 520 nm by a Helios Gamma UV-vis spectrophotometer (Thermo Electron, England) (Plate 3.3). Finally, the cell concentration was adjusted to final cell density of 1.5×10^7 cfu (colony forming unit)/mL in the reaction mixture.

Table 3.1 Chemical compositions of NS particles at the different spots in the same mine (wt%) (Li *et al.*, 2009a).

Spots	S	Zn	Fe	Cd	Mn	Ge	Se	Ga	Cu	Total
1	33.30	62.27	3.84	0.12	0.03	0.01	0.05	0.08	0.00	99.69
2	32.73	62.16	4.21	0.17	0.01	0.00	0.02	0.00	0.00	99.0
3	33.76	64.72	0.27	0.23	0.01	0.05	0.06	0.03	0.00	99.14
4	33.18	63.66	2.57	0.17	0.00	0.01	0.20	0.00	0.03	99.83
5	33.24	62.64	3.33	0.13	0.01	0.00	0.00	0.01	0.00	99.40
6	33.11	64.17	2.06	0.10	0.02	0.04	0.00	0.09	0.00	99.59
7	32.73	62.87	3.27	0.19	0.03	0.05	0.00	0.00	0.02	99.17
8	33.50	63.82	2.61	0.17	0.01	0.00	0.00	0.00	0.1	100.23
9	34.00	62.83	3.04	0.11	0.06	0.10	0.01	0.00	0.02	100.22
10	32.88	65.12	1.01	0.15	0.01	0.06	0.07	0.00	0.02	99.33

Plate 3.2 A Hermle Z323 centrifuge (Hermle Labortechnik, Germany).

Plate 3.3 A Helios Gamma UV-vis spectrophotometer (Thermo Electron, England).

3.2.3 The adsorption between natural sphalerite and bacterial cells

Cell suspension was added into 22.5 mL of NS suspension in 80 mL tube. The mixture was stirred, laid horizontally on a shaker platform, and shaken at 250 rpm to keep contents suspended, for 1 h at 25°C. At 15, 30 and 60 min, the tubes were again inverted to mix contents, samples were removed to sterile tubes, and NS was allowed

to settle for 30 min. Cells in the resulting supernatants were enumerated. One control which was bacteria alone without NS was carried out to prove the bacteria would not settle. The adsorption percentage was measured by the following Equation 3.1:

$$\text{Adsorption rate (\%)} = \frac{(CD_{control} - CD_{sample})}{CD_{control}} \times 100 \qquad \text{(Equation 3.1)}$$

Where:

$CD_{control}$ represents the cell density of the control at time zero

CD_{sample} represents the cell density of the treatment at different time

3.2.4 Photocatalytic disinfection of *E. coli* K-12

NS solution was homogenized by sonication with a Branson 2510 sonicator (Branson Ultrasonics B.V., Soest, NL, USA) (Plate 3.4) at 35 kHz for 1 min. Five mL of saline-washed *E. coli* K-12 was suspended in 45 mL sterilized saline solution containing NS. The reaction temperature was kept at 25°C and the reaction mixture was stirred with a magnetic stirrer throughout the experiment. The reactor (Plate 3.5) held six FTs (15 W, VELOX®, Thailand). The VL and UV intensities inside the reactor flask were measured by a light meter (LI-COR®, Lincoln, Nebraska, USA) and an UVX digital radiometer (UVP®, Upland, California, USA), respectively. At different time intervals, aliquots of the sample were collected and serially diluted with sterilized saline solution. Then, 0.1 mL of the diluted sample was immediately spread

on nutrient agar plates (Lancashire, UK) and incubated at 37°C for 24 h to determine the number of viable cells (in cfu/mL). As a comparison, a dark control (NS alone without light irradiation), a light control (light irradiation alone without the photocatalyst), and a negative control (without NS photocatalyst or light irradiation) were also conducted. A liquid filter (5 M sodium nitrite) was placed between the FTs and the sample flask to block all UV emission to determine whether NS was a real VLD photocatalyst. Each set of experiments was performed in triplicate.

Plate 3.4 A Branson 2510 sonicator (Branson Ultrasonics B.V., Soest, NL, USA).

3.2.5 Effect of scavengers

The scavenger experiments were carried out by adding individual scavenger to 50 mL reaction mixture containing about 1.5×10^7 cfu/mL *E. coli* K-12 and 1 g/L NS before the light irradiation. The stock concentrations of individual scavengers were 1 M $K_2Cr_2O_7$ (Merck, Darmstadt, Germany) for the quenching of e^-, 1 M isopropanol (Riedel-de Haën®, Seelze, Germany) for the scavenging of free $^{\bullet}OH$ ($^{\bullet}OH_{free}$), 1 M KI for the scavenging of h^+ and $^{\bullet}OH$ adsorption on the surface of the photocatalyst

($^{\bullet}OH_{ads}$), 100 mM Fe(II)-EDTA (Fe(II)-EDTA solution was prepared dissolving iron sulfate ($FeSO_4$) (90%, Ajax Chemicals, Sydney, Australia) with ethylenediaminetetraacetic disodium salt (Na_2EDTA) (Ajax Chemicals, Sydney, Australia) into distilled water) for the detection of H_2O_2. As a comparison, a dark control (NS alone without light irradiation in the presence of each scavenger) and a light control (light irradiation alone without the photocatalyst adding each scavenger) were conducted to find the maximum amount of scavenger without toxicity.

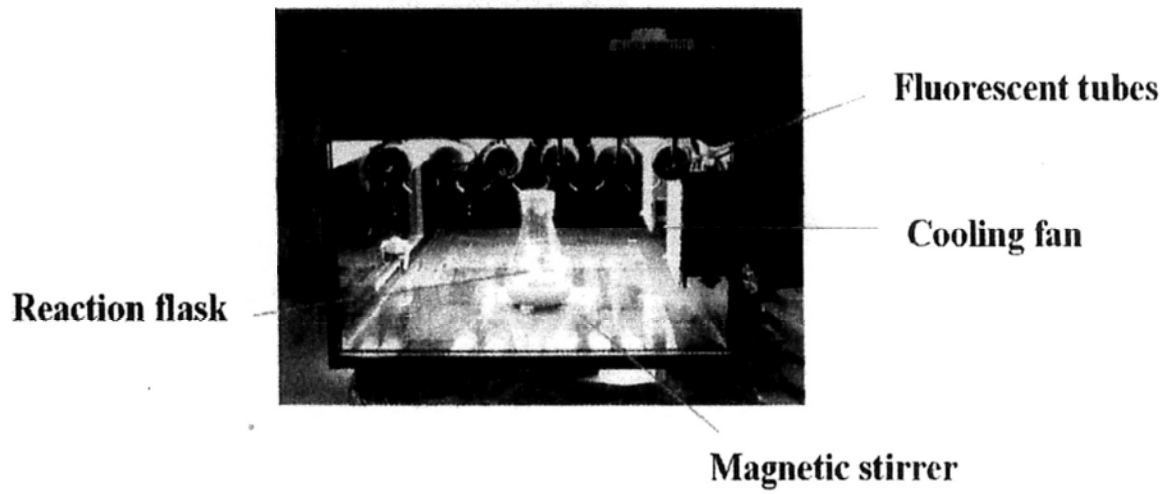

Plate 3.5 A photocatalytic disinfection reactor under FTs irradiation.

3.2.6 Partition system

To study whether direct contact between NS and *E. coli* K-12 was important for disinfection, the partition system (Kikuchi *et al.*, 1997; Zhang *et al.*, 2009b, 2010) was used to separate *E. coli* K-12 from the surface of NS. The setup of the partition system for this experiment was shown in Plate 3.6. Ten mL of *E. coli* K-12 suspension (1.5×10^7 cfu/mL) was pipetted into a semi-permeable container, and 50 mL of NS

suspension (1 g/L) was maintained outside of the membrane and stirred continuously to keep NS evenly distributed in the solution. At different intervals, aliquots of the cells inside the membrane were sampled and immediately diluted. The number of viable cells in the samples was determined by the same procedure as that described in Section 3.2.4.

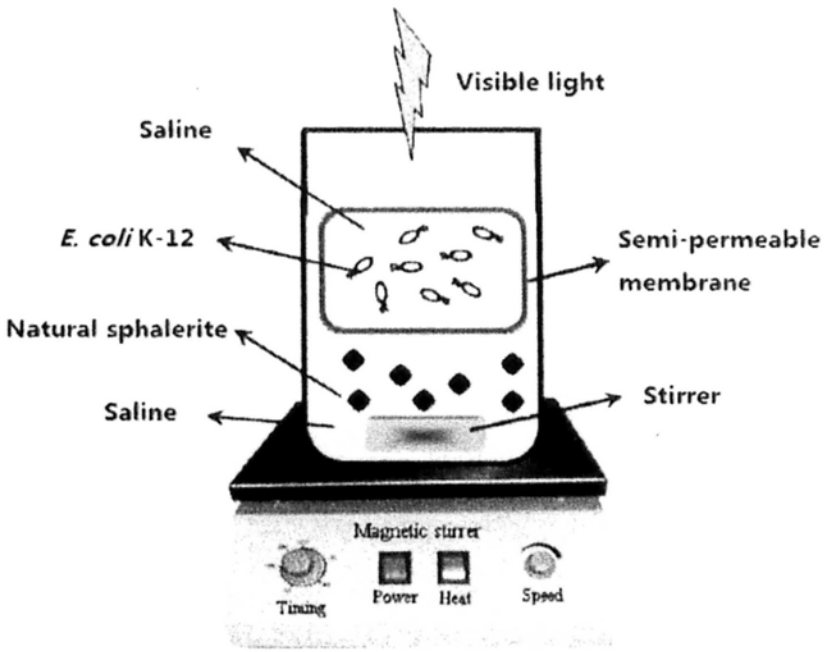

Plate 3.6 A schematic illustration of partition system used in the photocatalyitc disinfection of *E. coli* K-12 with NS under VL irradiation (Zhang *et al.*, 2010).

3.2.7 Analysis of hydrogen peroxide

The mechanism of analogy of H_2O_2 was based on peroxidase (POD)-catalyzed oxidation of other aromatic amines. The sequence of reactions leading to the oxidation of N,N-diethyl-*p*-phenylenediamine (DPD) consisted of oxidation by H_2O_2 of POD to a higher valent state, which in turn oxidized two molecules of DPD to the radial

cation, $DPD^{\bullet+}$ (Figure 3.2).

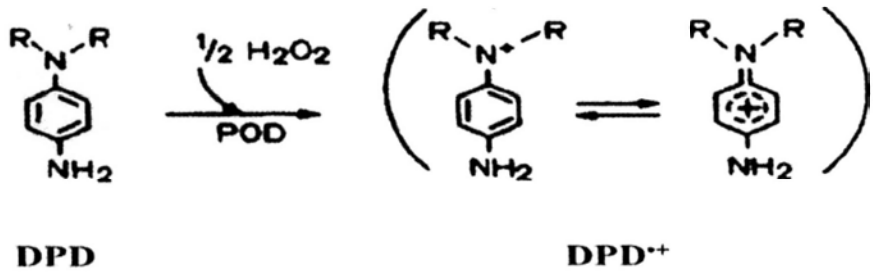

DPD **$DPD^{\bullet+}$**

Figure 3.2 Chemical reaction of DPD/POD method (Bader *et al.*, 1988).

The radical cation $DPD^{\bullet+}$ could form a fairly stable color, with the maximum absorption at 551 nm (Bader *et al.*, 1988). Due to the high specific absorption of $DPD^{\bullet+}$, the DPD/POD method permitted measurement of low concentrations of H_2O_2.

The photocatalytic reaction was started by turning on FTs. At different time intervals, 3 mL of the sample were collected and centrifuged to remove NS. 2.7 mL of the solution was pipette into a 10 mL beaker. 0.3 mL of PBS buffer (0.5 M Na_2HPO_4 and 0.5 M NaH_2PO_4 in distilled water were adjusted to pH 6.0 when this stock solution was diluted 10-fold) were added to achieve pH 6 in the final solution. Then 60 and 6 μM in final solution of DPD and POD reagents, respectively, were added in rapid succession. After at least 1 min, the solution was transferred into the photometric cell and measured the absorption spectrum from 450-600 nm by a UV-vis spectrophotometer.

3.2.8 Analysis of hydroxyl radical

Terephthalic acid was used as a probe molecule (Ishibashi *et al.*, 2000; Yu *et al.*, 2009) to detect the formation of $^{\bullet}OH$ of NS irradiated by FTs. Terephthalic acid readily reacted with $^{\bullet}OH$ to produce a highly fluorescent product, 2-hydroxyterephthalic acid. The intensity of 2-hydroxyterephthalic acid was proportional to the amount of $^{\bullet}OH$ produced by NS. 4×10^{-4} mol/L terephthalic acid and 2×10^{-3} mol/L NaOH were added to 50 mL of NS suspension (1 g/L). The photocatalytic reaction was started by turning on FTs. At different time intervals, aliquots (1 mL) of the sample were collected and analyzed by a fluorescence spectrophotometer (Tecan, Männedorf, Switzerland) after NS being removed by centrifugation. At the excitation wavelength at 315 nm, 2-hydroxyterephthalic acid gave a peak at the wavelength at 425 nm.

3.2.9 Analysis of superoxide radical

To identify $^{\bullet}O_2^-$ produced by NS during photocatalysis, electron spin resonance (ESR) signals of spin-trapped paramagnetic species with 5, 5-Dimethyl-1-pyrroline-*N*-oxide (DMPO) were recorded at ambient temperature on ESR spectrometer (Brucker ESR A300 spectrometer, Rheinstetten, Germany). The settings for ESR spectrometer were center field 3507 G, sweep width 80 G, microwave frequency 9.85 Hz, power 6.34 mW, modulation frequency 100 kHz, and modulation amplitude 1 G.

3.2.10 Transmission electron microscopy

TEM is a microscopic technique which a beam of electrons was transmitted through

an ultra thin specimen and interacted with the specimen as it passed through. An image was formed, magnified and focused onto a fluorescent screen or photographic film layer. TEM was capable of imaging at a significantly higher resolution and better improvement in depth of vision than light microscopes. Sample quality could be enhanced by staining heavy compounds as they could selectively deposit heavy atoms in the sample. The dense electron clouds of heavy atoms strongly interacted with the electron beam and thus enhanced the sample structural detail. To be noticed, the sample must be cut into ultra-thin sections of 70 nm so as to allow the vision of image (Hayat, 1985)

To study the morphological change of the bacterial cells and investigate the mechanism of photocatalytic disinfection, TEM images of *E. coli* K-12 before and after the photocatalytic reaction were observed. The mixture comprising NS and *E. coli* K-12 during different stages the photocatalytic reaction was collected and centrifuged. The bacterial cells were pre-fixed by glutaraldehyde (E.M. grade, Electron Microscopy Sciences, Hatfield, PA, USA) and trapped in low melting point agarose. The solidified encapsulated pellets were cut into small cubes with diameter less than 1 mm by the razor blade. After being post-fixed by osmium tetraoxide (E.M. grade, Electron Microscopy Sciences, Fort Washington, PA, USA), the small cell pellet was dehydrated by adding a graded series of ethanol concentrations (50, 70, 85, 95 and 100%), and was finally embedded in Spurr solution (Electron Microscopy Sciences, Fort Washington, PA, USA) for polymerization at 68°C for 16 h. Using an

ultra-microtome (Leica, Reichert Ultracuts, Wien, Austria) with a diamond knife (Plate 3.7) (DiATOME *ultra 45°*, Diatome Ltd., Biel, Switzerland), ultra-thin sections of 70 nm were made and placed on copper mesh grids with chloroform coating. Then they were stained with 2.5% uranyl acetate and 2% lead citrate on copper grids. Finally, the stained ultra-thin sections were examined by a H-7650C transmission electron microscope (Plate 3.8) (Hitachi Ltd, Tokyo, Japan) at 80 kV accelerating voltage.

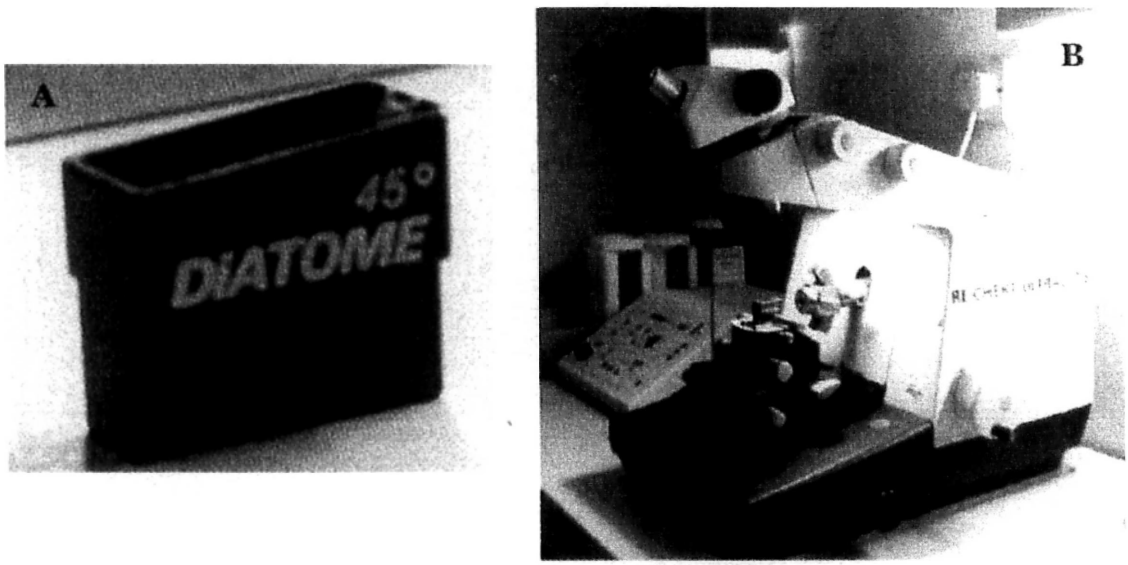

Plate 3.7 (A) A diamond knife (DiATOME *ultra 45°*, Diatome Ltd., Biel, Switzerland), and (B) An ultra-microtome (Leica, Reichert Ultracuts, Wien, Austria).

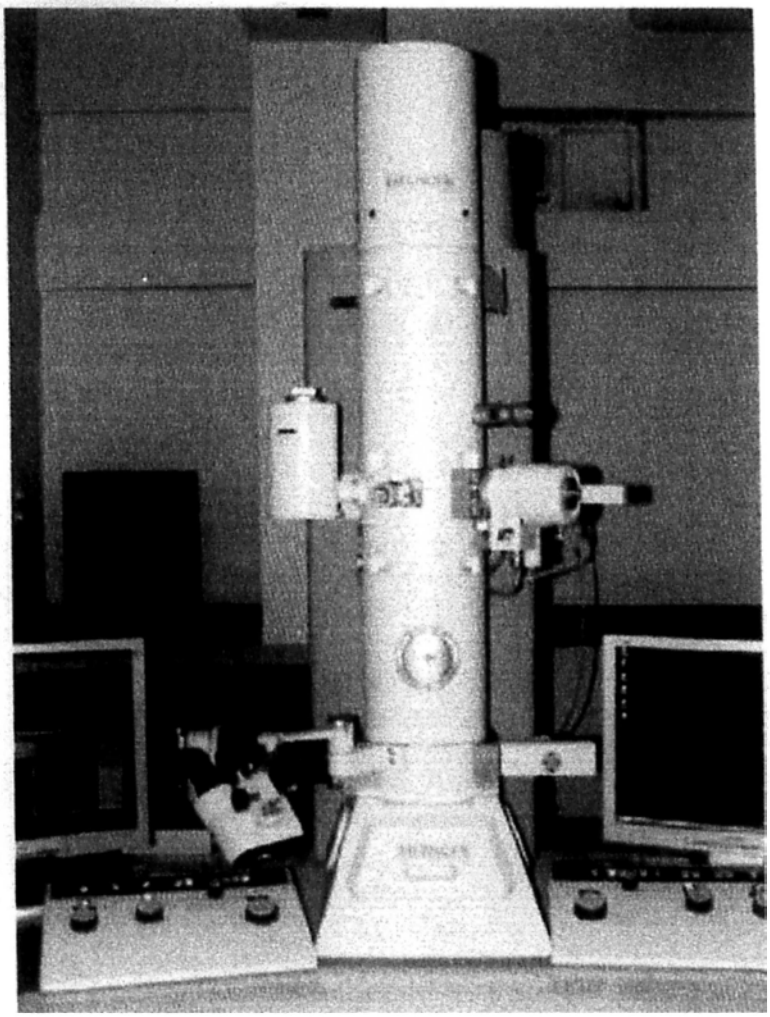

Plate 3.8 A H-7650C transmission electron microscope (Hitachi Ltd, Tokyo, Japan).

3.2.11 Atomic absorption spectrophotometry

To determine the metal ions eluted from NS during the photocatalytic disinfection process, 1 g/L NS suspension before and after turning on the FTs was collected and filtered through a Millipore filter with a pore size of 0.45 μm (Millipore Corporation, Ireland). The solution after filtration was withdrawn for atomic absorption spectrophotometry (AAS) analysis on a Z-2300 Polarized Zeeman atom absorption spectrophotometer (Hitachi High-Technologies, Tokyo, Japan) (Plate 3.9).

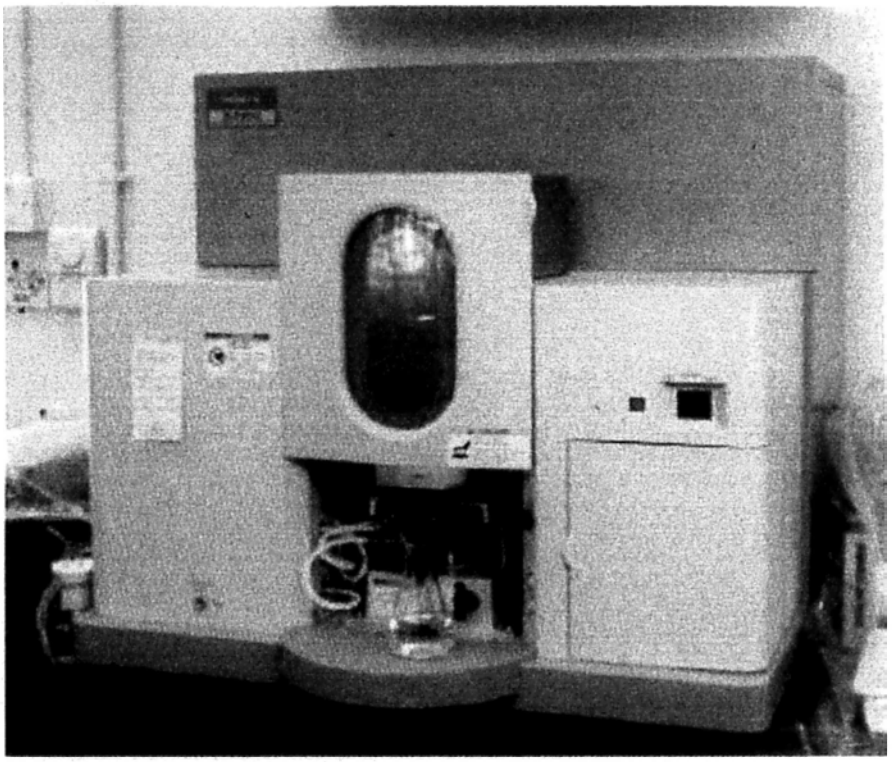

Plate 3.9 A Z-2300 Polarized Zeeman atom absorption spectrophotometer (Hitachi High-Technologies, Tokyo, Japan).

3.2.12 Total organic carbon analysis

Total organic carbon (TOC) analysis was conducted to determine whether total bacterial mineralization by photocatalytic disinfection could be obtained in prolonged VLD photocatalytic disinfection. A typical analysis for TOC measures was both the total carbon (TC) and inorganic carbon (IC), the latter representing the content of dissolved CO_2 and carbonic acid salts. Subtracting IC from TC yielded TOC.

150 mL reaction mixture containing the initial cell density of 1.5×10^8 cfu/mL with 1 g/L NS was under photocatalytic disinfection treatment with FTs irradiation. At different time intervals, two 12 mL samples was collected and centrifuged at 24,000 *g*

for 5 min. Cell pellets obtained were used for the solid-phase analysis while the supernatant was used for the aqueous-phase analysis following the protocol of the instruction manual (Shimadzu Corporation, 2011).

For the aqueous-phase analysis, 12 mL supernatant samples was put into pre-cleaned sample vial for TC and IC determination by auto-sample ASI-V connecting to the TOC analyzer TOC-$V_{CSH/CSN}$ (Shimadzu Corporation, Kyoto, Japan) (Plate 3.10A). For solid-phase analysis, the cell pellets harvested were resuspended in 0.2 mL saline solution, added into pre-weighed sample boat and dried at 105°C until steady weight was attained. Then one of the dried cell pellets was combusted in a furnace at 900°C for the determination of total CO_2 formed from TC, while the other dried cell pellets were put into react with 85% phosphoric acid at 200°C for the measurement of CO_2 formed from IC. A TOC analyzer TOC-$V_{CSH/CSN}$ with a solid sample measurement was used for the solid-phase measurement (Shimadzu Corporation, Kyoto, Japan) (Plate 3.10B).

Two control experiments were carried out for TOC analysis. One was the dark control containing only bacterial cells and photocatalyst at dark for monitoring the natural change of TOC from reaction mixture without photocatalysis. Another was the solution only containing photocatalyst for determining the background TOC content from 1 g/L of NS reaction mixture. All the above experiments were also conducted in triplicates.

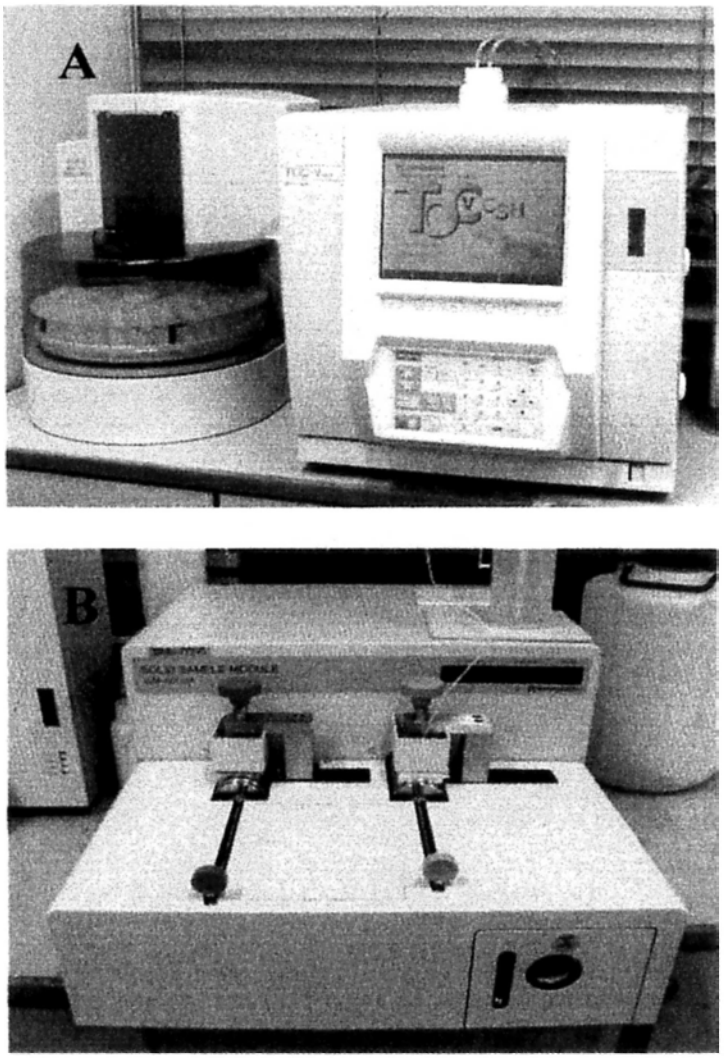

Plate 3.10 (A) An auto-sampler connecting to the TOC analyzer TOC-VCSH/CSN (Shimadzu Corporation, Kyoto, Japan) (B) A solid sample measurement module SSM-5000A (Shimadzu Corporation, Kyoto, Japan).

3.3 Results

3.3.1 Optimization the physicochemical conditions of disinfection

3.3.1.1 The adsorption effect

The effect of NS suspension adherence to bacterial cells on the photocatalytic disinfection was determined. *E. coli* K-12 suspended to levels of 10^7 cells/mL and 1 g/L of NS were mixing in saline solution. The adsorption results shows that

essentially all adsorption of photocatalyst to *E. coli* took place within 1 h, with little or no additional adsorption taking place over more time incubation (Figure 3.3). At the very beginning of the contact NS with bacterial cells, the adsorption rate was only 40%. With prolonged contact time, the adsorption rate increased significantly. After 1 h mixing of the photocatalyst and bacterial cells, the adsorption rate reached to almost 90%.

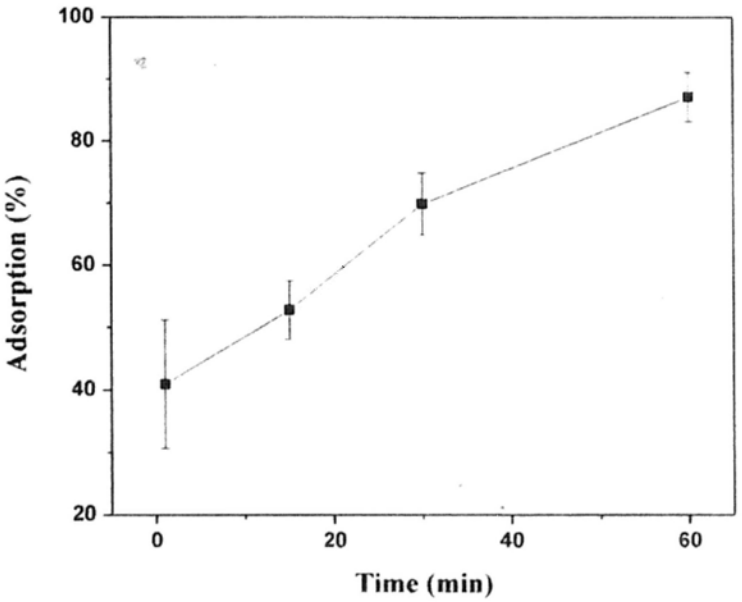

Figure 3.3 The adsorption of NS onto *E. coli* K-12. Each data point and error bar represents the means and standard deviation, respectively, of triplicates.

For better study the adsorption effect, Figure 3.4 shows the photocatalytic disinfection efficiency at no stirring or after stirring 1 h of the reaction mixture before the irradiation. The results show that at the condition of no stirring of the mixture before reaction, complete inactivation of *E. coli* K-12 was observed after 10 h of treatment. While after stirring the photocatalyst and bacterial cells for 1 h before photocatalytic

irradiation, which suggests 90% adsorption between the photocatalyst and bacterial cells (Figure 3.3), the total inactivation finished within 6 h, shorten 4 h compared with no stirring condition.

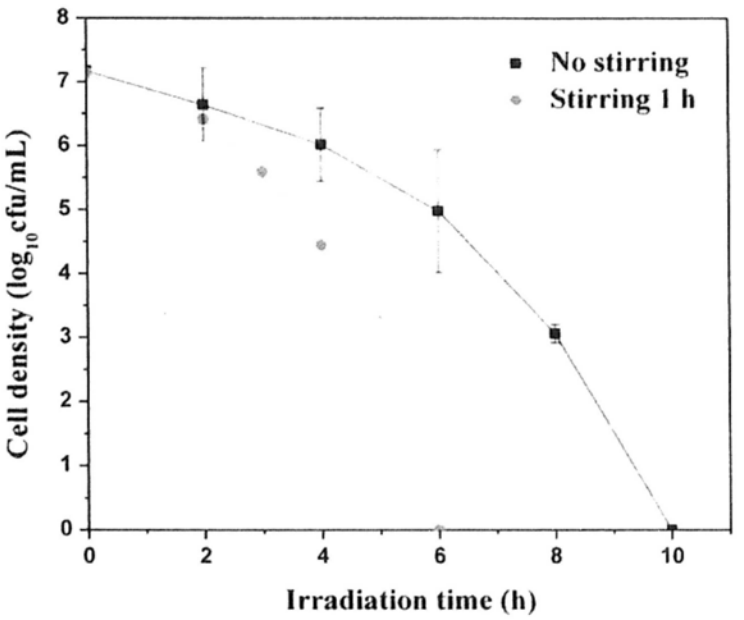

Figure 3.4 Disinfection efficiency of *E. coli* K-12 (1.5×10^7 cfu/mL) at the different adsorption between NS and bacterial cells under FTs irradiation.

3.3.1.2 The concentration of the photocatalyst effect

The concentration of NS was optimized for photocatalytic disinfection (Figure 3.5). The results show that 1 g/L was the optimal added concentration into the solution of NS. If the amount of NS decreased from 1 to 0.13 g/L, disinfection efficiency would reduce. Increasing the amount of NS to 1.25 g/L, the disinfection efficiency did not change compare with 1 g/L NS. And further increasing the concentration of photocatalyst would shield the light, and also resulted in reduced disinfection efficiency.

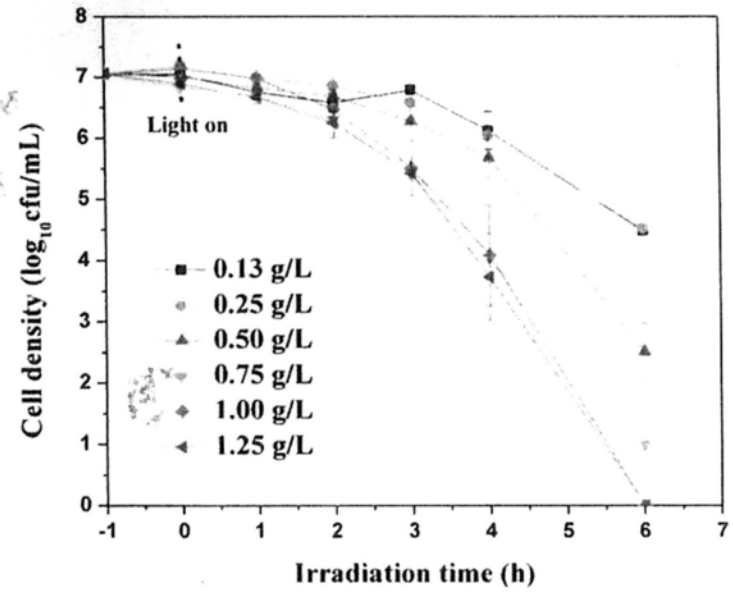

Figure 3.5 Disinfection efficiency of *E. coli* K-12 (1.5×10^7 cfu/mL) at the different concentration of NS under FTs irradiation.

3.3.1.3 The cell density effect

As shown the Figure 3.6, with the decreasing of cell density of *E. coli* K-12, the disinfection efficiency would increase by NS under FTs irradiation. NS could completely inactivate 10^3 cfu/mL *E. coli* K-12 within 1 h treatment. However, to compare the disinfection efficiency with some synthetic VLD photocatalysts, such as S-doping TiO_2 (Yu *et al.*, 2005) and Ag-coating TiO_2 (Zhang *et al.*, 2003), the similar cell density to them was chosen, which was about 10^7 cfu/mL.

3.3.2 Photocatalytic disinfection performance

After optimization the physicochemical conditions of disinfection, the photocatalytic disinfection of 1.5×10^7 cfu/mL *E. coli* K-12 by 1 g/L NS after 1 h adsorption of them

under FTs irradiation was studied. In dark, light and negative controls, the bacterial population remained constant after 6 h (Figure 3.7). When NS was irradiated by FTs, it exhibited high bactericidal activity, and total inactivation of *E. coli* K-12 was observed after 6 h treatment (Figure 3.7). Because the FTs emit not only VL but also trace amounts of UV (Table 3.2), to confirm that NS was a true VLD photocatalyst and the disinfection of *E. coli* K-12 was not due to UV photocatalysis, a sodium nitrite filter was placed between the light source and the flask to block all UV emission to ensure that the observed NS disinfection performance was only due to VL photocatalysis. When the liquid filter was used, the intensity of VL decreased to 2.7 mW/cm^2 and no measurable UV intensity was detected (Table 3.2). Under such conditions, total inactivation was achieved with 8 h of VL irradiation (Figure 3.8).

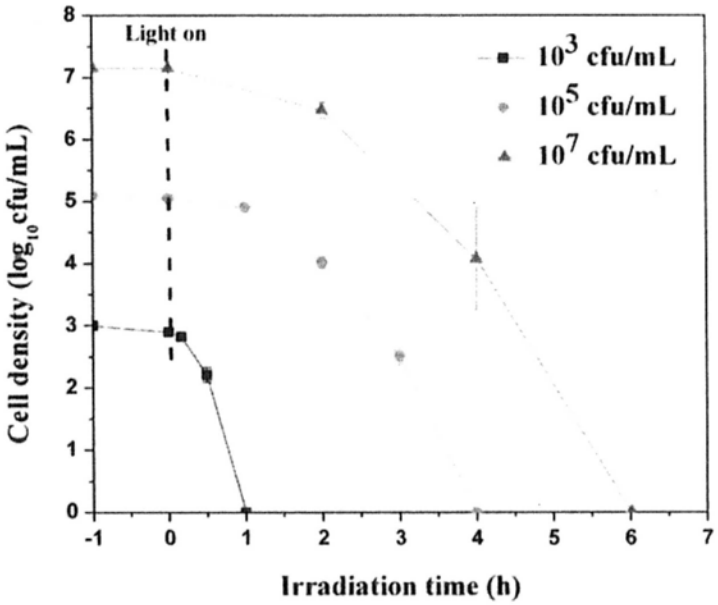

Figure 3.6 Photocatalytic disinfection of different cell density of *E. coli* K-12 by NS under FTs irradiation.

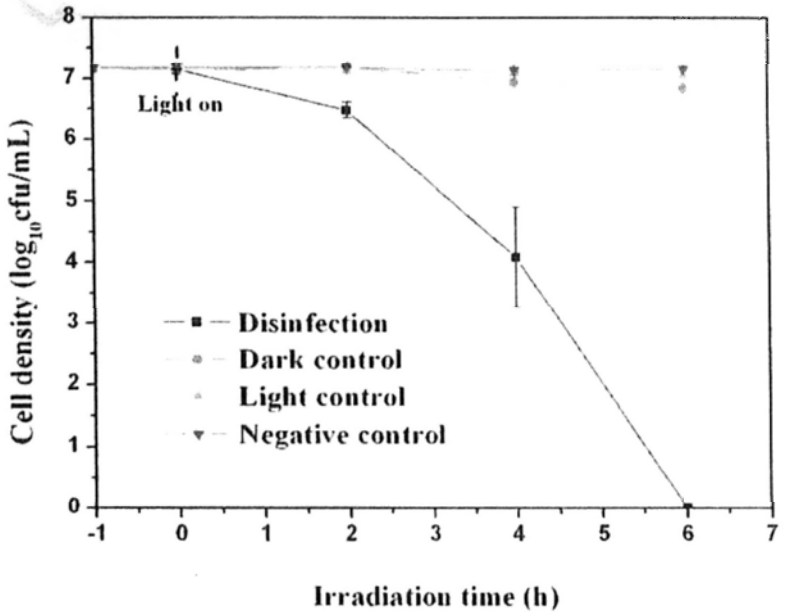

Figure 3.7 Photocatalytic disinfection of *E. coli* K-12 by NS under FTs irradiation. Experimental conditions: Photocatalyst concentration = 1 g/L; *E. coli* K-12 concentration = 1.5×10^7 cfu/mL; Dark control: 1 g/L NS at dark; Light control: saline solution under FTs; Negative control: saline solution at dark.

Table 3.2 The intensity of different domains of light sources.

Intensity (mW/cm^2)	UVA (315-400 nm)	UVB (280-315 nm)	UVC (200-280 nm)	VL (400-800 nm)
Fluorescence (no filter)	0.03	0.015	0.006	3.3
Fluorescence (liquid filter)	0	0	0	2.7
UVA lamp	0.03	0.05	0.01	–*

*Not applicable

To further confirm that 2.8 log-reduction of cell density using liquid filter compared with no filter at 6 h treatment was due to the decreasing intensity of VL or the effect of the UV domain of FTs, the disinfection effect of *E. coli* K-12 by NS under UVA lamps was studied (Figure 3.8). The intensity of UVA lamps (Table 3.2) was a little higher than the UV domain of FTs. The results shows that there was only a 0.7 log-reduction in the vial cells count obtained under UVA lamps irradiation after 6 h, which was lower than 2.8 log-reduction of cell density.

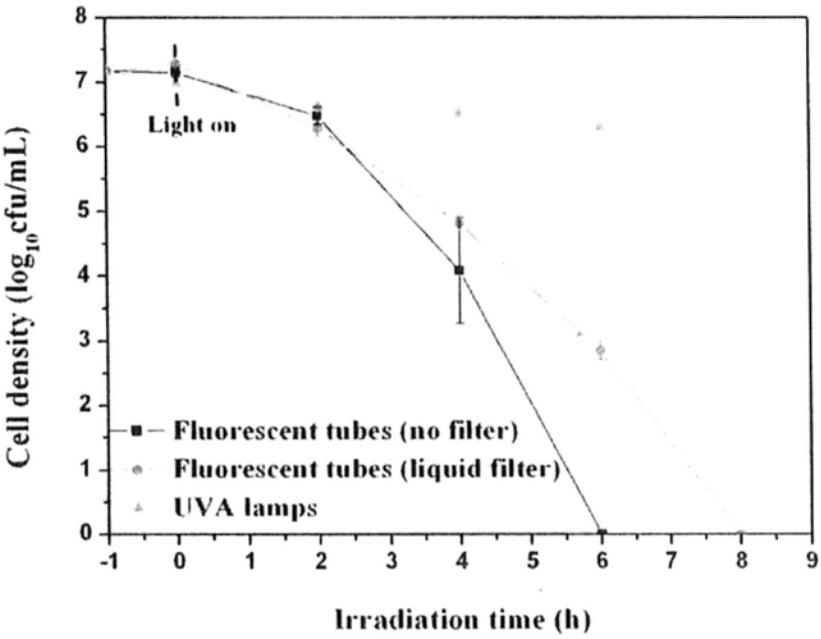

Figure 3.8 Disinfection efficiency of *E. coli* K-12 by NS using FTs (without and with a liquid UV filter) and UVA irradiation.

3.3.3 Photocatalytic disinfection mechanism

3.3.3.1 Optimization the concentrations of each scavenger

Photocatalysis is known to produce several reactive species ($^{\bullet}OH$, H_2O_2, $^{\bullet}O_2^-$, h^+, and e^-) that are potentially involved in the disinfection of bacterial cells. To determine which reactive species were involved in the photocatalytic disinfection process, different scavengers were used to remove the respective reactive species. KI was used to remove h^+ and $^{\bullet}OH_{ads}$ (Chen *et al.*, 2005), isopropanol to remove $^{\bullet}OH_{free}$ into the solution (Chen *et al.*, 2005; Khodja *et al.*, 2005), 4-hydroxy-2,2,6,6-tetramethylpiperidinyloxy (TEMPOL) to remove $^{\bullet}O_2^-$ (Lejeune *et al.*, 2006), Cr(VI) to remove e^- (Chen *et al.*, 2005), and Fe(II) to remove H_2O_2 (Zhang *et al.*, 2010).

The low concentration of scavengers could not remove all the relative species, and the excess concentration of scavengers would exhibit toxic effect on bacterial cells. Based on this information, the concentration of each scavenger was optimized to make sure the amount of scavengers was the maximum concentration and did not exhibit toxicity to bacterial cells. For h^+ and $^{\bullet}OH_{ads}$, increasing the concentration of KI to 50 mM, the photocatalytic inactivation efficiency was almost kept constantly as that at low concentration (5 mM) (Figure 3.9). In addition, the dark and light controls show that 5 mM of KI did not show toxic to bacterial cells. Thus, the optimal concentration of KI was 5 mM. The result of isopropanol was similar to that of KI, and the optimal concentration was 0.5 mM (Figure 3.10). For e^- scavenger, decreasing the concentration of Cr(VI) from 0.05 to 0.01 mM, the disinfection efficiency increased, suggesting that the amount of Cr(VI) was not enough to remove all the e^-. While

increasing the concentration of Cr(VI) to 0.1 mM, the photocatalytic inactivation efficiency was almost kept constant (Figure 3.11). So, the concentration of Cr(VI) was fixed at 0.05 mM. The result of Fe(II) was similar to that of Cr(VI), and the optimal concentration was 0.1 mM (Figure 3.12).

3.3.3.2 Scavenger effect in the non-partition system

The control experiments show that the addition of these scavengers did not result in any toxic effect to *E. coli* K-12 within 6 h (Figure 3.13B). Without the addition of a scavenger, the complete disinfection of *E. coli* K-12 was achieved in a 6 h treatment. When Fe(II) (H_2O_2 scavenger) was added, the cell density was reduced to 1×10^5 cfu/mL without H_2O_2 (Figure 3.13A), indicating that H_2O_2 is strongly involved in photocatalytic disinfection. In the presence of Cr(VI) (e^- scavenger), the cell density only decreased to 5×10^5 cfu/mL (Figure 3.13A), which suggests that e^- also plays an important role in the disinfection process. In the presence of KI (h^+ and $^{\bullet}OH_{ads}$ scavenger), isopropanol ($^{\bullet}OH_{free}$ scavenger), or TEMPOL ($^{\bullet}O_2^-$ scavenger), the level of bactericidal effect did not change much compared with the change when no scavenger was added (Figure 3.13A), indicating that h^+, $^{\bullet}OH_{free}$, $^{\bullet}OH_{ads}$, and $^{\bullet}O_2^-$ are not strongly involved in photocatalytic disinfection in this system.

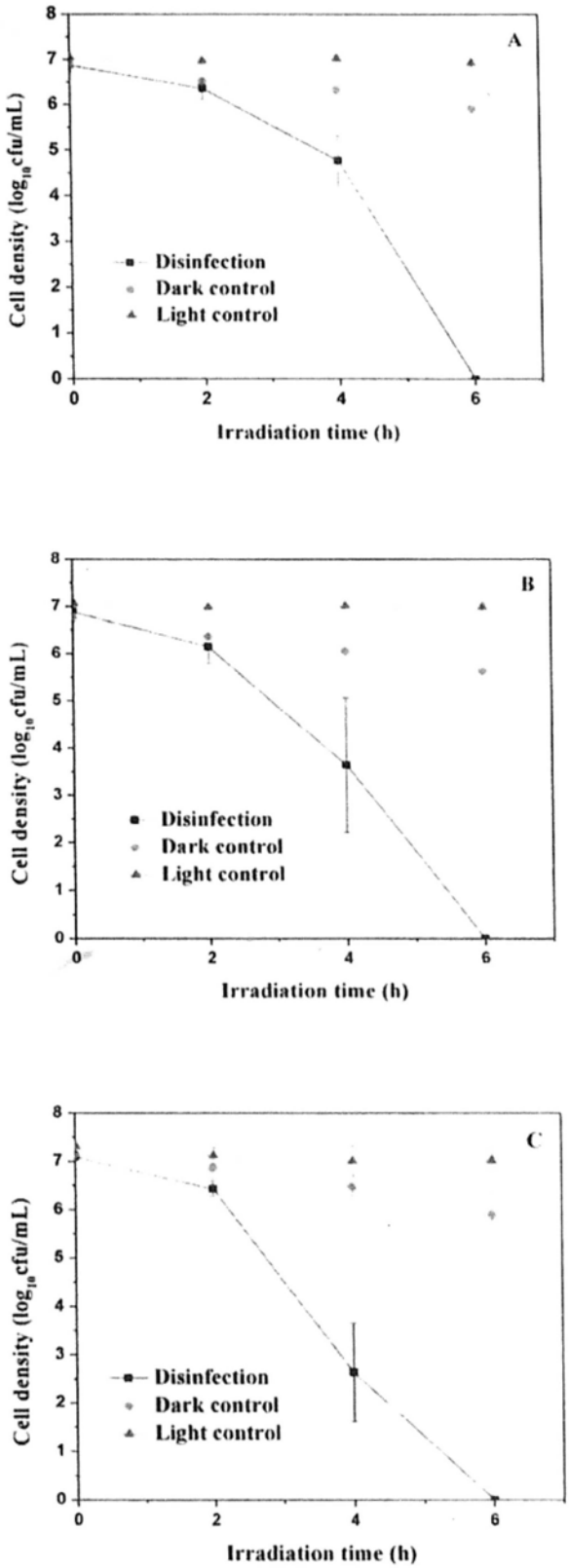

Figure 3.9 Disinfection efficiency of *E. coli* K-12 by NS under FTs irradiation with different concentrations of KI. (A) 5 mM, (B) 10 mM, and (C) 50 mM.

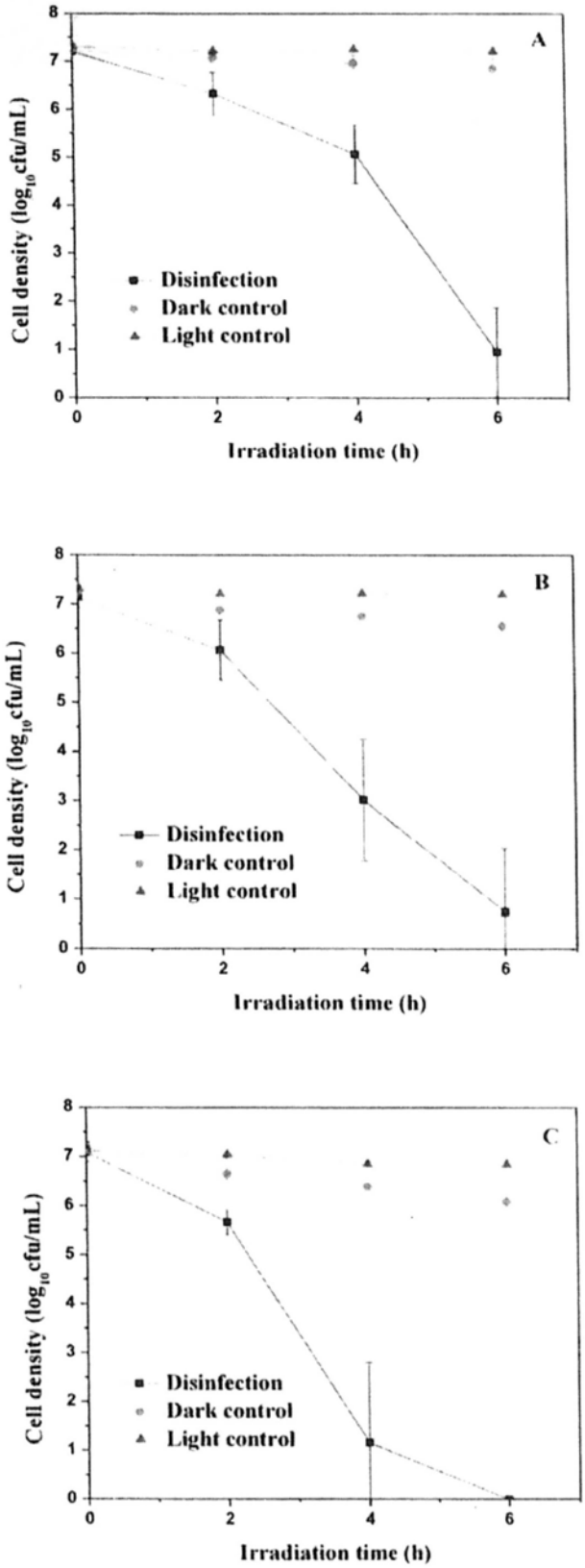

Figure 3.10 Disinfection efficiency of *E. coli* K-12 by NS under FTs irradiation with different concentrations of isoproponal. (A) 0.5 mM, (B) 5 mM, and (C) 50 mM.

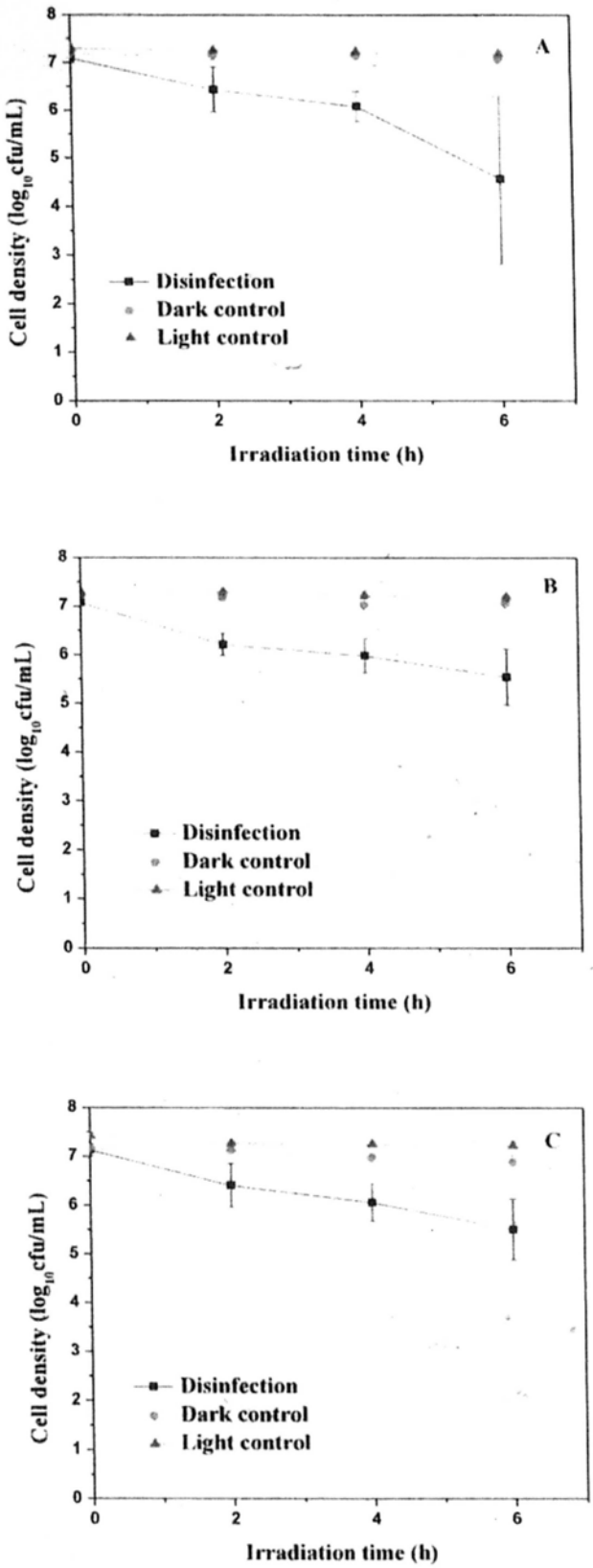

Figure 3.11 Disinfection efficiency of *E. coli* K-12 by NS under FTs irradiation with different concentrations of Cr(II). (A) 0.01 mM, (B) 0.05 mM, and (C) 0.1 mM.

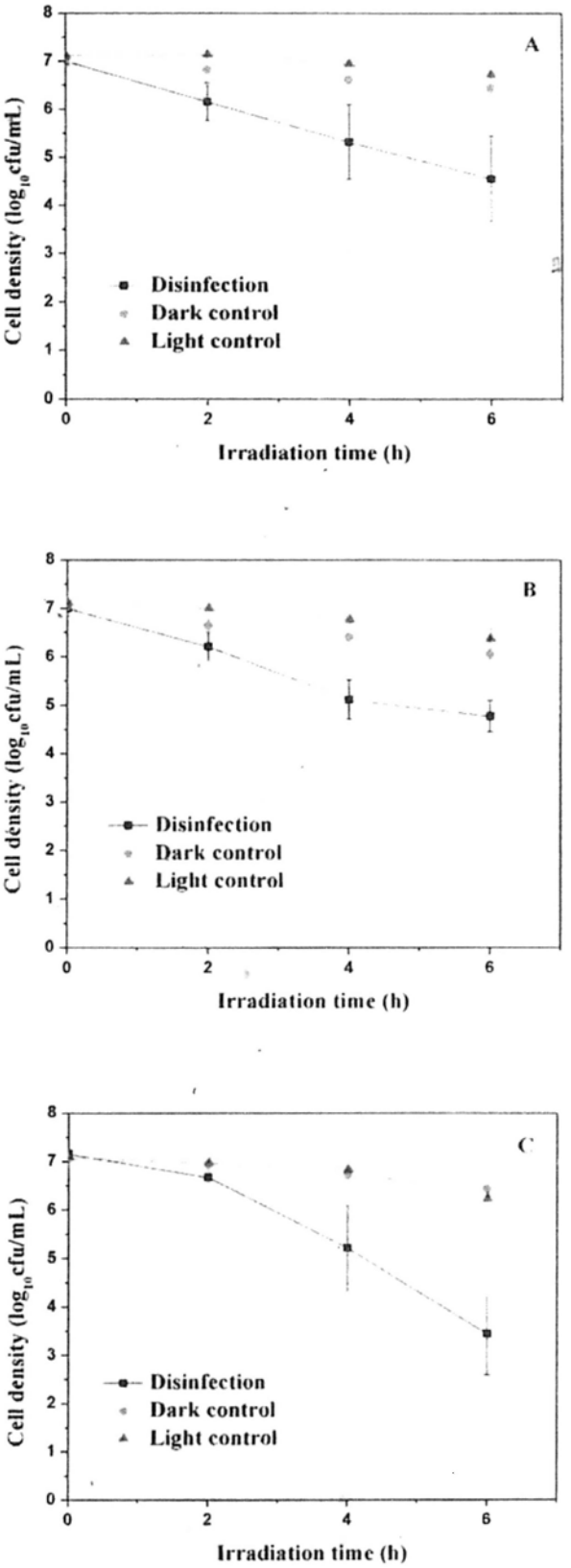

Figure 3.12 Disinfection efficiency of *E. coli* K-12 by NS under FTs irradiation with different concentrations of Fe-EDTA. (A) 0.05 mM, (B) 0.1 mM, and (C) 0.5 mM.

To further clarify whether e^- plays an important role in photocatalytic disinfection, quadruple scavengers, namely KI, isopropanol, Fe(II), and TEMPOL, were employed to remove the h^+, $^{\bullet}OH_{ads}$, $^{\bullet}OH_{free}$, H_2O_2, and $^{\bullet}O_2^-$ simultaneously (Figure 3.13A), so that only e^- was left in the disinfection system. Interestingly, the presence of e^- resulted in a 5-log decrease in cell density after 6 h of treatment (Figure 3.13A), which indicates that e^- is a powerful reactive specie for disinfecting *E. coli* K-12. This is probably due to the positioning of the conduction band of NS at a much more negative potential (-1.4 V vs. SCE) (Zang *et al.*, 1995), which gives e^- the energy to inactivate bacterial cells.

To further confirm the role of e^-, the photocatalytic disinfection of *E. coli* K-12 was conducted under anaerobic conditions (the reactor was sealed after 30 min of purging with argon (Ar) gas to eliminate O_2) in the presence of h^+ scavenger (KI) (Figure 3.13A). In this system, no oxidative radicals were found either on the conduction band or on the valence band, and only e^- was involved in the disinfection. The result shows that the disinfection efficiency was higher under anaerobic than under aerobic conditions, which further confirms the involvement of e^- in photocatalytic disinfection by NS under FTs irradiation.

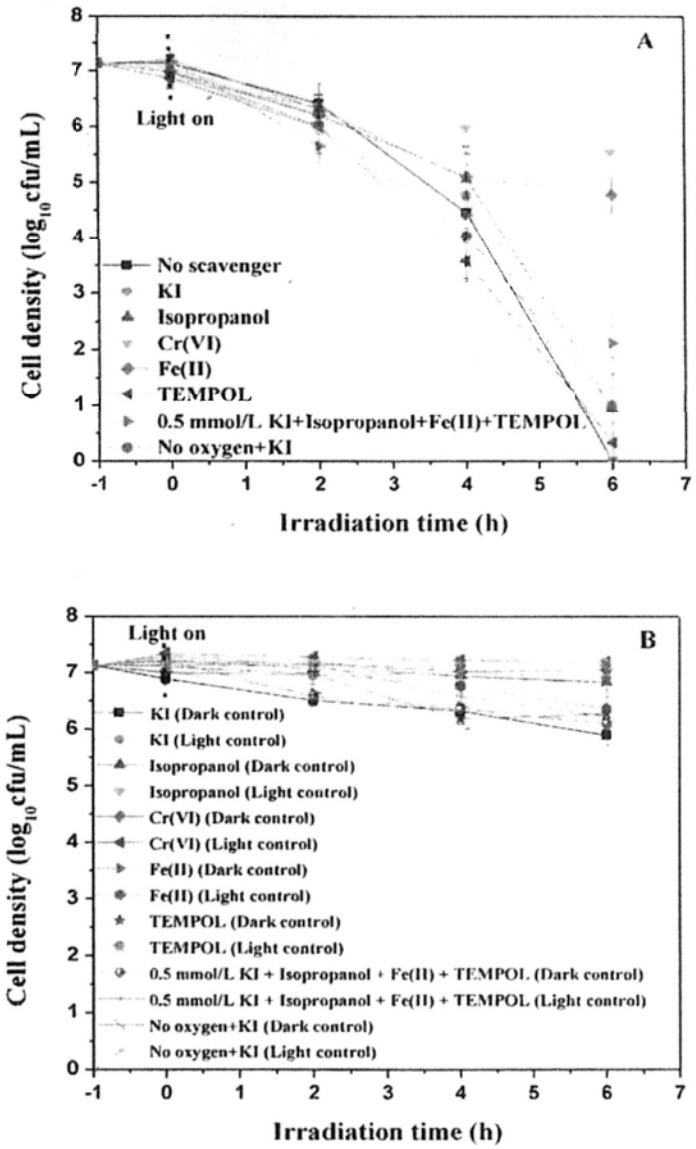

Figure 3.13 Disinfection efficiency of *E. coli* K-12 by NS under FTs irradiation with different scavengers. (A) Photocatalytic disinfection, and (B) Dark and light controls. Experimental conditions: Photocatalyst concentration = 1 g/L; *E. coli* K-12 concentration = 1.5×10^7 cfu/mL; KI concentration = 5 mmol/L; Isopropanol concentration = 0.5 mmol/L; Cr (VI) concentration = 0.05 mmol/L; Fe(II)-EDTA concentration = 0.1 mmol/L; TEMPOL concentration = 2 mmol/L.

3.3.3.3 Scavenger effect in the partition system

To further determine the role of H_2O_2 in disinfection, we conducted a photocatalytic disinfection of *E. coli* K-12 using a partition system (Kikuchi *et al.*, 1997; Zhang *et al.*, 2009b, 2010). As shown in Plate 3.6, the *E. coli* K-12 suspension was injected into a semipermeable membrane container and NS suspension was dispersed outside of the container. The molecular weight cut-off (MWCO) of the semipermeable membrane was 12-14×10^3 Daltons, which only allowed smaller molecules such as $^{\bullet}OH_{free}$ and H_2O_2 to freely enter. The larger targets, such as NS (particle sizes < 40 μm) and *E. coli* K-12 (which has a molecular weight of about 2.6×10^6 Daltons), cannot pass through the membrane. Figure 3.14 shows the disinfection efficiency of *E. coli* K-12 inside the membrane container when the outside system was placed under different conditions. For the light and negative controls, the bacterial population showed no change after 6 h of treatment, which indicates no toxic effect of light or the membrane on the cells. In the presence of NS without light irradiation (dark control), only a 1.7-log reduction of *E. coli* K-12 was observed (Figure 3.14), which was probably due to adsorption between the membrane and the cells of *E. coli* K-12. Interestingly, the complete inactivation of *E. coli* K-12 was observed after 6 h of treatment when the outer system was NS suspension irradiated by FTs (Figure 3.14).

The experiment has been carried out to prove the adsorption between the membrane and bacterial cells in the presence of NS. In non-partition system, one layer of semipermeable membrane was added in the solution of 1.5×10^7 cfu/mL *E. coli* K-12

and 1 g/L NS. After 6 h mixing without light irradiation, there were only 2.5-log bacterial cells in the solution (Figure 3.15). Then the membrane was picked out, put it into pure water, sonicated it for 30 min and then spread the sample on the plate to count the colony of bacterial cells. The results show that there were 1×10^6 cfu/mL cells on the membrane, which suggests bacterial cells are adsorbed onto the membrane.

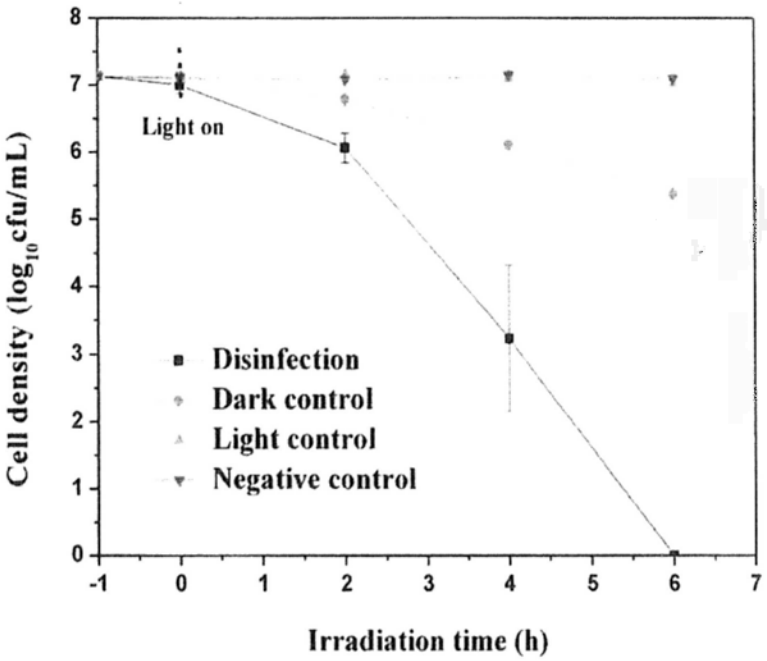

Figure 3.14 Photocatalytic disinfection of *E. coli* K-12 (1.5×10^7 cfu/mL) inside a semipermeable packaged container and outside of the membrane is NS suspension (1 g/L) under FTs irradiation.

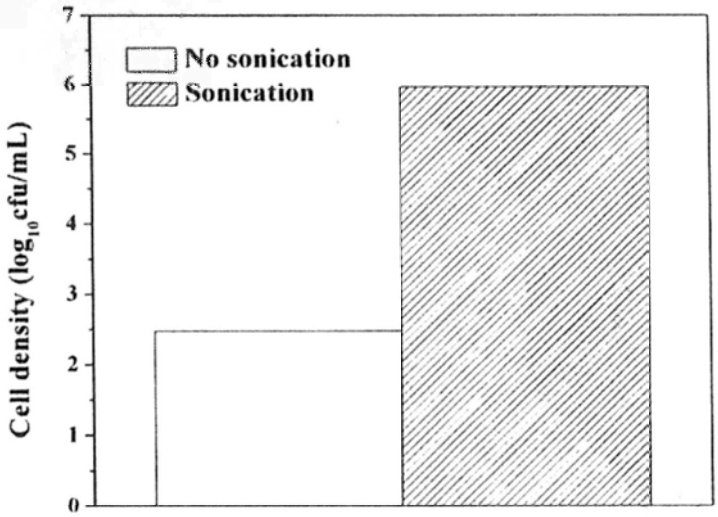

Figure 3.15 The adsorption between the membrane and bacterial cells in the presence of NS.

To find out which diffusing reactive species ($^{\bullet}OH_{free}$, H_2O_2 or both) are involved in the disinfection process in the partition system, different scavengers were added into the outside of the membrane container to remove the respective reactive species. As shown in Figure 3.16B, the dark control shows an approximately 1.5-log reduction in disinfection, which was similar to the result of the dark control with no scavenger in the partition system (Figure 3.14), and indicates that none of the scavengers are toxic to the cells. The addition of KI (h^+ and $^{\bullet}OH_{ads}$ scavenger) (Figure 3.16A) did not change the level of bactericidal performance from that when no scavenger was involved, which demonstrates that reactive species bound to the surface of the photocatalyst are not involved in the partition system or in the slurry system. When isopropanol (scavenger for $^{\bullet}OH_{free}$) was added, no obvious decrease in photocatalytic

disinfection efficiency was observed compared with no scavenger (Figure 3.16A), which suggests that $^{\bullet}OH_{free}$ is also not involved in the bactericidal effect in this partition system. In the presence of TEMPOL ($^{\bullet}O_2^-$ scavenger), there was about a 4-log reduction in cell density after 6 h irradiation. This decrease in disinfection efficiency was probably not due to the disinfection effect of $^{\bullet}O_2^-$, but to the inhibition effect of H_2O_2 produced because of the removal of $^{\bullet}O_2^-$ by the scavenger.

The addition of Fe(II), which is the scavenger for H_2O_2, suppressed the bactericidal effect (Figure 3.16A). This result was similar to that in the non-partition system (Figure 3.13A), which indicates that H_2O_2 plays an important role in both partition and non-partition systems in the photocatalytic disinfection of *E. coli* K-12.

In the partition system (Figure 3.16A), there was about a 5-log reduction in cell density in the presence of Cr(VI) (e^- scavenger) after 6 h of irradiation, which suggests that e^- is not strongly involved in the disinfection in this system. In the non-partition system (Figure 3.13A), there was a slight decrease in cell density after the removal of e^- by adding Cr(VI) due to the important disinfecting role of e^-. In the partition system, the cell density was greatly reduced after adding Cr(VI) because of the lack of disinfection effect of e^-. Quadruple scavengers (KI, isopropanol, Fe(II), and TEMPOL) simultaneously were also added to study the role of e^- in the partition system. The results show that cell density decreased by 2-log (Figure 3.16A), and were similar to that of the dark control (Figure 3.16B), which indicates that e^- is probably not

involved in disinfection in the partition system.

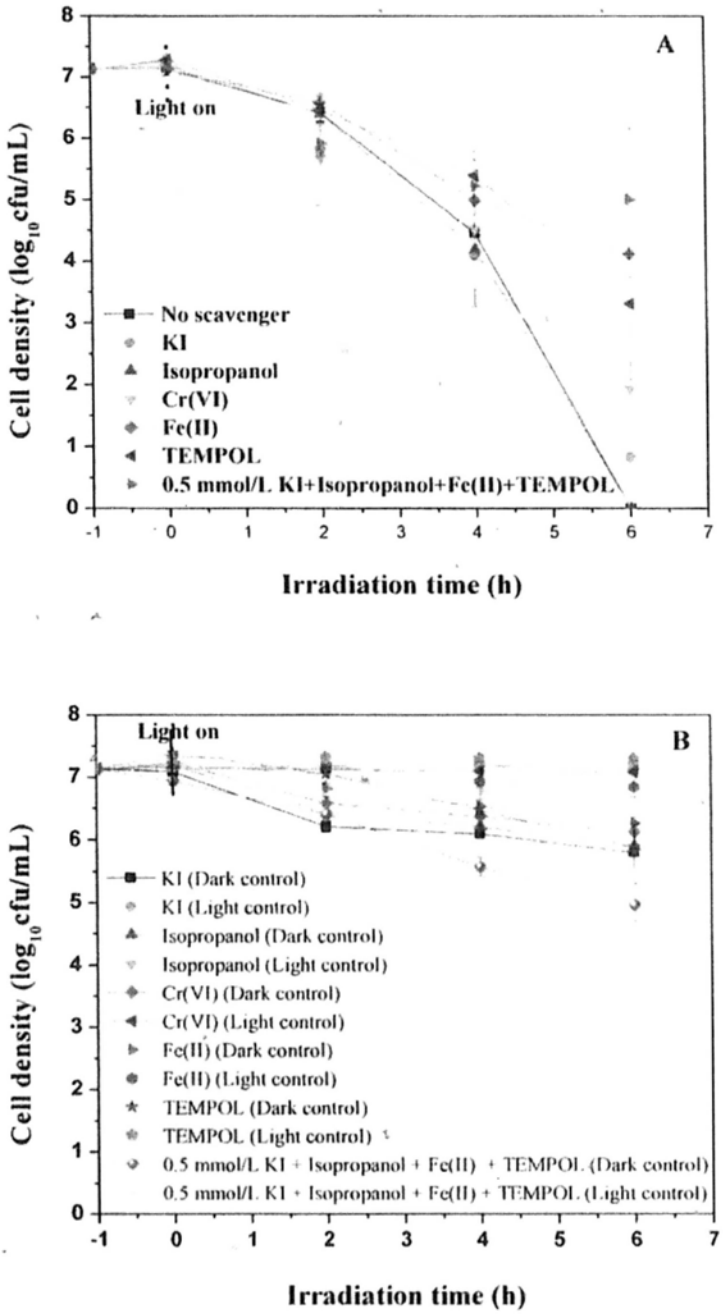

Figure 3.16 Disinfection efficiency of *E. coli* K-12 by NS in partition system under FTs irradiation with different scavengers. (A) Photocatalytic disinfection, and (B) Dark and light controls.

3.3.4 Analysis of reactive species

3.3.4.1 Analysis of hydrogen peroxide

H_2O_2 produced by NS was further determined by a photometric method using POD (Bader *et al.*, 1988). Figure 3.17 shows the absorbance (at 551 nm) of H_2O_2 against irradiation time in the non-partition and partition systems, and clearly demonstrated that H_2O_2 was accumulated in both systems.

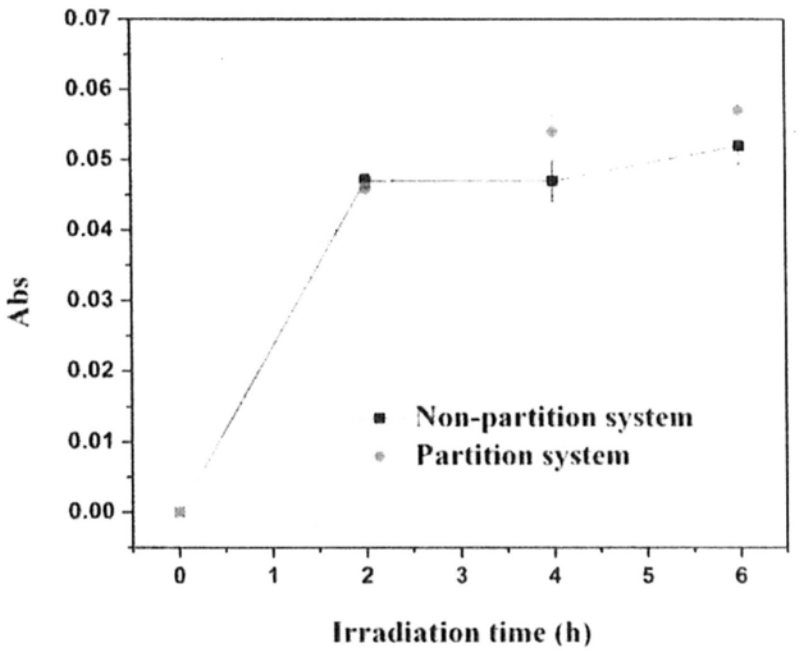

Figure 3.17 Absorption intensity (551 nm) of DPD/POD reagent after reaction with H_2O_2 against illumination time in the non-partition and partition systems.

3.3.4.2 Analysis of hydroxyl radical

To study whether $^{\bullet}OH$ involved in the photocatalytic disinfection, terephthalic acid was used as a probe molecule to detect the formation of $^{\bullet}OH$ of NS under FTs irradiation. Because FTs could emit trace amounts of UVA, UVB and UVC, which were sufficient to irradiate P25 TiO_2 to produce $^{\bullet}OH$ and inactivate bacterial cells

(Leung *et al.*, 2008). For comparison, the P25 TiO_2 irradiated by FTs was also studied under the same condition.

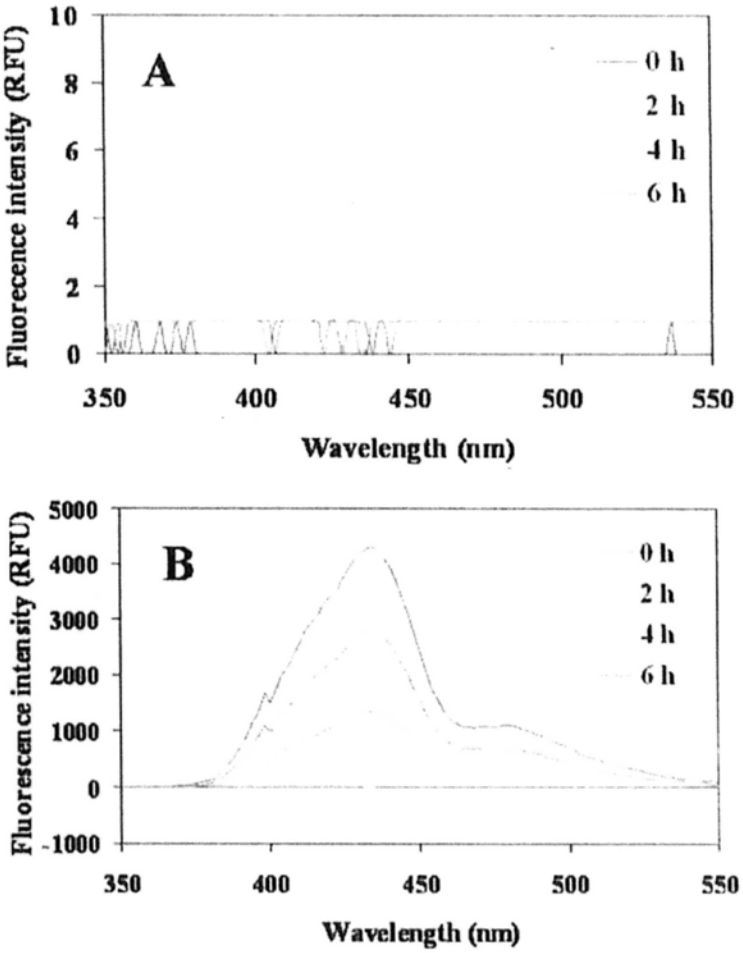

Figure 3.18 Fluorescence emission spectral changes observed during the FTs irradiation of (A) NS, and (B) A P25 TiO_2 suspension in a 4×10^{-4} mol/L terephthalic acid and 2×10^{-3} mol/L NaOH (excitation at 315 nm). The fluorescent spectra were recorded every 2 h.

Figure 3.18 shows fluorescence emission spectral changes observed during the FTs illumination of NS and P25 TiO_2 suspension in a 4×10^{-4} mol/L terephthalic acid and 2×10^{-3} mol/L NaOH (excitation at 315 nm). The results show that no emission peak at

425 nm was observed in the NS-FTs system (Figure 3.18A), which was similar with the results of synthetic ZnS-UV system (Yu *et al.*, 2009). This indicates that no $^{\bullet}OH$ is detected in the NS-FTs system. However, in the case of P25 TiO_2-FTs (Figure 3.18B), a gradual increase peak signal at about 425 nm was observed with irradiation time increasing, which indicates the production of $^{\bullet}OH$.

3.3.4.3 Analysis of superoxide radical

The ESR technique was used to measure $^{\bullet}O_2^-$ involved in irradiated NS suspension. Figure 3.19 shows the ESR spectrum recorded at ambient temperature in NS suspension under FTs irradiation. It was found that there was no $^{\bullet}O_2^-$ signal peak detected.

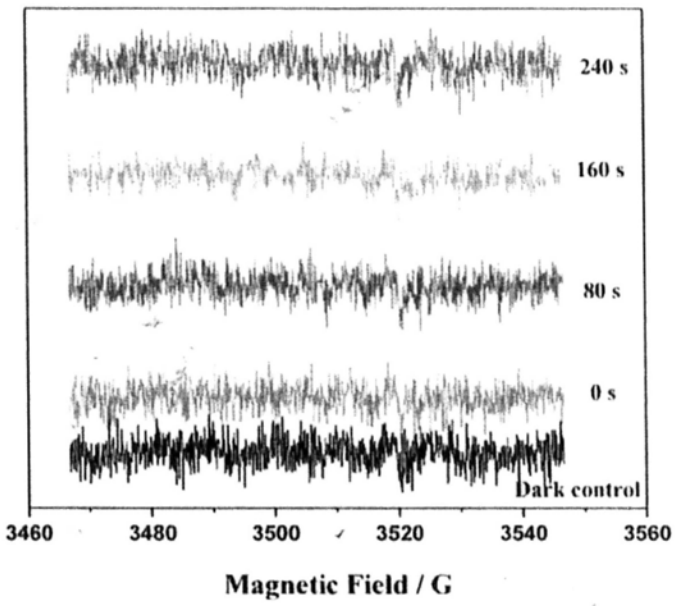

Figure 3.19 DMPO spin-trapping ESR spectra recorded at ambient temperature in methanol dispersion (for DMPO- $^{\bullet}O_2^-$) under FTs irradiation of NS.

3.3.5 Transmission electron microscopy

To further confirm the destruction process of *E. coli* K-12 by e^- or H_2O_2 produced by NS irradiated by FTs, the changes of cell morphology of *E. coli* K-12 during photocatalytic disinfection were studied by TEM.

3.3.5.1 Electron disinfection effect

Figure 3.20 shows e^- disinfection effect after the addition of quadruple-scavengers (KI, isopropanol, Fe(II), and TEMPOL) at different stages of photocatalytic disinfection. In the initial stage of disinfection, *E. coli* K-12 exhibited an intact cell structure and an obvious cell wall (Figure 3.20A). After 6 h of irradiation treatment (Figure 3.20B), an electron translucent region appeared at the center of the cell, indicating that the outer membrane of the cell is damaged and thus a leakage of the interior components has occurred. After 12 h of treatment (Figure 3.20C), the cell had lost most of its interior components and the cell wall was partially destroyed, which suggests that the attack by e^- of the bacteria starts from the outer membrane and then progresses to the cell wall. Eventually, as the irradiation time was extended to 30 h (Figure 3.20D), the cell became increasingly translucent and the cell wall was largely destroyed, indicating the complete destruction of *E. coli* K-12.

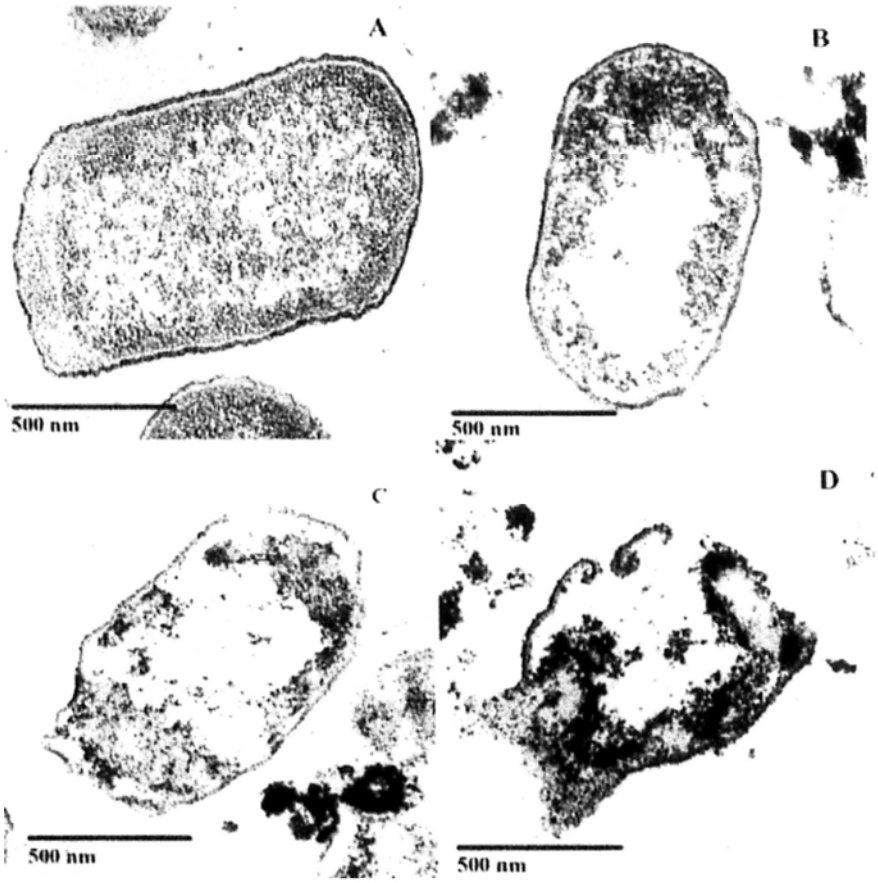

Figure 3.20 TEM images of *E. coli* K-12 photocatalytically treated with NS under FTs irradiation adding quadruple scavengers (KI, isopropanol, Fe(II) and TEMPOL). (A) 0 h, (B) 6 h, (C) 12 h, and (D) 30 h.

3.3.5.2 Hydrogen peroxide disinfection effect

In order to further confirm the destruction process of *E. coli* K-12 by H_2O_2 produced by NS irradiated by FTs, the morphology of *E. coli* K-12 was studied by TEM in the partition system (Figure 3.21). At the very beginning of disinfection, *E. coli* K-12 exhibited an intact structure of cell and an obvious cell wall (Figure 3.21A). After 6 h irradiated treatment (Figure 3.21B), an electron translucent region appeared at the centre of the cell, which indicates a leakage of the interior component. After 12 h of treatment (Figure 3.21C), cell lost most of the interior component and the cell wall

was partly destroyed. Eventually, with the irradiation time prolonging to 30 h (Figure 3.21D), the cell became more and more translucent and the cell wall was greatly ruptured, which indicates a complete destruction of *E. coli* K-12.

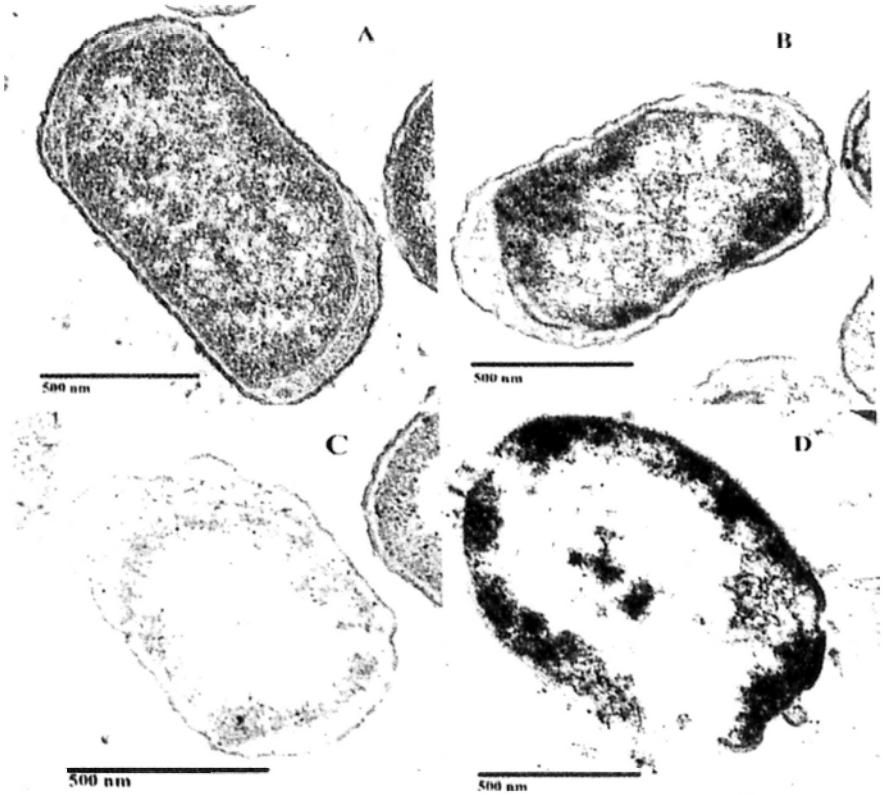

Figure 3.21 TEM images of *E. coli* K-12 photocatalytically treated with NS under FTs irradiation in the partition system (A) 0 h, (B) 6 h, (C) 12 h, and (D) 30 h.

Surprisingly, the e^- effect (Figure 3.20) was similar to the effect of H_2O_2 in the partition system (Figure 3.21). At present, it is confirmed that e^- produced by NS plays an important role in disinfection, but the details of the mechanism of inactivation by e^- remain unknown. The TEM images suggest that the mechanism by which e^- disinfects bacterial cells is similar to that of H_2O_2. However, further investigation is needed to explain why e^- induced bacterial cell damage is similar to damage induced by H_2O_2.

3.3.6 Photocorrosion and reuse of natural sphalerite

The experiment to determine the photocorrosion of NS by the irradiation of FTs used in this study was investigated. The stability of NS was assessed with the released amount of Zn^{2+} in solution resulting from dissolution or photocorrosion by AAS analysis. The results show that NS in the solution of pH 6.8 (the reaction pH used in this study) was much stable and there was almost no photocorrosion (i.e. no Zn^{2+} released into the solution within 10 h irradiation by the FTs).

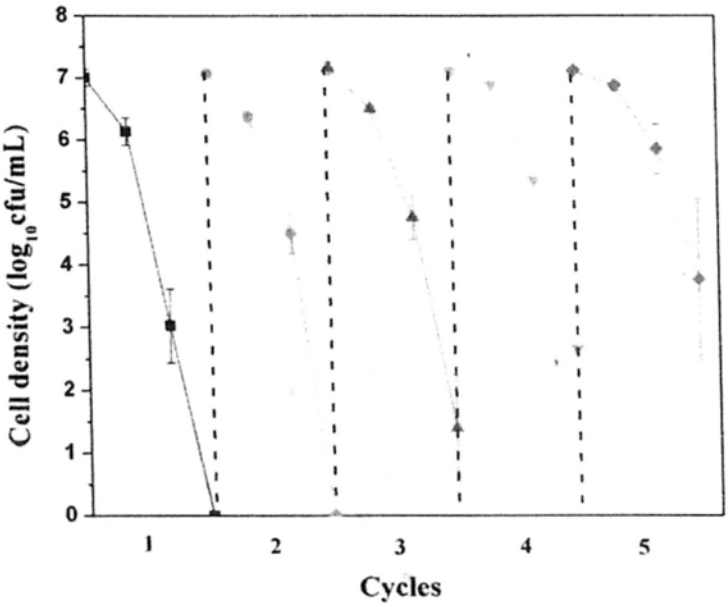

Figure 3.22 Effect of recycling of NS on the photocatalytic disinfection of *E. coli* K-12 in the partition system.

To investigate the reusability of NS in the photocatalytic disinfection, the durability test was carried out in partition system. The photocatalytic disinfection of *E. coli* K-12 in every cycle was shown in the following Figure 3.22. The total inactivation of *E. coli* K-12 by NS within 6 h irradiation was maintained for 2th cycle. And then the

disinfection efficiency decreased with the increasing the reuse cycle. There was about 4-log cell density reducing in the 5th cycle.

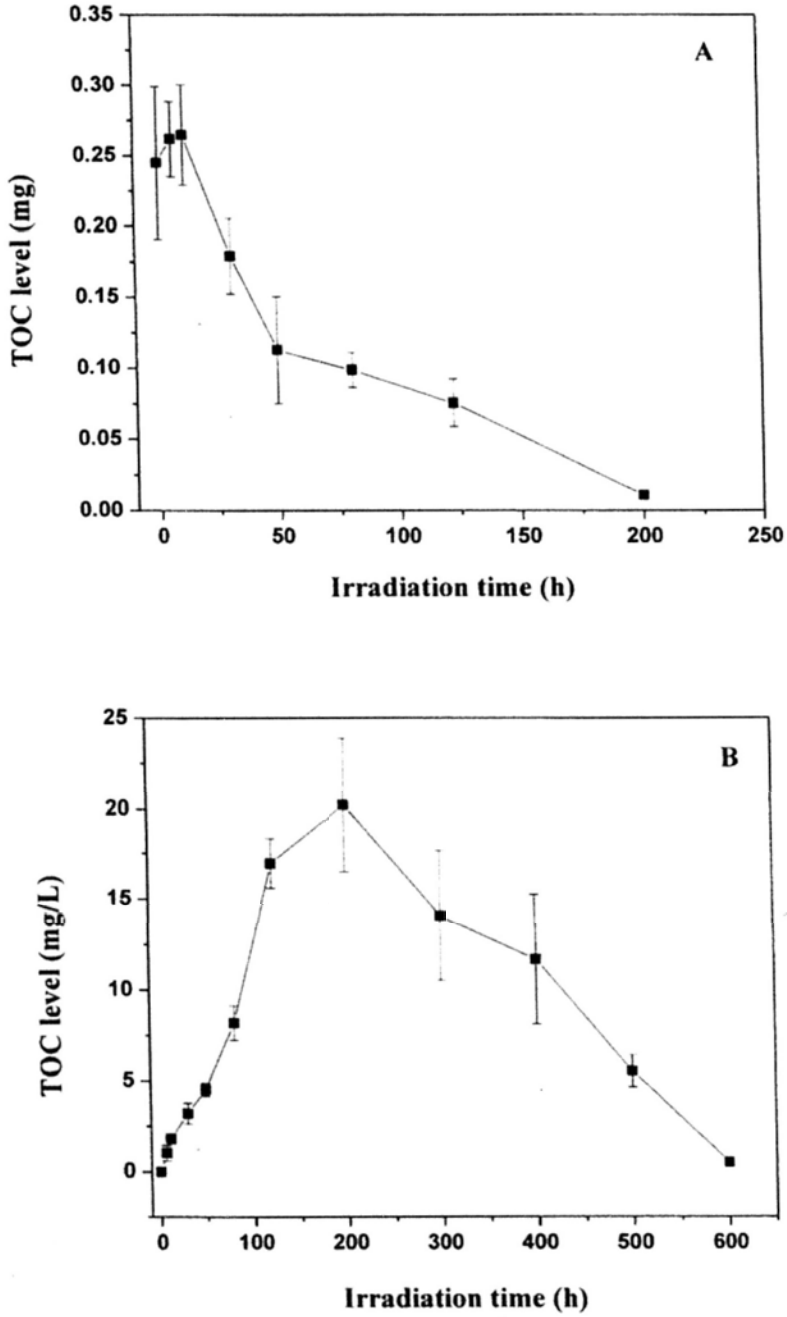

Figure 3.23 The TOC content of *E. coli* K-12 under (A) Solid-phase, and (B) Liquid-phase measurement during photocatalytic disinfection. Experimental condition: Photocatalyst concentration = 1 g/L; *E. coli* K-12 concentration = 1.5×10^{8} cfu/mL.

3.3.7 Total organic carbon analysis

TOC analysis on photocatalytic disinfection of *E. coli* K-12 by NS under FTs irradiation was conducted. In solid-phase measurement, TOC level gradually dropped from 0.27 to 0 mg after 200 h disinfection treatment (Figure 3.23A). For liquid-phase analysis, the time for complete mineralization of organic carbon was much longer than solid-phase. TOC level rapidly increased from 0 to 200 h, and then gradually drop to undetectable TOC level at 600 h (25 d).

3.4 Discussion

3.4.1 Optimization the physicochemical conditions of disinfection

To investigate the photocatalytic disinfection efficiency and mechanism of *E. coli* K-12 with NS under FTs irradiation, the optimal physicochemical conditions of inactivation were first determined, including the optimal adsorption time, the optimal concentration of NS and the cell density of bacterial cells.

Firstly, because the photoexcited e^- and h^+, from which the ROSs are produced, locate on the surface of the photocatalyst, some researchers suggest that the adsorption capacities of the photocatalyst and pollutants are significant for the photocatalytic degradation of organic pollutants and decolorization of azo dyes (Fu *et al.*, 2005; Zhang *et al.*, 2009). However, the most interesting question whether the direct contact between the bacterial cells and photocatalyst is a prerequisite for the efficient inactivation of bacterial cells during the photocatalysis, is still not answered. To solve

this problem, the effect of adsorption time on the photocatalytic disinfection efficiency is investigated. The result shows the adsorption of NS onto *E. coli* K-12 needed some time (Figure 3.3) and the equilibrium adsorption time between bacterial cells and photocatalyst had significant effect on the photocatalytic disinfection efficiency (Figure 3.4), which suggests that the reactive species produced on the surface of NS play important roles in the disinfection of bacterial cells.

Secondly, the concentration of the photocatalyst is another important parameter to influence the photocatalytic disinfection efficiency. The results revealed that along with the increasing the amount of the photocatalyst, the efficiency of inactivation also increased due to more reactive species produced during the photocatalytic process (Figure 3.5). However, a detrimental effect was noticed when further increase in the concentration of the photocatalyst. There are several explanations for this detrimental effect. Reddy *et al.* (2008) revealed that high amount of photocatalyst might increase the turbidity of solution which would reduce the penetration of light irradiation and thus produced less amount of reactive species, that eventually leaded to the decrease in bactericidal efficiency. Benabbou *et al.* (2007) found the greater the amount of photocatalyst, the more it formed several layers on the bacterial outer membrane. Thus there would be increasingly limited reactive species diffusion to the bacterial cells. As a consequence, more e^- would quickly recombine with the positive h^+, and eventually decreased the disinfection efficiency. Based on this information, the optimal amount of NS was fixed at 1 g/L (Figure 3.5).

Finally, at high cell density of bacteria (10^7 cfu/mL), NS showed good photocatalytic disinfection efficiency under FTs irradiation (Figure 3.6). For the water purification, the concentration of bacterial cells is only 10^2 cfu/mL, which is much lower than 10^7 cfu/mL. Thus, the photocatalytic disinfection of NS irradiated by FTs will be also effective at realistic pathogen concentration lower than 10^2 cfu/mL (Figure 3.6).

3.4.2 Photocatalytic disinfection performance

The results of all of the control experiments suggest that NS has no toxic effect on bacterial cells and FTs irradiation causes no photolysis in *E. coli* K-12 (Figure 3.7). Moreover, the observed bactericidal effect of NS (Figure 3.8) is not due to UV photocatalysis, and NS is a true VLD photocatalyst.

Compared with UV irradiation alone, such as UVA-TiO_2 system, NS displayed relatively low disinfection efficiency (Figure 3.7). However, although UV light sources can emit high energy irradiation which is highly effective for bacterial disinfection, they are still costly, less easily available and hazardous, and require higher energy consumption. In this study, the FT as the VL source is selected because of its low cost and commonly used for household lighting. Leung *et al.* (2008) compared the TiO_2 photocatalytic disinfection using UVA with FTs irradiation. The results show that complete inactivation of 7-log *Alteromonas alvinellae* was achieved within 20 min for UVA lamp, while 3 h for FTs irradiation. Thus, although TiO_2 is a good efficient photocatalyst, it still displays different disinfection efficiency according

to different light sources. In addition, S-doping TiO_2 (Yu *et al.*, 2005) and Ag-coating TiO_2 (Zhang *et al.*, 2003) are common synthetic VLD photocatalysts. Although these synthetic photocatalysts show high photocatalytic efficiency (1 h) under VL, only small amounts can be synthesized and the synthesized semiconductor modification involves complicated techniques and is thus costly. In contrast, NS occurs in large quantities on the earth's surface and is easily obtained, making it much less costly than synthetic photocatalysts. More importantly, the most common VL sources for synthetic photocatalysts are Xenon lamps and halogen lamps, which have a high light intensity. However, these light sources cannot be widely used in wastewater treatment because of their high cost and high energy consumption. Most importantly, the cheap and large amounts of the natural photocatalysts coupled with 24 h turning on FTs are more facile in the photocatalytic disinfection of bacterial cells. Thus, it is concluded NS shows good photocatalytic efficiency and has more promising than artificial photocatalysts for the photocatalytic disinfection of bacterial cells.

3.4.3 Photocatalytic disinfection mechanism

To find out the exact reactive specie(s) playing important role(s) in the inactivation process, the photocatalytic disinfection of *E. coli* K-12 by NS adding different scavengers is investigated. The scavenger concentration in this project is enough for complete inhibition of inactivation pathway via different specific active species.

In the non-partition system, during the VLD photocatalytic disinfection process mediated by NS, the addition of KI (h^+ and $^{\bullet}OH_{ads}$ scavenger), isopropanol ($^{\bullet}OH_{free}$ scavenger) and TEMPOL ($^{\bullet}O_2^-$ scavenger) did not influence the photocatalytic disinfection efficiency compared with no scavenger added (Figure 3.13A). The positive h^+ and parts of $^{\bullet}OH_{ads}$ and $^{\bullet}OH_{free}$ are produced by the oxidative pathway. While $^{\bullet}O_2^-$ and the others $^{\bullet}OH$ are generated via the reductive pathway. Because the produced $^{\bullet}OH$ and $^{\bullet}O_2^-$ in water is very unstable, it will subsequently undergo facile disproportionation to produce H_2O_2, thus they are not involved in the photocatalytic disinfection in this system. When Fe(II) (H_2O_2 scavenger) and Cr(VI) (e^- scavenger) were added, the photocatalytic disinfection partially inhibited (Figure 3.13A), indicating that H_2O_2 produced on both reductive and oxidative pathways and e^- generated on the reductive pathway are strongly involved in the inactivation.

In order to clarify the function of e^-, quadruple scavengers are used simultaneously to remove all the reactive species except e^-. The results show that e^- could directly decrease the cell density with the light irradiation (Figure 3.13A). Under anaerobic conditions in the presence of h^+ scavenger, there was also only e^- left in the reaction system (Figure 3.13A). But due to no oxygen reacting with photogenerated e^- to produce other reactive species, the amount of e^- is more than that of adding quadruple scavengers. The function of h^+ scavenger is used to inhibit the recombination of e^- and h^+ to further increase the amount of e^-. Under anaerobic condition, the disinfection efficiency is higher than under aerobic condition, which further confirms the role of e^-

in the NS-FTs system.

To further confirm the role of H_2O_2 in disinfection, scavengers coupled with the partition system are used to investigate H_2O_2. As mentioned previously, NS and *E. coli* K-12 are separated by a semi-permeable membrane in the partition system. This means the reactive species on NS surface, such as e^-, h^+, $^{\bullet}O_2^-$, and $^{\bullet}OH_{ads}$, shall not have been involved in the disinfection in the partition system, and only diffusing reactive species, such as $^{\bullet}OH_{free}$ and H_2O_2, can pass through the membrane to inactivate *E. coli* K-12 inside the membrane container. The results (Figure 3.16A) proved that all the reactive species on the surface of the photocatalyst did not play roles in the disinfection. Only addition of Fe(II) (H_2O_2 scavenger) could greatly inhibit the photocatalytic disinfection, suggesting that only H_2O_2 is strongly involved in the inactivation in partition system.

In the partition system, the separation effect by the semipermeable membrane means that *E. coli* K-12 cannot contact with the surface of NS, so the e^- on the surface does not display a bactericidal effect, and only H_2O_2 diffuses through the membrane to inactivate the *E. coli* K-12 inside the membrane container. In the non-partition system, because *E. coli* K-12 contacts the surface and also reacts with NS solution, both e^- and H_2O_2 are likely to be strongly involved in photocatalytic disinfection. This is the first time that the bactericidal effect of e^- has been reported.

3.4.4 Analysis of reactive species

H_2O_2 is directly analyzed photometrically by the DPD/POD method (Figure 3.17), which is commonly used method to detect H_2O_2 during photocatalytic disinfection. These results confirm that H_2O_2 did generate both in the non-partition and partition systems of the NS-FTs system and had more chance to inactivate bacterial cells.

The $^{\bullet}OH$ analysis (Figure 3.18) shows that there was no $^{\bullet}OH$ signal produced in FTs irradiated suspension of NS. The ESR technique is used to examine the generation of $^{\bullet}O_2^-$ during the photocatalytic disinfection process. No $^{\bullet}O_2^-$ signal was detected under FTs irradiation (Figure 3.19). These facts indirectly confirm that $^{\bullet}OH$ and $^{\bullet}O_2^-$ are not mainly involved in photocatalytic disinfection in the NS-FTs system.

Several previous studies have focused on the bactericidal effects of ROSs. Some studies have suggested that $^{\bullet}OH$ is the primary attacking agent in the photocatalytic bactericidal effect due to its powerful oxidative ability (Watts *et al.*, 1995; Cho *et al.*, 2005; Zhang *et al.*, 2010). Other studies have suggested that the main bactericidal agent in photocatalytic disinfection is not $^{\bullet}OH$ but H_2O_2, because $^{\bullet}OH$ has a very short life-time (Strul *et al.*, 1993; Blake *et al.*, 1999), whereas H_2O_2 can diffuse through the cell membrane and produce a long-range bactericidal effect (Bors *et al.*, 1979; Rincón and Pulgarin, 2004). In the NS-FTs system, $^{\bullet}OH$ may not be the bactericidal agent due to its short life-time, and that instead H_2O_2, because of its long life-time and ability to diffuse into the bacterial cells, is the main agent in the disinfection process.

3.4.5 Transmission electron microscopy

Because there are two reactive species (e^- and H_2O_2) involved in the NS-FTs system, the effect of individual is studied by TEM. After adding quadruple scavengers (KI, isopropanol, Fe(II), and TEMPOL) in the non-partition system, only e^- is left in the system. In the partition system, e^- produced on the surface of the photocatalyst cannot directly contact with the bacterial cells due to the separation effect of semipermeable membrane, so there is only H_2O_2 playing a role in the disinfection. Both the effect of e^- and H_2O_2 shows similar destruction process of *E. coli* K-12. Before the photocatalysis reaction start, *E. coli* K-12 have an intact interior component and a well-defined cell wall. With the irradiation time prolong, the cells lost more and more interior components and further lost the outer cell wall, eventually completely destruction (Figures 3.20 and 3.21).

The results of TEM suggest that the mechanism of e^- to disinfect bacterial cells (Figure 3.20) is similar to that of H_2O_2 (Figure 3.21). Thus, it is speculated that e^- may react with some substrate (X) to produce oxidative radical ($^{\bullet}X$). This substrate X may be in the solution outside of the bacterial cells or inside of the bacterial cells. Then, based on the component of the solution (NaCl and NS), the experiment is carried out to detect the radicals using ESR method. The result does not find the speculation $^{\bullet}X$, which suggests that $^{\bullet}X$ is not produced outside the bacterial cells, and is probably produced inside the bacterial cell. However, the component of the bacterial cell is very complex, and any substrate has opportunity to produce $^{\bullet}X$. At present, no suitable

method has found to detect the radical produced inside the bacterial cell.

3.4.6 Photocorrosion and reuse of natural sphalerite

The photocorrosion is a problem for pure metal sulfide semiconductors, such as ZnS and CdS, when they are used in photocatalytic reaction (Dunstan *et al.*, 1990; Tang and Huang, 1995). It is because the pure ZnS will release Zn^{2+} in solution with increasing irradiation time. To investigate this issue, the experiment is carried out to determine the photocorrosion of NS by the irradiation of FTs used in this study. The results show that NS was much stable and there was no Zn^{2+} further released during the photocatalysis. Thus, the VL photocorrosion of NS in this study is not serious.

Li *et al.* (2006) reported the photocorrosion of NS, and found that after 9 h irradiation by a 500W tungsten halogen lamp, the Zn atom percentage on NS surface decreased from 27.5 to 24.4%, which corresponded to a loss of 3.1% of the ZnS particles. Thus, this result suggests that NS is stable, and the photocorrosion is small under the irradiation of strong tungsten halogen lamp. However, adding h^+ scavenger and the solution of sulfide or sulfite ions (S_2^- or SO_3^{2-}) may provide a positive effect against the photocorrosion of the sphalerite surface, which has been proven to be stable.

The cycling runs in the photocatalytic disinfection of *E. coli* K-12 mediated by NS under FTs irradiation further confirm the stability of NS in VLD photocatalytic process (Figure 3.22).

3.4.7 Total organic carbon analysis

Jacoby *et al.* (1998) firstly reported the complete degradation of organic compounds in the bacterial cells into CO_2 by photocatalysis. To quantitatively investigate the level of mineralization of *E. coli* K-12 by photocatalytic disinfection, TOC analysis is carried out. Because the organic compounds in the bacterial cells are insoluble, they can be studied by solid-phase measurement. On the other hand, the organic compounds released from the bacterial cells into water are soluble, so they can be studied by liquid-phase measurement. The results show that complete mineralization of *E. coli* K-12 by NS under FTs irradiation did occur after prolonging treatment (Figure 3.23).

3.5 Conclusions

The photocatalytic disinfection capability of a natural semiconducting mineral, NS, is studied for the first time. NS can completely inactivate 1.5×10^7 cfu/mL *E. coli* K-12 within 6 h of FTs irradiation. The photocatalytic disinfection mechanism for NS is investigated by using multiple scavengers. For the first time, the critical role of the e^- played in the bactericidal actions is experimentally demonstrated. The involvement of H_2O_2 in the photocatalytic disinfection is also confirmed using the partition system combined with different scavengers. There is no $^{\bullet}OH$ and $^{\bullet}O_2^-$ produced due to the low potential valence band edge of NS. Moreover, the photocatalytic destruction of the bacterial cells is observed in TEM analysis. NS is very stable and difficult photocorrosion irradiated by FTs. The natural photocatalyst is abundant and easy to be

obtained. It possesses excellent VL photocatalytic activity. These superior properties make it an excellent solar-driven photocatalyst for large-scale cost-effective wastewater treatment.

4. Photocatalytic inactivation of *Escherichia coli* by natural sphalerite: Effects of spectrum, wavelength and intensity of visible light

4.1 Introduction

The basic mechanism of photocatalysis is well-established by the example of TiO_2 photocatalyst irradiated by UV (Ollis, 1985; Rincón and Pulgarin, 2003; Cho *et al.*, 2004). Since the photon excitation of the photocatalyst is the initial step for the activation of the whole photocatalytic system, it is required that the energy of the photon is sufficient to excite the photocatalyst. Some semiconductors, such as TiO_2, SnO_2 and ZnS, can be activated by UV (Sökmen *et al.*, 2001; Yin *et al.*, 2001; Ma *et al.*, 2005), while other photocatalysts, such as Fe_2O_3 and CdS, can absorb VL (Kawahara *et al.*, 2006; Li *et al.*, 2009c). Besides the pure semiconductors, many studies have been devoted to synthesize excellent photocatalysts for disinfection using VL (Zhang *et al.*, 2003; Yu *et al.*, 2005; Zhang *et al.*, 2010). Thus, the selection of the light sources is a very crucial factor to strongly determine the final disinfection efficiency (Leung *et al.*, 2008).

However, there are only limited studies focusing on the effect of different parameters of light sources (Fujishima *et al.*, 2000; Rincón and Pulgarin, 2004a; Rincón and Pulgarin, 2005; Benabbou *et al.*, 2007; Chen *et al.*, 2009). For UV irradiation, the inactivation efficiency is strongly dependent on the spectral distribution of the light source of photons. In terms of the emitting wavelength, the electromagnetic spectrum of UV irradiation can be classified as UVA, UVB and UVC (Rincón and Pulgarin,

2005). If a lamp emitting UVC, the disinfection effect is very fast, even in the absence of the photocatalyst. The results of Benabbou *et al.* (2007) showed that at equivalent intensity, the UVC/TiO_2 system was more lethal for *E. coli* than the UVA/TiO_2 and UVB/TiO_2 systems. The light intensity is another parameter that affects the degree of photocatalytic disinfection, however, the disinfection results of 5 W/m^2 at 2 h irradiation may not be equal to the results obtained under 10 W/m^2 for 1 h irradiation (Chen *et al.*, 2009). The results of Benabbou *et al.* (2007) also showed the disinfection efficiency improved along with the increasing of light intensity.

Although UVB and UVC with high energy are effective for bacterial disinfection, they are hazardous and only accounted for less than 4% of the sunlight. Thus, VL sources have greater potential applications in the water purification and wastewater treatment. Unfortunately, to the best of my knowledge, there has no study to clarify the effect of different parameters of VL, for instance, the light spectrum, wavelength and intensity, on the photocatalytic disinfection of bacterial cells. Therefore, in order to obtain a cost-effective light parameter for bacterial disinfection, it is important to evaluate those three effects on disinfection efficiency.

In this part, the photocatalytic disinfection ability of *E. coli* K-12 by NS under different VL irradiation is described. The main goal of this project is to study the effect of the following parameters: (a) spectra of different VL sources, (b) wavelength of VL, and (c) intensity of VL, on the photocatalytic disinfection of *E. coli* K-12 in

the NS-VL system.

4.2 Materials and methods

4.2.1 Materials

The natural photocatalyst was the same with Section 3.2.1. NS used in this work was collected from the HSP deposit of Hunan Province and sued after pretreatment as reference (Li *et al.*, 2009).

4.2.2 Preparation of *E. coli* K-12 culture

Similar processes were conducted as mentioned in Section 3.2.2. *E. coli* K-12 were chosen for the study. The bacterial cells were cultured in NB (BioLife, Milano, Italy) solution at 37°C and agitated at 200 rpm for 16 h. The cultures were then washed twice with saline solution by centrifugation at 24,000 *g* for 5 min, and the cell pellet was resuspended in saline solution. Finally, the cell concentration was adjusted to final cell density of 1×10^7 cfu/mL in the reaction mixture.

4.2.3 Visible light sources

The main VL source was LED lamps (2.5 W, OPTILED, United States), including white, blue, green, yellow and red colored lamps. The reactor of LED lamp (Plate 4.1) could hold maximum 16 LED lamps. To investigate the spectrum effect of VL, the other two VL sources were chosen: FT (15 W, VELOX®, Thailand) and Xenon lamp (300 W, PLS-SXE-300, Beijing Perfect Light Co. Ltd., Beijing). The reactor of FT

(Plate 3.5) could hold 6 FTs and a liquid filter (5 M sodium nitrite), placed between FTs and sample flask, was used to block all the UV emission. The reactor of Xenon lamp was shown in Plate 4.2. Light was passed through a UV cutoff filter ($\lambda \geq 400$ nm), and then was focused onto the sample flask. Table 4.1 showed the maximum VL intensity of each light source, which was measured by a light meter (LI-COR®, Lincoln, Nebraska, USA). The intensity of each light source was adjusted by changing the number of lamp and the distance from the light source to the sample flask.

4.2.4 Photocatalytic disinfection reaction

Similar processes were conducted as mentioned in Section 3.2.4. Fifty mg of NS was suspended in 45 mL sterilized saline solution. Then the solution was homogenized by sonication at 35 kHz for 1 min with a sonicator (Branson Ultrasonics B.V., Soest, NL, USA). After that, 5 mL of saline-washed bacterial cell was suspended in 45 mL sterilized saline solution containing 1 g/L of photocatalyst. The photocatalytic disinfection was initiated by turning on light. At different time intervals, aliquots of the sample were extracted and serially diluted with saline solution. 0.1 mL of the diluted sample were then immediately spread on nutrient agar (Lancashire, UK) plates and incubated at 37°C for 24 h to determine the number of viable cells (in cfu/mL). In parallel with the photocatalytic disinfection, three control experiments: a light control (light irradiation alone without photocatalyst), a dark control (photocatalyst alone without light irradiation) and a negative control (without light irradiation or photocatalyst), were carried out to prove the occurrence of photocatalytic disinfection

required the coexistence of light irradiation and photocatalyst.

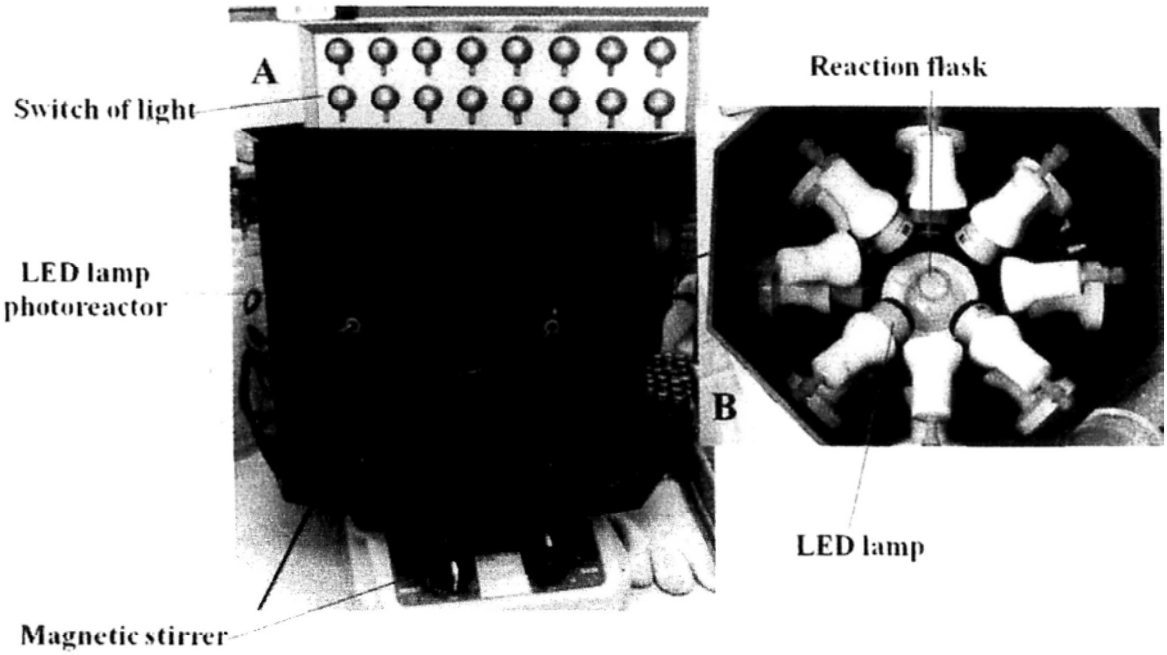

Plate 4.1 A photocatalytic disinfection reactor under LED lamps irradiation.

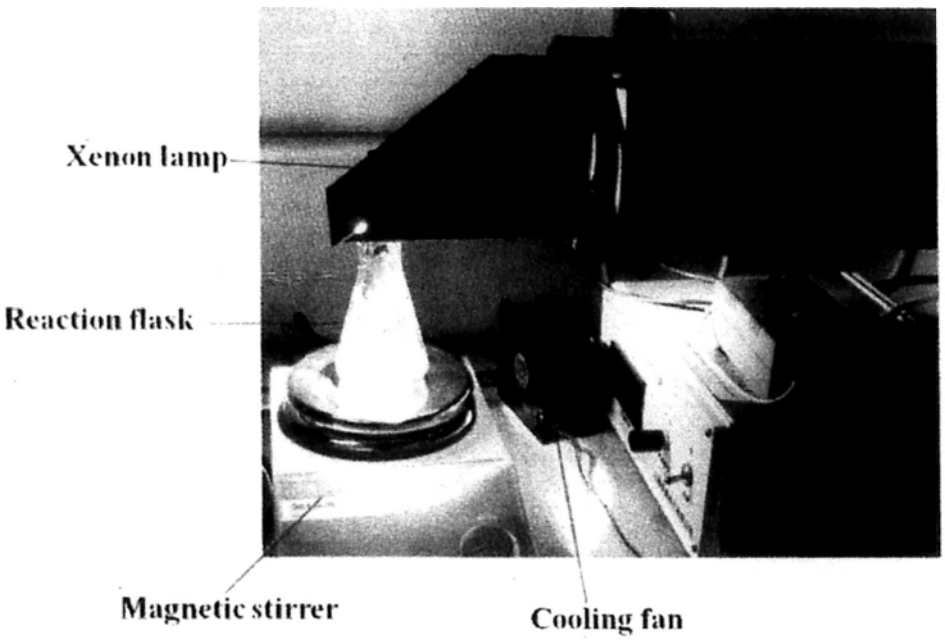

Plate 4.2 A photocatalytic disinfection reactor under Xenon lamp irradiation.

Table 4.1 The maximum VL intensity of each light source.

Light source	Maximum VL intensity (mW/cm^2)
White LED lamp (16 lamps)	223
Blue LED lamp (16 lamps)	193
Green LED lamp (16 lamps)	87
Yellow LED lamp (16 lamps)	97
Red LED lamp (16 lamps)	467
FTs (6 tubes)	3
Xenon lamp (1 lamp)	209

4.2.5 Effect of pH on photocatalytic disinfection

To determine the effect of pH on photocatalytic disinfection, the pH level was monitored by adjusting the initial pH with the addition of a few drops of 0.5 mM HCl and 0.5 mM NaOH to the reaction mixture using pH meter. The beginning pH levels were chosen including pH of 5.0±0.2, 6.0±0.2, 7.0±0.2 and 8.0±0.2, and the pH values were monitored at each testing point. The photocatalytic disinfection reaction and enumeration of cell viability were carried out and determined as described in Section 4.2.4. At each varied pH, a light control (light irradiation alone without photocatalyst) and a dark control (photocatalyst alone without light irradiation) were carried out to ensure the effect of pH and light or pH and photocatalyst on bacterial survival was negligible.

4.2.6 Transmission electron microscopy

The mixture of NS and bacterial cells before and after photocatalytic reaction was collected and centrifuged. The procedures were the same with those used in the Section 3.2.10. The bacterial cells were pre-fixed by glutaraldehyde and trapped in low melting point agarose. After being post-fixed by osmium tetraoxide in PBS (E.M. grade, Electron Microscopy Sciences, Fort Washington, PA, USA), the cell pellet was dehydrated by adding a graded series of ethanol and finally embedded in Spur solution (Electron Microscopy Sciences, Fort Washington, PA, USA) for polymerization. By using ultra-microtome (Leica, Reichert Ultracuts, Wien, Austria), ultra-thin sections of 70 nm were made and stained with uranyl acetate and lead citrate on copper grids. Finally, the stained ultra-thin sections were examined by a JEM-1200 EXII transmission electron microscope (JEOL Ltd, Tokyo, Japan).

4.2.7 Bacterial regrowth ability test

To investigate the ability of *E. coli* K-12 to undergo repair after photocatalytic disinfection under VL, after achieving complete bacterial inactivation by disinfection treatment, whole reaction mixture in a flask was aseptically removed from the photocatalytic reactor and kept in dark at 37°C with 200 rpm agitation to allow bacterial repair. After 10 min and at every 24 h dark incubation (until recovery time reaching 96 h), 500 μL aliquots of samples were taken and directly plated onto the nutrient agar plates, and then incubated at 37°C for 24 h for any observable colony formation. To ensure detection of any recovered cells, 100 μL disinfected samples

were transferred to 5 mL of NB solution at 37°C for 24 h at the above mentioned time intervals. After incubation, 500 μL aliquots of samples were plated onto the nutrient agar plates and incubated at 37°C for 24 h to confirm any occurrence of regrowth after photocatalytic disinfection. Control experiments were performed by (i) adding 100 μL sterilized ultrapure water and (ii) adding 100 μL sample without irradiated by VL (dark control) to NB medium.

4.3 Results

4.3.1 Effect of spectra of visible light sources

There were three different VL sources used in the study. White LED lamp, which emitted VL without UV domain, has achieved market dominance in applications due to its low energy use recently. In addition, FTs and Xenon lamp also emitted VL only after filtering UV emission. The effect of the different VL sources was studied under the same VL intensity of 3 mW/cm^2 at pH 8. As shown in Figure 4.1, the inactivation of *E. coli* K-12 was much more efficient under FTs than white LED lamp and Xenon lamp. Total inactivation 7-log of bacterial cells was achieved after 8 h irradiated by FTs. And there was an induction period (observed in the first 4 h), where the reactive species began to attack the bacterial cells but not caused serious damage leading to the inactivation of bacterial cells. However, at an equivalent intensity, the white LED lamp and Xenon lamp were less effective than the FTs. Within 10 h treatment, both LED lamp and Xenon lamp could only result in the reduction of a 3-log cell density. It was interesting to note that the disinfection process observed in the presence of LED

lamp and Xenon lamp was very similar. And there was no obvious induction period observed during the photocatalytic disinfection process of LED lamp and Xenon lamp.

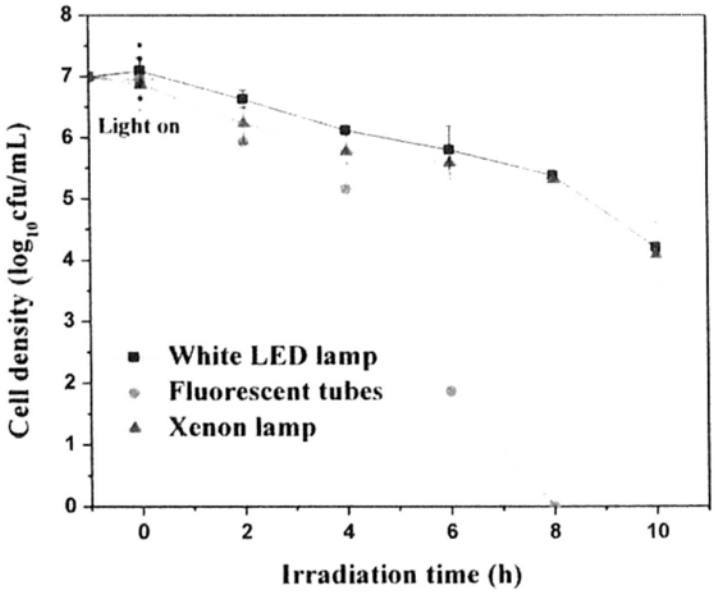

Figure 4.1 Spectral effect of VL on the inactivation of *E. coli* K-12 by NS at pH 8. Experimental conditions: NS concentration = 1 g/L; *E. coli* K-12 concentration = 1×10^7 cfu/mL; Intensity of VL = 3 mW/cm^2; each data point and error bar represent the means and standard deviation, respectively, of triplicates.

To find out the reason why photocatalytic disinfection efficiency of FTs was much higher than the others, the spectra of three light sources were compared. From Figure 4.2, the most difference of the spectra of three light sources are the number of peaks. For white LED lamp and Xenon lamp, the whole spectrum is continuous (continuous spectrum). Interestingly, the spectrum of FTs is totally different from "continuous spectrum", which consisted of several major discreted peaks (discreted peak

spectrum). The result of Figure 4.1 shows that the "discreted peak spectrum" had more strong bactericidal effect than "continuous spectrum" in the photocatalytic disinfection mediated by NS (i.e. NS-VL system).

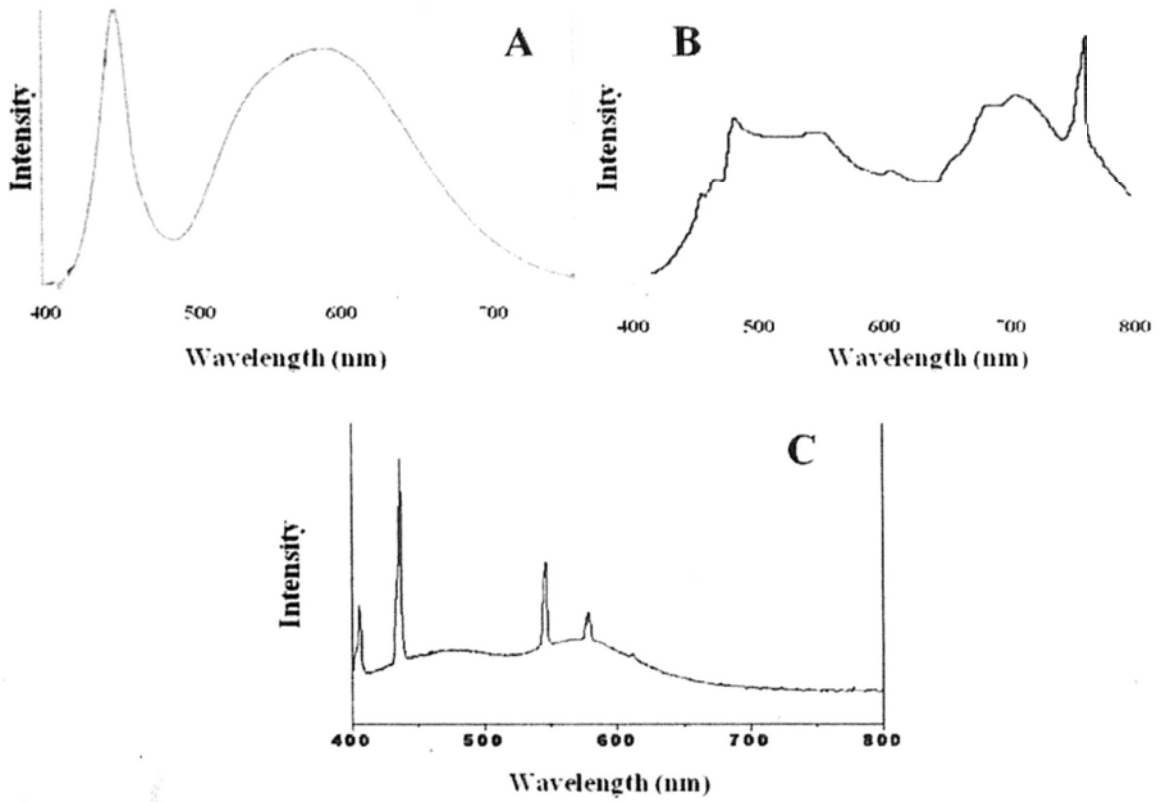

Figure 4.2 The spectra of (A) White LED lamp, (B) Xenon lamp and (C) FTs. The spectra of white LED lamp and Xenon lamp were from OPTILED Lighting International Ltd. and the Beijing Perfect Light Co. Ltd., respectively. The FTs spectrum was measured by spectroradiometer (International Light Technologies, USA).

4.3.2 Effect of wavelength of visible light

The effect of VL wavelengths on bacterial disinfection was investigated under the same VL intensity (87 mW/cm^2) at pH 8 using different colored LED lamps (blue,

green, yellow, red and white LED lamps). As shown in Figure 4.3, the disinfection efficiencies under blue and yellow LED lamps were higher than that under green LED lamps, and much higher than that under red LED lamps. The inactivation process of blue LED lamps was similar to that of yellow LED lamps, and both of them could totally disinfect 1×10^7 cfu/mL *E. coli* K-12 within 8 h treatment. Green LED lamps could result in the reduction of a 5-log cell density after 10 h treatment. However, within 10 h red LED lamps irradiation, there was no cell density decreasing, which means the red range of VL has no effect on the photocatalytic disinfection.

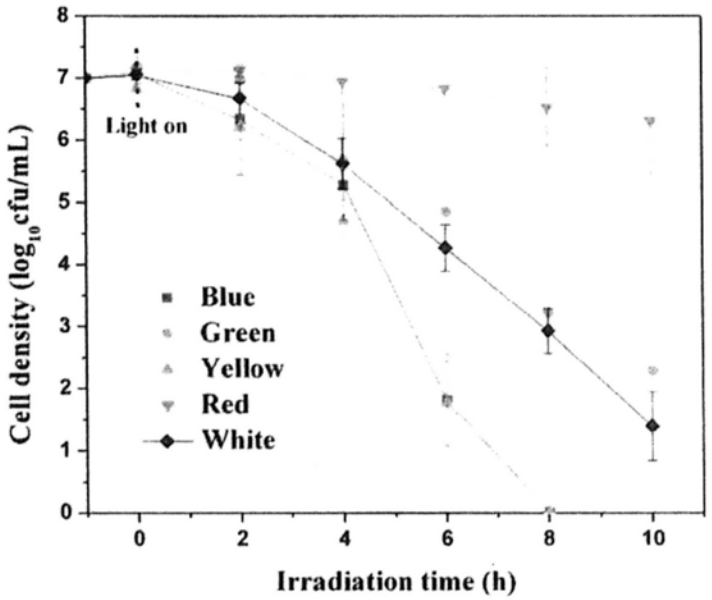

Figure 4.3 Wavelength effect of VL on the inactivation of *E. coli* K-12 by NS at pH 8. Experimental conditions: NS concentration = 1 g/L; *E. coli* K-12 concentration = 1×10^7 cfu/mL; Intensity of VL = 87 mW/cm^2.

To analyze the results of wavelength effect on photocatalytic disinfection, the wavelength of LED lamp and the absorption spectra of NS were compared. Table 4.2

shows the dominant wavelength of each color LED lamps. Figure 4.4 showes the diffuse reflectance UV-vis absorption spectra of NS. Two absorption regions, a steep absorption edge at about 420 nm and a broad shoulder band in the range of 450-620 nm, were observed (Li *et al.*, 2009).

Table 4.2. The parameters of four colored LED.

Light	Dominant wavelength (nm)	Spectrum
Red	625	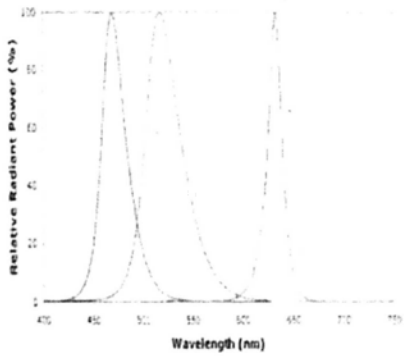
Yellow	590	
Green	520	
Blue	465	

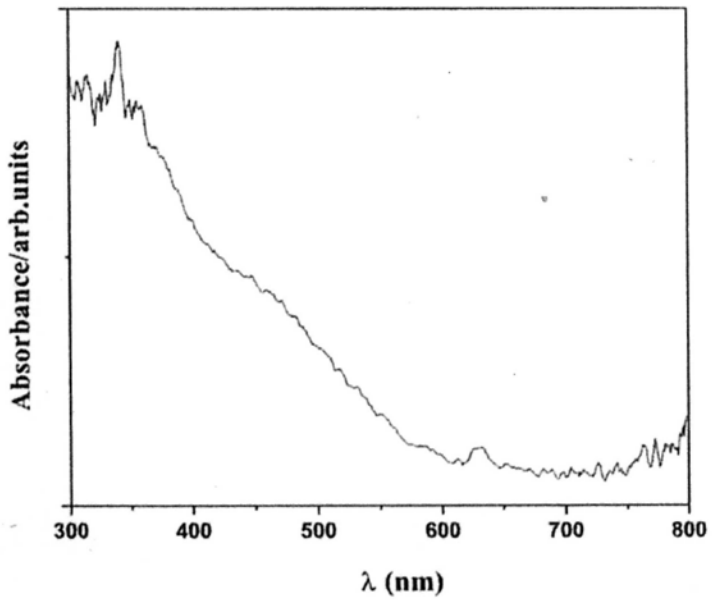

Figure 4.4 Diffuse reflectance UV-vis absorption spectra of NS.

4.3.3 Effect of intensity of visible light

Experiments to investigate the light intensity effect on photocatalytic disinfection efficiency of NS were performed using white LED lamps. Figure 4.5 shows that the disinfection efficiency increased with the increasing of VL intensity from 3 to 223 mW/cm^2. At the lower light intensity (3 and 15 mW/cm^2) and in presence of photocatalyst, there was only a little decrease in cell density. Along with the increasing of VL intensity (87 and 200 mW/cm^2), the disinfection efficiency also increased and there was an induction period at the first 2 h. Further increasing the VL intensity to 223 mW/cm^2, the induction period was disappeared, and the completely inactivation 7 log of bacterial cells was achieved within 6 h irradiation. In the light control with the intensity of 223 mW/cm^2 (Figure 4.5), the bacterial population remained constant after 8 h treatment.

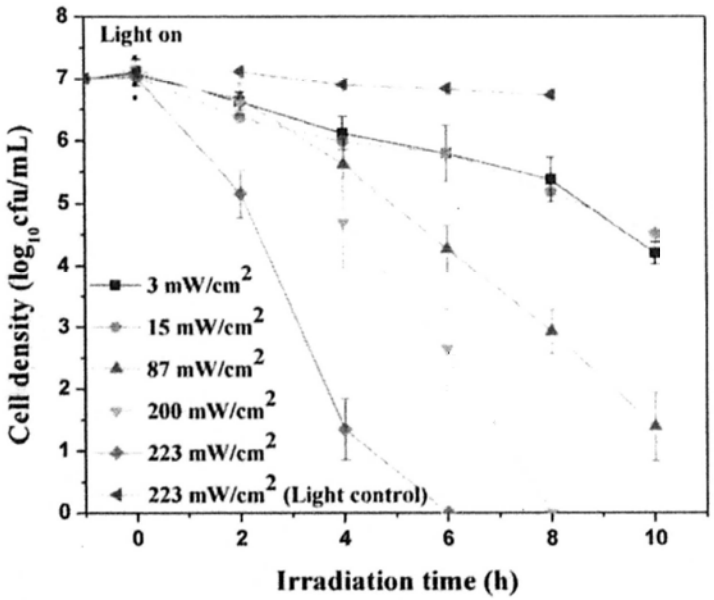

Figure 4.5 Effect of intensity of VL on the inactivation of *E. coli* K-12 by NS at pH 8.

4.3.4 Effect of pH on photocatalytic disinfection

Figure 4.6 shows pH effect on the photocatalytic disinfection of *E. coli* K-12 by NS under white LED lamps irradiation with the intensity of 200 mW/cm^2. The pH value was adjusted at the beginning of the photocatalytic reaction by addition of NaOH or HCl (0.5 mM) to the mixture of NS and bacterial cells, and the pH value did not change within the reaction time. In dark and light controls, at studied range of pH 5-8 (Figure 4.6B), the cell density did not change after 10 h, which suggests that no disinfection effect or photolysis to *E. coli* K-12 by NS or white LED irradiation at different pH. Total inactivation of 1×10^7 cfu/mL *E. coli* K-12 was achieved after 8 h treatment at pH 8 (Figure 4.6A). While at more acidic or neutral pH, the cell density decreased only 2.5 log within 10 h irradiation.

4.3.5 Destruction process of *E. coli* irradiated by visible light

Furthermore, the destruction process of the morphology of *E. coli* K-12 at different VL irradiation time with the intensity of 200 mW/cm^2 at pH 8 was observed by TEM analysis. Figure 4,7A shows the appearance of *E. coli* K-12 before photocatalytic reaction. Characteristics of the *E. coli* K-12 were the well-defined cell wall as well as evenly rendered interior of the cell. The morphology of *E. coli* K-12 irradiated for 8 h greatly changed (Figure 4.7B). Part of the cell wall was decomposed, and an electron translucent region appeared at interior of the cell, indicating that the outer cell membrane is damaged leading to the leakage of the interior component. The further destruction was also observed at 15 and 30 h (Figures 4.7C and 4.7D, respectively).

With a prolonged irradiation, the cell became more and more translucent and the cell wall was greatly ruptured, which indicates that the cell membrane and cell wall of the bacterial cells are destroyed by the reactive species.

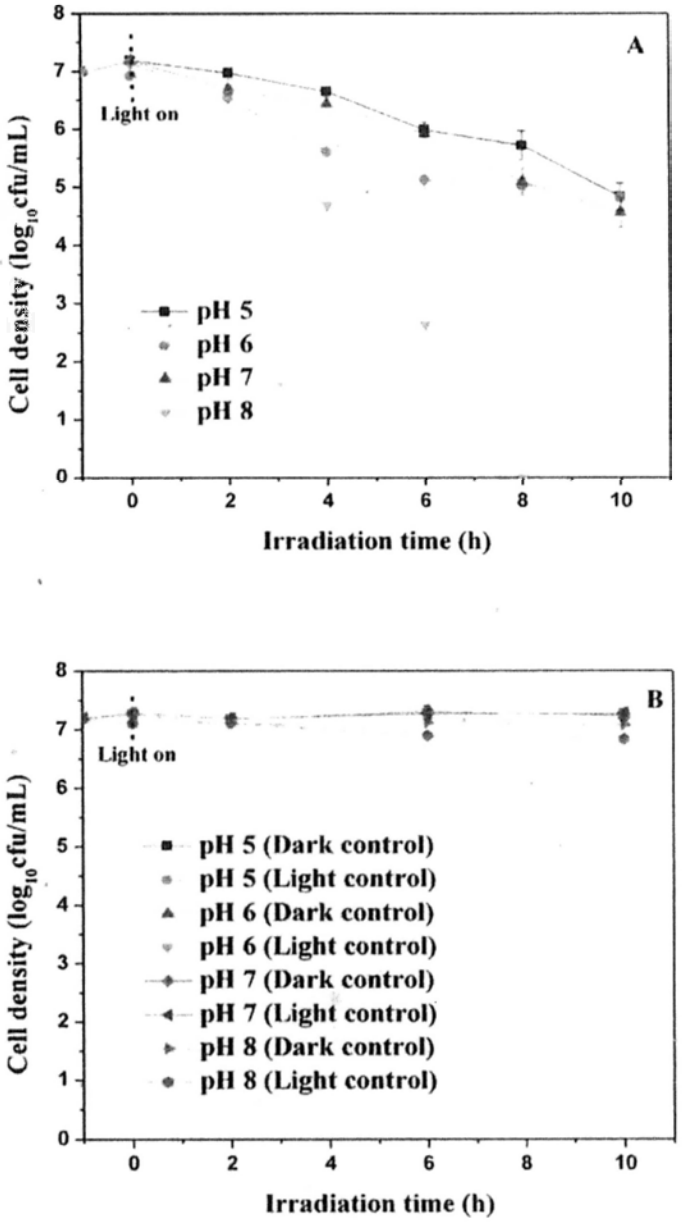

Figure 4.6 Photocatalytic disinfection of *E. coli* K-12 by NS under (A) White LED irradiation, and (B) Dark and light controls at different pH.

4.3.6 Regrowth ability test

Bacterial regrowth test was conducted to evaluate the effectiveness of inactivation bacterial cells by the photocatalytic disinfection process. As mentioned before, *E. coli* K-12 was completely inactivated after 8 h photocatalytic disinfection by NS under white LED lamps with the intensity of 200 mW/cm^2 at pH 8 (Figure 4.5). After that, the reaction mixture was sampled and undergone a 96 h recovery period for bacterial regrowth. The results (Table 4.3) indicate that no detectable bacterial colony is observed after 96 h incubation period.

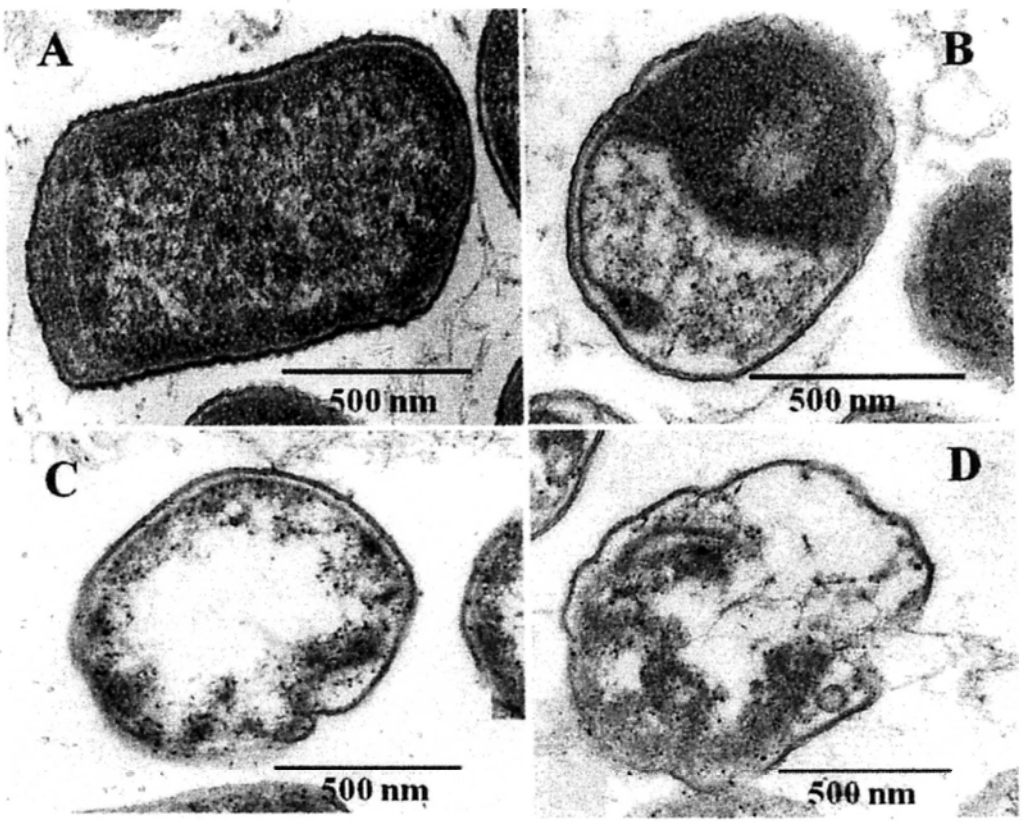

Figure 4.7 TEM images of *E. coli* K-12 photocatalytically treated with NS under VL irradiation. (A) 0 h, (B) 8 h, (C) 15 h, and (D) 30 h.

Table 4.3 Regrowth ability (cfu/mL) of *E. coli* K-12 after photocatalytic disinfection by NS under VL irradiation.

Experiment	0 h	24 h	48 h	72 h	96 h
1	N.D.	N.D.	N.D.	N.D.	N.D.
2	N.D.	N.D.	N.D.	N.D.	N.D.

N.D. = Not detectable

4.4 Discussion

As mentioned in Chapter 3, NS has proved as a real VLD photocatalyst to disinfect bacterial cells. However, there is no report to discuss which parameter(s) of VL can influence the photocatalytic disinfection efficiency. Here, it is discovered that there is an apparent correlation between the spectrum, wavelength and intensity of VL and bacterial disinfection.

4.4.1 Effect of spectra of visible light sources

As shown in Figure 4.1, at the same intensity of VL, the inactivation of *E. coli* K-12 was much more efficient under FTs irradiation than white LED and Xenon lamp irradiation. Compared the disinfection efficiency of FTs with the other two lamps, there is an obvious induction period at the first 4 h irradiation, which indicates that large amount of reactive species are produced under FTs irradiation and bacterial cells have their own defense system against risk from reactive species in the environment. The induction period indicates that the bacterial defense system is efficient to protect bacterial cell, but still insufficient as regards the accumulation of irradiation due to

more efficient in photocatalytic disinfection after 4 h treatment.

The differences among three VL sources are the spectra of light. The spectrum of FTs is obvious different from those of white LED lamp and Xenon lamp. There are more number of peaks of FTs than those of white LED lamp and Xenon lamp. Thus, it is hypothesized that the "discreted peak spectrum" supplies more photons to induce e^-/h^+ pairs so that better photocatalytic disinfection is achieved under illuminant with "discreted peak spectrum".

4.4.2 Effect of wavelength of visible light

Under the same intensity, the wavelength effect of VL on photocatalytic disinfection of bacterial cells is studied. Five different colors of LED lamps, which are blue, green, yellow, red and white, are chosen. The results (Figure 4.3) show that under blue and yellow LED lamps irradiation, the disinfection efficiency was higher than that under green, white and red LED lamps. The data in Table 4.2 shows that red is in the longest wavelengths range of approximately 610-650 nm, yellow light covers with a wavelength of 570-620 nm, green is at a wavelength range of 470-570 nm, and blue is at a wavelength range of roughly 440-490 nm. Based on the results of Figure 4.3, the most effective range of VL was the wavelength of 440-490 and 570-620 nm for NS. The longest wavelength of VL from 610-650 nm was not functional for the photocatalytic disinfection by NS, which suggests that the red range of VL is not involved in the photocatalytic disinfection due to the weak energy.

To find a correlation between the wavelength of VL and photocatalytic disinfection efficiency, the diffuse reflectance UV-vis absorption spectra of NS is measured. If some wavelength range of LED lamp is covered by the most absorption spectra of NS, that color of LED lamp will have most absorption efficiency by NS so that it has the best efficiency to inactivate bacterial cells. Due to the photon energy of blue range is higher than other color LEDs, the shorter wavelength of 440-490 nm is more effective than the longer wavelengths. In addition, in the wavelength region of 620-750 nm, there is no light absorption for NS (Figure 4.4), which suggests that the wavelength of 620-750 nm has no effect on the photocatalytic disinfection. This observation is well matched with the previous study (Figure 4.3) that red wavelength range is not contribute to the disinfection efficiency. At equivalent intensity, the disinfection efficiency under white LED lamps is lower than that under blue and yellow LED lamps (Figure 4.3), which is probably because of the non-functional red wavelength in white LED lamps occupying parts of the intensity of lamps. Thus, selecting an appropriate wavelength range of VL can improve the disinfection efficiency and save energy.

4.4.3 Effect of intensity of visible light

The result of light control (Figure 4.5) suggests that no photolysis to *E. coli* K-12 at high intensity of VL. The lowest disinfection efficiency at 3 and 15 mW/cm^2 of VL indicates that low photon is inducing the limited photocatalysis reaction. The disinfection efficiency increases at 87 and 200 mW/cm^2 of VL, suggesting that higher

photons are produced and exciting more e^-/h^+ pairs to inactive bacterial cells. The induction period at the first 2 h indicates that the bacterial defense system is response to protect bacterial cell. At the highest intensity of VL (223 mW/cm^2), the induction period disappears, which suggests that the self-defense system of bacterial cell does not function at high flux of photos. Thus, the intensity of VL is also one of the most important parameters in the photocatalytic disinfection.

4.4.4 Effect of pH on photocatalytic disinfection

The disinfection efficiency at pH 8 was much higher than that at pH 5, 6 and 7 (Figure 4.6). The results show the inactivation of bacterial cells is more sensitive at alkaline pH than at acidic and neutral pH. This phenomenon probably can be explained by considering that the number of reactive species produced increases as a function of pH or a strong adsorption between NS and bacterial cells is observed at alkaline pH. In Chapter 5, it will further discuss about the pH effect on the photocatalytic disinfection.

4.4.5 Destruction process of *E. coli* irradiated by visible light

In order to ensure the destruction of bacterial cells by the photocatalytic disinfection irradiated by VL, the structural changes of the bacterial cells during different stages of photocatalysis are studied by TEM. Before photocatalytic disinfection, it is observed that the cell structure remained intact (Figure 4.7A), suggesting the bacterial cells have not damaged. When photocatalytic disinfection is started by turning on the LED

lamps, the damage of the bacterial cell is proceeding along with irradiation time. More and more electron translucent regions appeared inside the bacterial cells and the cell wall was destroyed, eventually the bacterial structure collapsed when the irradiation time was extended to 30 h (Figure 4.7B-D). The photocatalysis can produce various reactive species to attack the bacterial cells. TEM results suggest that the reactive species produced by NS irradiated by the white LED lamps have the powerful ability to gradually degrade the interior cell membrane and the cell wall, which leads to the distortion of bacterial structure.

4.4.6 Regrowth ability test

In Experiments 1 and 2, no bacterial colony was observed after 96 h incubation time, which means that 8 h photocatalytic disinfection for *E. coli* K-12 with NS is an effective disinfection time (Rincón and Pulgarin, 2004), which is defined as the time required for complete bacterial inactivation without regrowth in a subsequent dark period for 96 h. This result also suggests that photocatalytic disinfection by NS under VL led to irreversible damage to *E. coli* K-12, or brought the damaged bacterial cells to a state called "viable but non-culturable" (VBNC) state, which means the bacterial cells could no longer grow on conventional media unless favorable condition is provided (Dunlop *et al.*, 2002). This result illustrates that the photocatalytic disinfection system using NS under white LED lamps irradiation with the intensity of 200 mW/cm^2 will not result in the bacterial recontamination, thus it can be concluded that photocatalysis is a safe and effective disinfection method in the real wastewater

treatment.

4.5 Conclusions

The photocatalytic disinfection of *E. coli* K-12 under different spectra, wavelengths and intensities of VL emitted from LED lamps, is firstly investigated by using NS as a VLD photocatalyst. The spectral effect of VL on disinfection efficiency is studied by using white LED lamp, FTs and Xenon lamp, which indicates that the "discreted peak spectrum" is more effective than "continuous spectrum" to inactivate bacterial cells. Besides, the photocatalytic disinfection of bacterial cells is conducted under the single spectrum (blue, green, yellow and red) LED lamp, respectively, which aims at investigation the VL wavelength effect on disinfection efficiency. The results show that the most effective range of VL for photocatalytic disinfection by NS is the wavelengths of 440-490 and 570-620 nm. Furthermore, a positive relationship is obtained between the disinfection efficiency and the VL intensity. NS can completely inactivate 1×10^7 cfu/mL *E. coli* K-12 within 8 h irradiation by white LED lamps with the intensity of 200 mW/cm^2 at pH 8. Moreover, the destruction process of the cell wall and the cell membrane is directly observed under TEM. Finally, no bacterial colony can be detected in a 96 h bacterial regrowth test, which reveals that the VL-photocatalytic disinfection leads to an irreversible damage to the bacterial cells.

5. Visible-light-induced photocatalytic disinfection of wastewater bacteria by natural sphalerite

5.1 Introduction

Photocatalytic disinfection is still a scientific and technical challenge since conventional disinfection methods used in water purification and wastewater treatment, such as chlorination and ozonation (Wert *et al.*, 2007; Shin and Sobsey, 2008), have exhibited their advantages and photocatalysis has shown disadvantages related to low utility of sunlight and high cost of synthetic photocatalysts.

Several studies have reported the feasibility of photocatalytic processes for bacterial inactivation (Matsunaga *et al.*, 1985; Sunada *et al.*, 2003; Kambala *et al.*, 2009). However, only a few studies have reported the photocatalytic inactivation of bacterial cells in real water samples (Subrahmanyam *et al.*, 2008; Backhaus *et al.*, 2010) and most of them have only used the model bacterial group, *E. coli*. Considering that some differences in photocatalytic disinfection response for different type of bacteria with different chemical composition, more efforts should be focus on the establishment of possible differences in the photocatalytic inactivation efficiency depending on different type of bacterial cells.

The most commonly accepted photocatalytic disinfection mechanism is based on the attack of ROSs to the bacterial cell wall (Cho *et al.*, 2004), cumulative damage leading to the cell membrane disorder, increasing the leakage of K^+ (Huang *et al.*,

2000), and finally the cell lysis and death. Therefore, since the attack occurs on the cell wall of bacterial cells, more attention must be paid on the differences of cell wall structure which may lead to different photocatalytic disinfection efficiency. In this sense, the differences between Gram –ve and Gram +ve bacteria could be considered as an example. Gram –ve bacteria have a thinner peptidoglycane cell wall than Gram +ve bacteria.

Recently, controversial conclusions have been obtained about the photocatalytic disinfection of Gram +ve and Gram –ve bacteria. Van Grieken *et al.* (2010) believed that the photocatalytic inactivation efficiency and the mechanism of the Gram –ve bacterium, *E. coli*, and Gram +ve bacterium, *Enterococcus faecalis*, results in no significant difference in both TiO_2 suspension and immobilized TiO_2. However, Čík *et al.* (2006) found that the photocatalytic activity of ZSM-5 polythiophene photocatalyst illuminated by VL for the inactivation of Gram –ve bacterium, *E. coli*, was more efficient than that of the Gram +ve bacterium, *Staphylococcus aureus.* Pal *et al.* (2007) compared the photocatalytic inactivation of Gram –ve bacterium, *E. coli* K-12, and Gram +ve bacterium, *Bacillus subtilis*, showing that *E. coli* K-12 was the most effectively inactivated whereas *B. subtilis* exhibited less response to photocatalytic treatment. Hence, it is important to evaluate the photocatalytic disinfection efficiency of different bacteria by NS under VL irradiation.

To test the feasibility of applying the NS-VL systems to large-scale disinfection, a

study of photocatalytic disinfection of different bacteria by NS is required. In this work, we describe the applicability of NS and compare the disinfection ability of the Gram –ve bacterium, *E. coli*, which is common in wastewater, with another common wastewater Gram +ve bacterium, *M. barkeri*. The effect of pH on the photocatalytic bacterial disinfection is investigated and according to the amount of ROSs present and the electrostatic interaction between bacterial cells and the photocatalyst. A possible inactivation mechanism involving e^- is proposed by comparing two different classes of wastewater bacteria using TEM and K^+ leakage studies.

5.2 Materials and methods

5.2.1 Materials

NS used in this work was collected from the HSP deposit. NS sample was mechanically crushed and milled at the mine. All NS particles were ground into powder and then sieved through 340-mesh into grains, corresponding to particle sizes below 45 μm (Li *et al.*, 2009a). The detail information of NS was shown in Section 3.2.1.

5.2.2 Bacterial culture preparation

M. barkeri (Figure 5.1) isolated from a sludge sample collected from the Shatin Sewage Treatment Works in Hong Kong, and were characterized and identified by the MIDI Sherlock system and 16S rRNA gene sequence analysis.

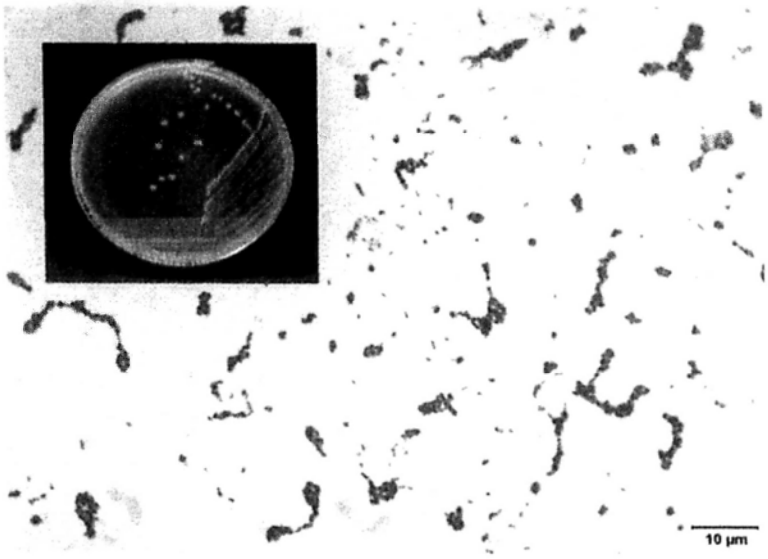

Figure 5.1 Microscopic view of Gram +ve bacterium, *M. barkeri.* The inset contains the colony appearance of *M. barkeri.*

A single colony of *M. barkeri* was grown in 50 mL NB solution overnight for the starter. After that, 1 mL of cultured solution was added to a new 50 mL NB solution and the absorbance at 540 nm (the maximum absorption wavelength for the culture of *M. barkeri*) was measured at every 2 h for 24 h in order to obtain a conclude growth curve (lag, log, stationary and death phases). The growth curve (Figure 5.2) was constructed by measuring absorbance at 540 nm against time in h.

The bacterial cells were cultured in NB solution at 37°C and agitated at 200 rpm for 16 h. The cultures were then washed twice with saline solution by centrifugation at 24,000 *g* for 5 min, and the cell pellet was resuspended in saline solution. Finally, the cell concentration was adjusted to a final cell density of 1.5×10^7 and 1.5×10^5 cfu/mL for *E. coli* and *M. barkeri*, respectively, in the reaction mixture. The pH value was adjusted to 6.8.

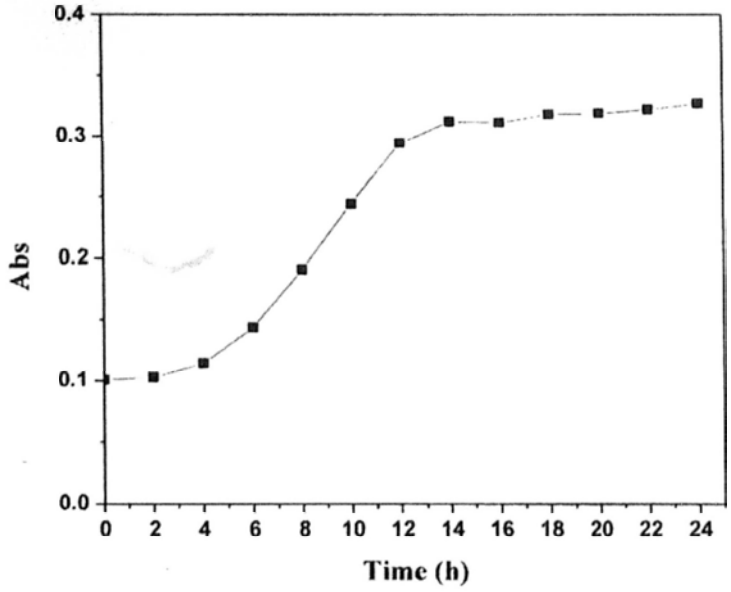

Figure 5.2 The growth curve of *M. barkeri.*

5.2.3 Photocatalytic disinfection performance

Similar processes were conducted as mentioned in Section 3.2.4. NS (final concentration 1 g/L) was suspended in 45 mL sterilized saline solution. The solution was then uniformed by sonication at 35 kHz for 1 min with a sonicator (Branson Ultrasonics B.V., Soest, NL, USA). After that, 5 mL of saline-washed bacterial cell was suspended in 45 mL sterilized saline solution containing 1 g/L of photocatalyst. The pH value of the mixture was 6.8. FTs were selected as the VL source because of their low cost and wide use for household lighting. The photocatalytic disinfection was conducted inside a photocatalytic reactor that could hold six FTs (Plate 3.5) (15 W, VELOX®, Thailand). The FTs could emit most of the VL spectrum (Figure 5.3) ($\lambda \geq 400$ nm), with an intensity of 3.3 mW/cm^2 measured by a light meter (LI-COR®, Lincoln, Nebraska, USA). Disinfection was initiated by turning on the FTs and at

different intervals, aliquots of the sample were collected and serially diluted with saline solution. 0.1 mL of the diluted sample was immediately spread onto nutrient agar (Lancashire, UK) plates and incubated at 37°C for 24 h to determine the number of viable cells. In parallel with the photocatalytic disinfection, three control experiments were carried out to prove that photocatalytic disinfection requires both light irradiation and the semiconductor photocatalyst. They comprised a light control (FTs irradiation alone without photocatalyst), a dark control (1 g/L photocatalyst alone without FTs irradiation), and a negative control (without FTs or photocatalyst). Each set of experiments was performed in triplicate.

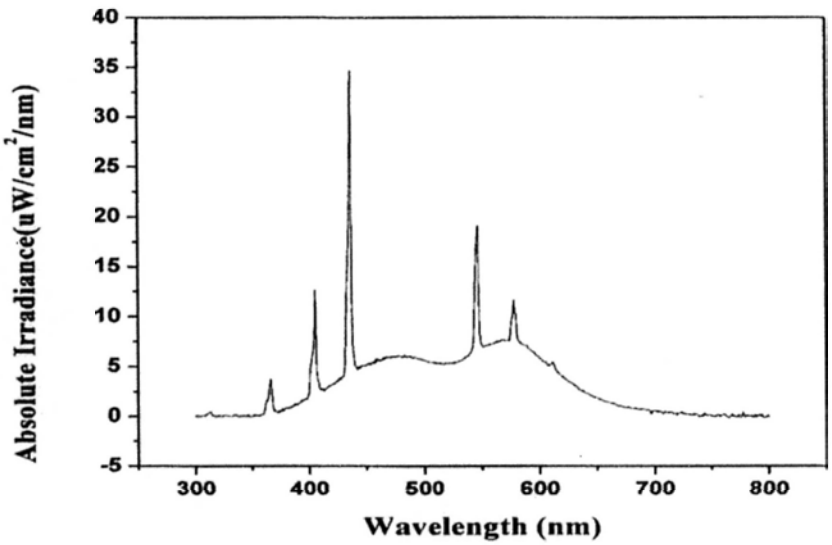

Figure 5.3 The spectrum of light emitted from the FTs.

5.2.4 The effect of pH

Similar processes were conducted as mentioned in Section 4.2.5. To determine the effect of pH on photocatalytic disinfection, the pH level was monitored by adjusting the initial pH with the addition of a few drops of 0.5 mM HCl and 0.5 mM NaOH to

the reaction mixture using pH meter. The beginning pH levels were chosen including pH of 5.0±0.2, 6.8±0.2, 8.0±0.2 and 10.0±0.2, and the pH value was monitored at each testing point. The photocatalytic disinfection reaction and enumeration of cell viability were carried out and determined as described in Section 5.2.3. At each pH, light control (light alone without photocatalyst) and dark control (photocatalyst alone without light) were carried out to ensure the effect of pH and light or pH and photocatalyst on bacterial survival were negligible.

5.2.5 Analysis of zeta potential

The zeta potential of NS and bacteria cells in NaCl solution (0.1 M) were measured by a zeta potential analyzer equipped with a data system of ZetaPlus 3.57 version and Model ZetaPlus (Brookhaven Instruments Corporation, New York, USA) at 25°C (Plate 5.1). The suspension for the zeta potential analysis contained 1 g/L NS or cell density of 1.5×10^7 or 1.5×10^5 cfu/mL for *E. coli* and *M. barkeri* in the presence of 0.1 M NaCl at different pH value. The pH value of the suspension was adjusted by 0.5 mM HCl and 0.5 mM NaOH solutions.

5.2.6 Analysis of hydrogen peroxide

H_2O_2 was analyzed photometrically by the DPD/POD method (Bader *et al.*, 1988). The following procedures were the similar with described in Section 3.2.7. One g/L NS at different pH value suspension was irradiated by FTs. After 2 h irradiation, the sample were collected and centrifuged to remove NS. PBS buffer, DPD and POD

reagents were added in rapid succession. After at least 1 min, the solution was transferred into the photometric cell and measured the absorption spectrum from 450-600 nm by a UV-vis spectrophotometer.

Plate 5.1 A zeta potential analyzer (Model ZetaPlus, Brookhaven Instruments Corporation, NY, USA), equipped with a data analysis system of ZetaPlus version 3.57.

5.2.7 Effect of scavengers

The scavenger experiments were carried out by adding individual scavenger to 50 mL reaction mixture containing about bacterial cells and NS before the light irradiation. The stock concentrations of individual scavengers are 1 M $K_2Cr_2O_7$ (Merck, Darmstadt, Germany) for the quenching of e^-, 1 M isopropanol (Riedel-de Haën®, Seelze, Germany) for the scavenging of $^{\bullet}OH_{free}$, 1 M KI (Merck KGaA, Darmstadt,

Germany) for the scavenging of h^+ and $^{\bullet}OH_{ads}$, 100 mM Fe(II)-EDTA for the detection of H_2O_2.

5.2.8 Measurement of bacterial catalase activity

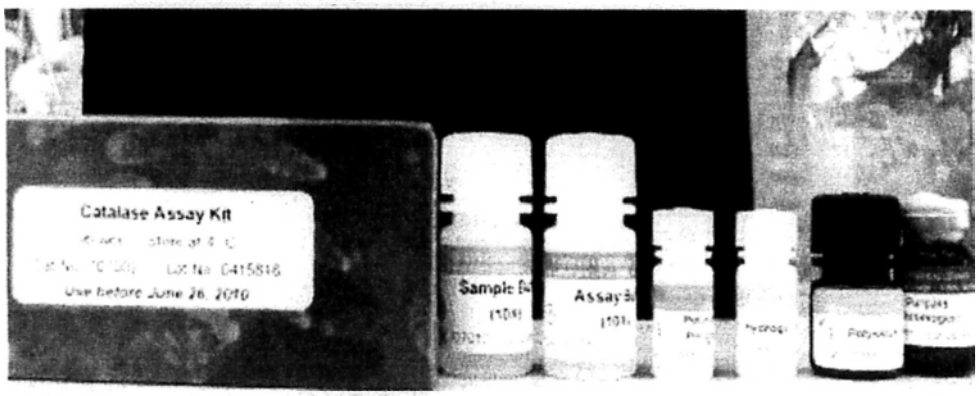

Plate 5.2 A CAT detection kit (Cayman Chemical Company, 2009).

CAT activity determination was conducted using the CAT Assay Kit (Plate 5.2), following the protocol in the instruction manual (Cayman Chemical Company, 2009). The assay kit utilized the peroxidative function of CAT for the determination of enzyme activity. The method was based on the reaction of the enzyme with methanol in the presence of an optimal concentration of H_2O_2. The formaldehyde produced was measured colorimetrically with 4-amino-3-hydrazino-5-mercapto-1,2,4-triazole (Purpald) as the chromogen. Purpald specifically formed a bicyclic heterocycle complex with aldehydes, and the complex was further oxidized to a purple color compound which was measured spectrophotometrically at 540 nm. CAT activity was determined by the following Equation 5.1:

CAT activity (nmol/min/mL)

$$= \frac{\text{Sample absorbance} - (\text{y-intercept of standard curve})}{\text{Slope of standards curve} \times 20\ \text{min}} \times \text{Sample dilution}$$

(Equation 5.1)

where the standard curve was the corrected absorbance of standards as a function of final formaldehyde concentration. One unit CAT activity was defined as the amount of enzyme that would cause the formation of 1.0 nmol of formaldehyde per min at 25°C.

5.2.9 Transmission electron microscopy

The procedures were the same with those used in the Section 3.2.10. Mixtures of NS and bacterial cells before and after photocatalytic reaction were collected and centrifuged. The bacterial cells were pre-fixed by glutaraldehyde and trapped in low melting point agarose. After being post-fixed by osmium tetraoxide in PBS (E.M. grade, Electron Microscopy Sciences, Fort Washington, PA, USA), the cell pellet was dehydrated by adding a graded series of ethanol and finally embedded in Spur solution (Electron Microscopy Sciences, Fort Washington, PA, USA) for polymerization. By using ultra-microtome (Leica, Reichert Ultracuts, Vienna, Austria), ultra-thin sections of 70 nm were made and stained with uranyl acetate and lead citrate on copper grids. Finally, the stained ultra-thin sections were examined by a JEM-1200 EXII transmission electron microscope (JEOL Ltd, Tokyo, Japan).

5.2.10 Measurement of the leakage of potassium ion into the medium

To determine the change of K^+ from the two wastewater bacteria during the photocatalytic disinfection process, at 2 h intervals, 1.5 mL of the illuminated NS/bacterial suspension was collected and filtered through a Millipore filter (pore size 0.45 μm). After filtration, AAS analysis was performed using a Z-2300 Polarized Zeeman atomic absorption spectrophotometer (Hitachi High-Technologies, Tokyo, Japan). Each set of experiments above was performed in triplicate.

5.3 Results

5.3.1 Photocatalytic disinfection performance

Two wastewater bacteria, the Gram -ve bacterium, *E. coli*, and the Gram +ve bacterium, *M. barkeri*, were used to test the performance of photocatalytic disinfection. Figures 5.4 and 5.5 show the photocatalytic disinfection of two bacterial species by NS under VL irradiation provided by the FTs at different pH. The pH was adjusted at the beginning of the irradiation by addition of NaOH or HCl (0.5 mM) to the mixture. The total inactivation of 1.5×10^7 cfu/mL of *E. coli* was achieved after a 3 h treatment at pH 10 (Figure 5.4A) and disinfection efficiency decreased with the decrease of the pH value from 10 to 5. As a comparison, a dark control (only photocatalyst in the dark) and light control (light irradiation alone without photocatalyst) were also conducted. In these two controls, the bacterial population remained constant after treatment (Figure 5.4B), which indicates that no toxic effect or photolysis is caused by NS or FTs irradiation at different pH values.

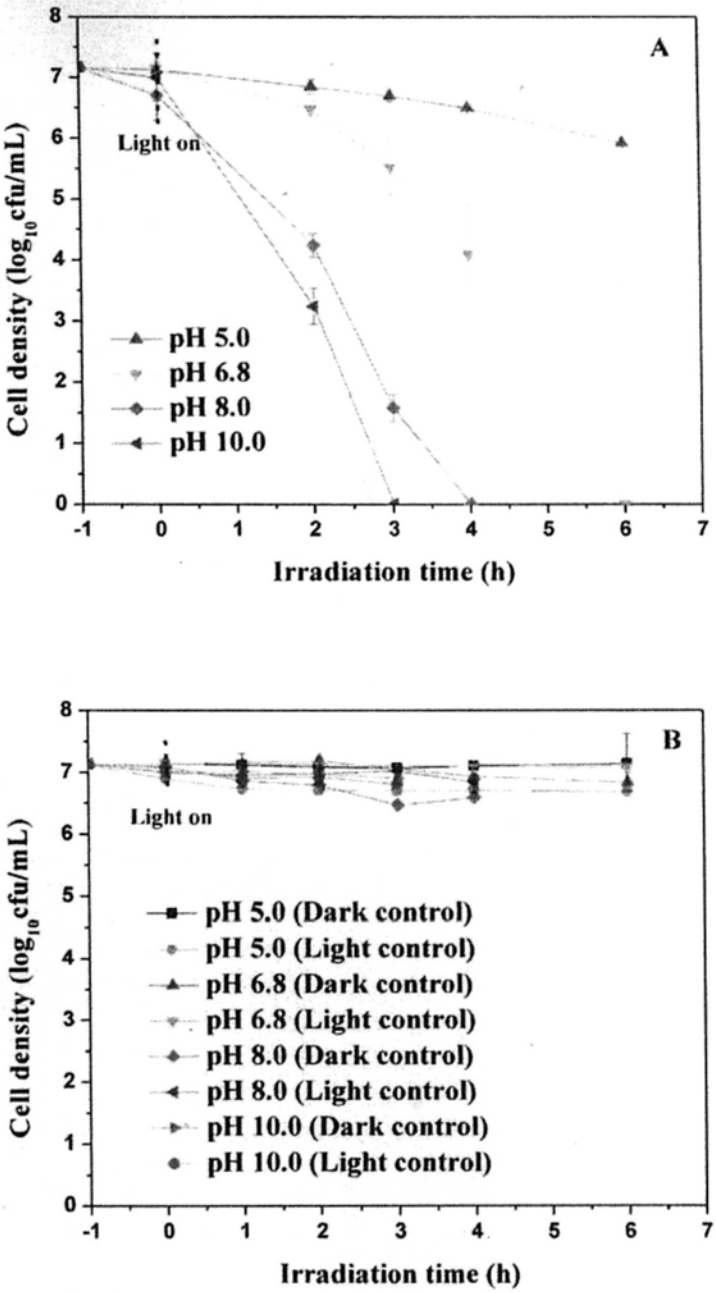

Figure 5.4 Photocatalytic disinfection of *E. coli* by NS under FTs irradiation at different pH values (A) Photocatalytic disinfection, and (B) Dark and light controls. Experimental conditions: NS concentration = 1 g/L; Bacterial cell concentration = 1.5×10^7 cfu/mL; Each data point and error bar represents the mean and standard deviation, respectively, of triplicates.

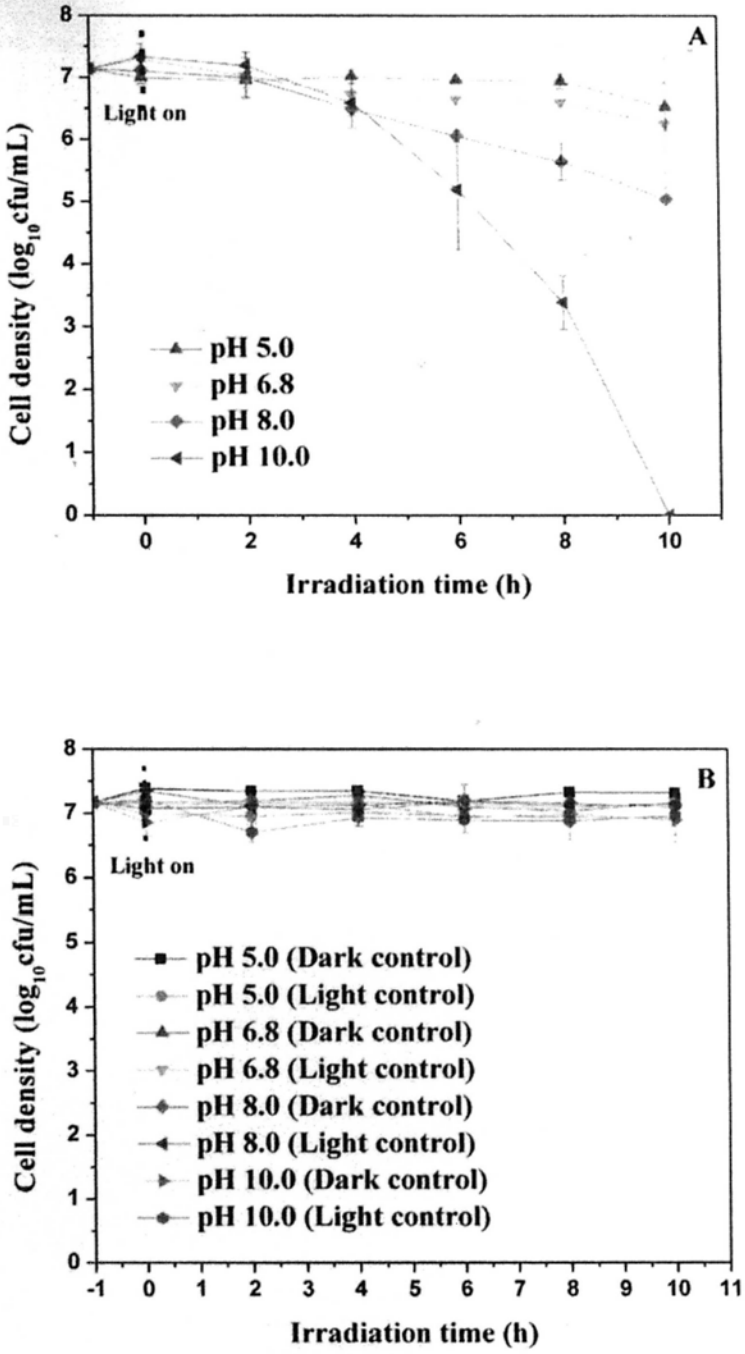

Figure 5.5 Photocatalytic disinfection of *M. barkeri* by NS under FTs irradiation at different pH values (A) Photocatalytic disinfection, and (B) Dark and light controls. Experimental conditions: NS concentration = 1 g/L; Bacterial cell concentration = 1.5×10^7 cfu/mL.

Similar results were obtained for *M. barkeri*. Figure 5.5A shows that the total inactivation of 1.5×10^7 cfu/mL of *M. barkeri* was observed after 10 h treatment at pH 10 and the disinfection efficiency declined with the reduction of the pH value from 10 to 5. The control results (Figure 5.5B) show that no toxic effect was caused by the photocatalyst itself and no photolysis was produced by FTs irradiation at different pH values. For both wastewater bacteria, higher disinfection efficiency was achieved at higher pH values.

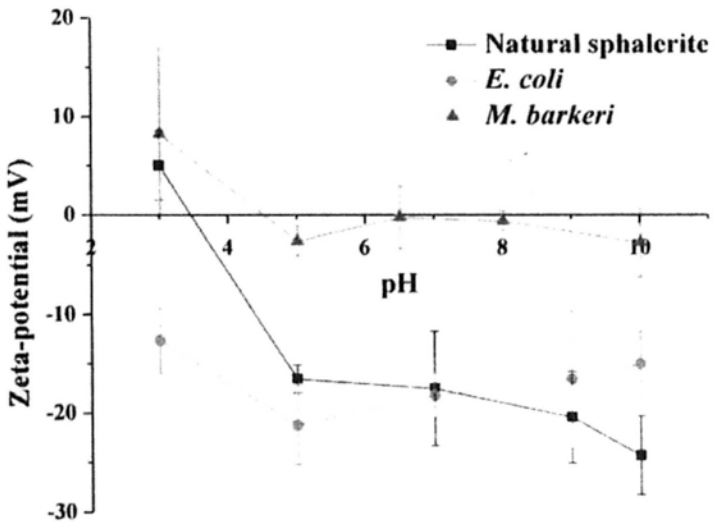

Figure 5.6 Zeta potentials for suspensions of NS, *E. coli* and *M. barkeri* in the presence of NaCl (0.1 M).

To determine whether electrostatic interaction influenced the disinfection efficiency at different pH values, the zeta potentials of NS and the two wastewater bacteria were measured as a function of solution pH. As shown in Figure 5.6, the point of zero

charge (PZC) of NS was approximately 3.5 pH units. In the range of pH 3.5-10, the surface of NS was negatively charged, whereas the overall charges of *E. coli* were negative and those of *M. barkeri* were nearly neutral. In addition, the zeta potentials of each sample were similar in the range of pH 5-10.

To ascertain the possible causes for the changes in photocatalytic disinfection efficiencies, the amount of H_2O_2 produced by NS was determined at different pH values. Figure 5.7 shows the spectrum of the absorbance of H_2O_2 after 2 h irradiation at pH values of 6.8 and 10. Obviously, the absorbance (at 551 nm) at pH 10 was higher than pH 6.8, which suggests that more H_2O_2 is produced at more alkaline pH.

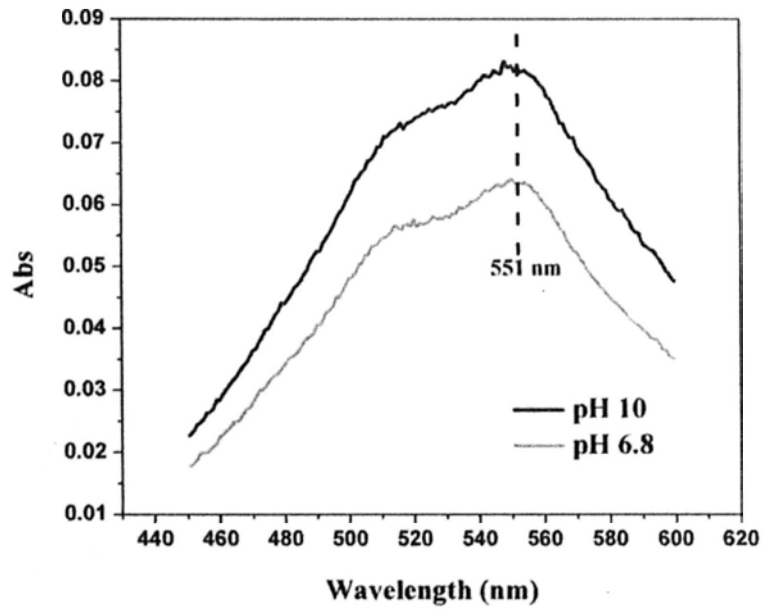

Figure 5.7 Absorption spectra of the DPD/POD after reaction with H_2O_2 produced by the FTs irradiation for 2 h at different pH values.

As the pH of normal wastewater is near neutral, the photocatalytic disinfection of *E. coli* and *M. barkeri* by NS under FTs irradiation were conducted at pH 6.8 in the following experiment. The cell densities of *E. coli* and *M. barkeri* were adjusted to 1.5×10^7 and 1.5×10^5 cfu/mL, respectively. As shown in Figure 5.8, a 7 log-reduction of *E. coli* was obtained within 6 h (Figure 5.8A), and a 5 log-reduction of *M. barkeri* was observed within a 10 h treatment at neutral pH (Figure 5.8B).

5.3.2 Photocatalytic disinfection mechanism

5.3.2.1 Reactive species analysis

Photocatalysis can produce several reactive charged or oxidative species ($^{\bullet}OH$, H_2O_2, $^{\bullet}O_2^-$, h^+ and e^-), which potentially play an important role in disinfection. To study which reactive species are involved and whether there is a difference between Gram –ve and Gram +ve bacteria in the photocatalytic disinfection, scavengers were used to remove their respective reactive species: KI for h^+ and $^{\bullet}OH_{ads}$ (Chen *et al.*, 2005), isopropanol for $^{\bullet}OH_{free}$ (Khodja *et al.*, 2005), TEMPOL for $^{\bullet}O_2^-$ (Lejeune *et al.*, 2006), Cr(VI) for e^- (Chen *et al.*, 2005), and Fe(II) for H_2O_2 (Zhang *et al.*, 2010).

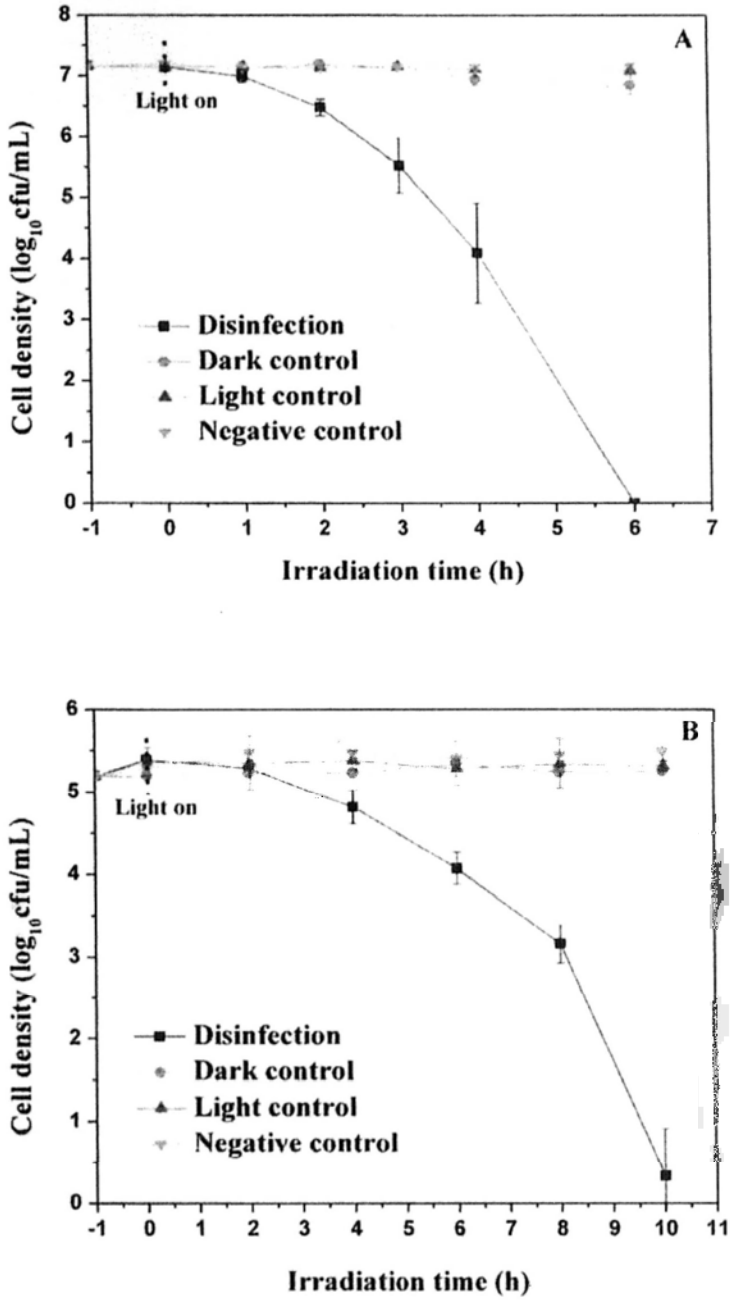

Figure 5.8 Photocatalytic disinfection of (A) *E. coli* and (B) *M. barkeri* by NS under FTs irradiation at neutral pH. Experimental conditions: Photocatalyst concentration = 1 g/L; Dark control: 1 g/L NS in the dark; Light control: saline solution under FTs; Negative control: saline solution in the dark.

For *E. coli* (Figure 5.9A), in the dark and light controls, after the addition of each scavenger, the bacterial population remained constant after 6 h (Figure 5.9B), which showed that these scavengers were non-toxic to bacterial cells. Without the addition of any scavengers, complete disinfection was achieved within 6 h at neutral pH (Figure 5.9A). With the addition of isopropanol ($^{\bullet}OH_{free}$ scavenger), KI (h^+ and $^{\bullet}OH_{ads}$ scavenger) and TEMPOL ($^{\bullet}O_2^-$ scavenger), the level of bactericidal effect did not change compared with that of no scavenger (Figure 5.9A), suggesting that h^+, $^{\bullet}OH$ and $^{\bullet}O_2^-$ are not involved in the photocatalytic inactivation. Interestingly, in the presence of Fe(II) (H_2O_2 scavenger) and Cr(VI) (e^- scavenger), the cell density reduced to 1×10^4 and 5×10^5 cfu/mL after 6 h irradiation, respectively (Figure 5.9A). These results indicate that the disinfection efficiency decreases only by 3 log without H_2O_2 and 1.5 log without e^-, inferring that H_2O_2 and e^- are strongly involved in the photocatalytic disinfection. To further study the role of e^- in the photocatalytic disinfection of *E. coli*, four scavengers (isopropanol, KI, Fe(II), and TEMPOL) were used to remove the $^{\bullet}OH$, h^+, H_2O_2 and $^{\bullet}O_2^-$, respectively (Figure 5.9A), and only e^- remained in the disinfection system. The results show that only e^- could result in the reduction of a 5.5-log cell density after 6 h treatment (Figure 5.9A).

For *M. barkeri* (Figure 5.10A), without any scavengers, the disinfection finished within 10 h at neutral pH. With the addition of KI, isopropanol, TEMPOL and Cr(VI), the level of bactericidal effect did not change compared with that of no scavengers (Figure 5.10A), indicating that h^+, both $^{\bullet}OH_{free}$ and $^{\bullet}OH_{ads}$, $^{\bullet}O_2^-$ and e^- are not involved

in the photocatalytic disinfection. Interestingly, in the presence of Fe(II) (H_2O_2 scavenger), the cell density reduced to 1×10^4 cfu/mL after 10 h irradiation (Figure 5.10A), indicating that the disinfection efficiency decreases only by 1 log without H_2O_2. To further clarify the role of e^-, four scavengers (isopropanol, KI, Fe(II), and TEMPOL) were also employed simultaneously. The results show that only e^- did not show any bactericidal effect on *M. barkeri* after 10 h treatment (Figure 5.10A), which indicates that the e^- is not strongly involved in photocatalytic disinfection of *M. barkeri*. In the dark and light controls, after the addition of each scavenger, the bacterial population remained constant after 10 h (Figure 5.10B), which suggests that these scavengers are non-toxic to *M. barkeri*.

To further confirm the role of H_2O_2, the effect of CAT (Figure 5.11), a well-known antioxidant enzyme that catalyzes the decomposition of H_2O_2 to water and oxygen, was investigated. The CAT activity of *E. coli* is shown in Figure 5.11. During the first 2 h, CAT activity increased rapidly, which indicates that a large amount of H_2O_2 is produced to attack the bacterial cells at the beginning of photocatalytic disinfection, and the bacterial defense system increases CAT activity to protect the cell. After 2 h, CAT activity rapidly decreased with the disinfection process (Figure 5.11). This suggests that *E. coli* is damaged severely, including its defense system, so that CAT activity decreases. For *M. barkeri* (Figure 5.11), during the first 2 h, CAT activity also increased rapidly indicating an increase in the concentration of H_2O_2 at the beginning of the photocatalytic disinfection. At longer irradiation times of 2-10 h, CAT activity

decreased very slowly and even became constant with further increase in disinfection time (Figure 5.11).

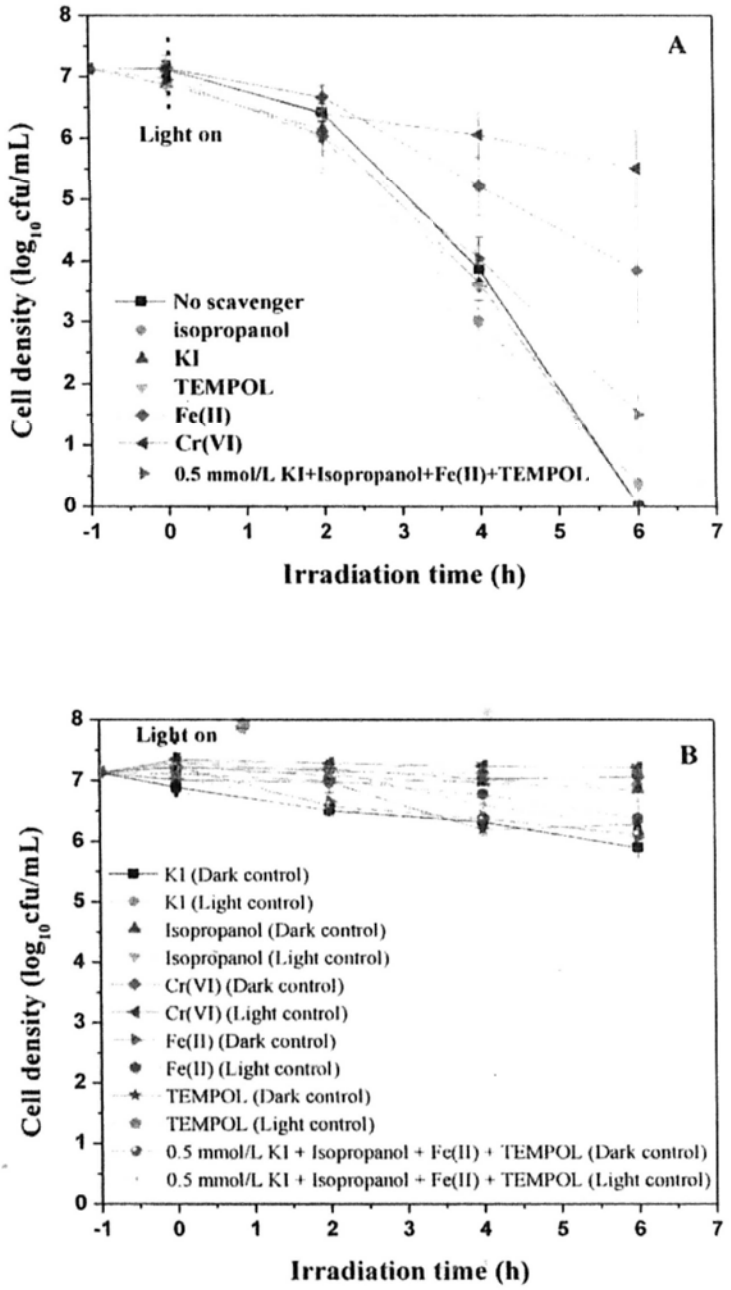

Figure 5.9 Photocatalytic disinfection of *E. coli* by NS with different scavengers (5 mmol/L KI, 0.5 mmol/L isopropanol, 0.05 mmol/L Cr(VI), 0.1 mmol/L Fe(II)-EDTA, 2 mmol/L TEMPOL) under FTs irradiation (A) Photocatalytic disinfection, (B) Dark and light controls.

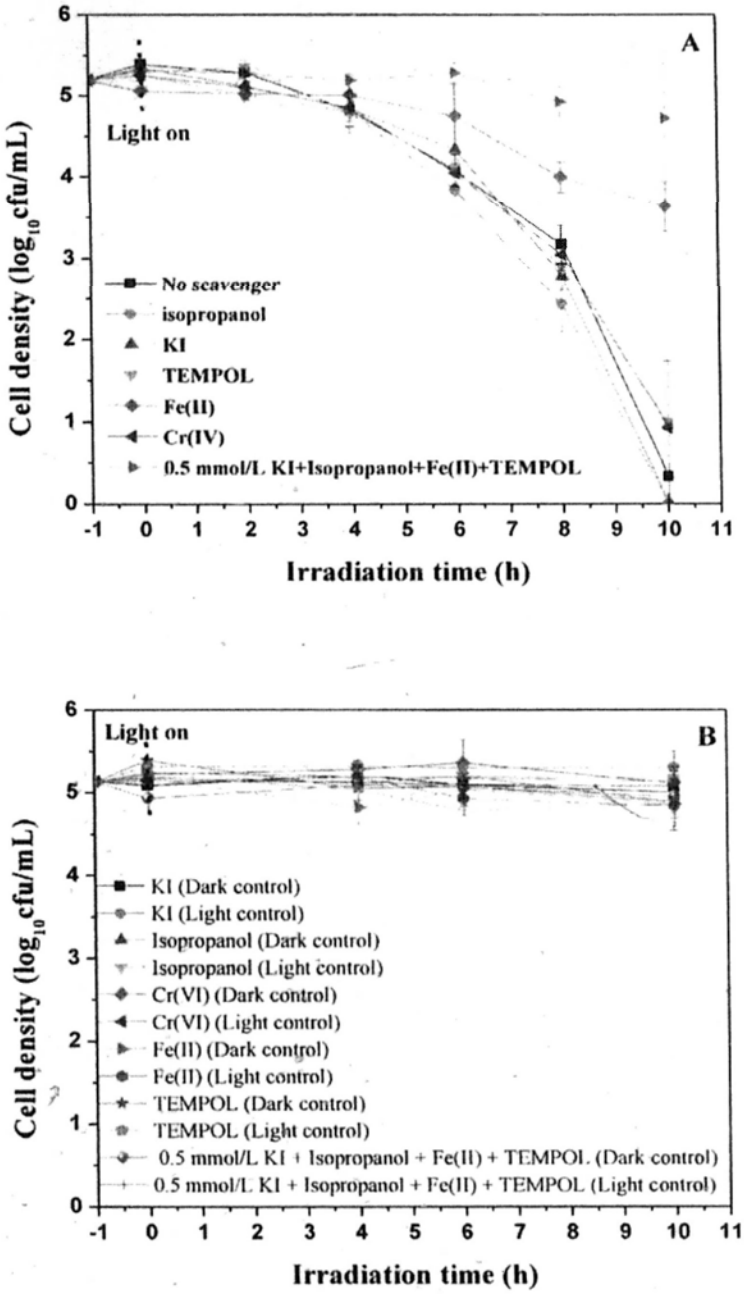

Figure 5.10 Photocatalytic disinfection of *M. barkeri* by NS with different scavengers (5 mmol/L KI, 0.5 mmol/L isopropanol, 0.05 mmol/L Cr(VI), 0.1 mmol/L Fe(II)-EDTA, 2 mmol/L TEMPOL) under FTs irradiation (A) Photocatalytic disinfection, (B) Dark and light controls.

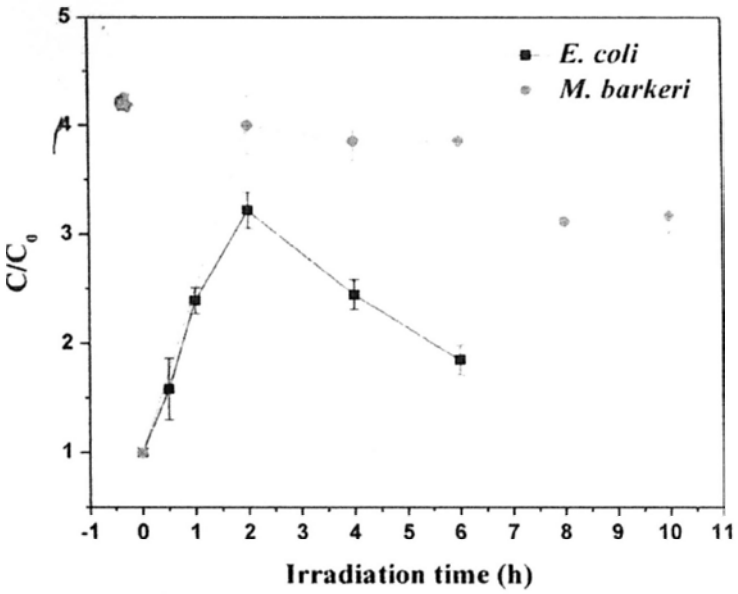

Figure 5.11 The change of CAT activity under photocatalytic disinfection of two wastewater bacteria by NS under FTs irradiation.

5.3.2.2 Destruction process of wastewater bacteria

To further confirm the destruction process, the bacterial cell morphology was studied by TEM analysis before and after photocatalytic disinfection. Figure 5.12 shows the disinfection effect of *E. coli* at the different stages of photocatalytic disinfection. At the beginning of disinfection, *E. coli* exhibited an intact cell structure including the obvious cell wall and evenly rendered interior of the cell (Figure 5.12A). After 6 h irradiation treatment (Figure 5.12B), an electron translucent region appeared at the center of the cell and the intracellular cell membrane shrank. After 12 h of treatment (Figure 5.12C), the cell lost most of the cytoplasmic components, which indicates that the intracellular membrane of the cell is damaged severely and the cell wall is partly destroyed. After 30 h irradiation (Figure 5.12D), the cell became increasingly

translucent and the cell wall was greatly ruptured, indicating a complete destruction of *E. coli*. The TEM images suggest that the destruction process of *E. coli* starts from the intracellular cell membrane to the outer cell wall.

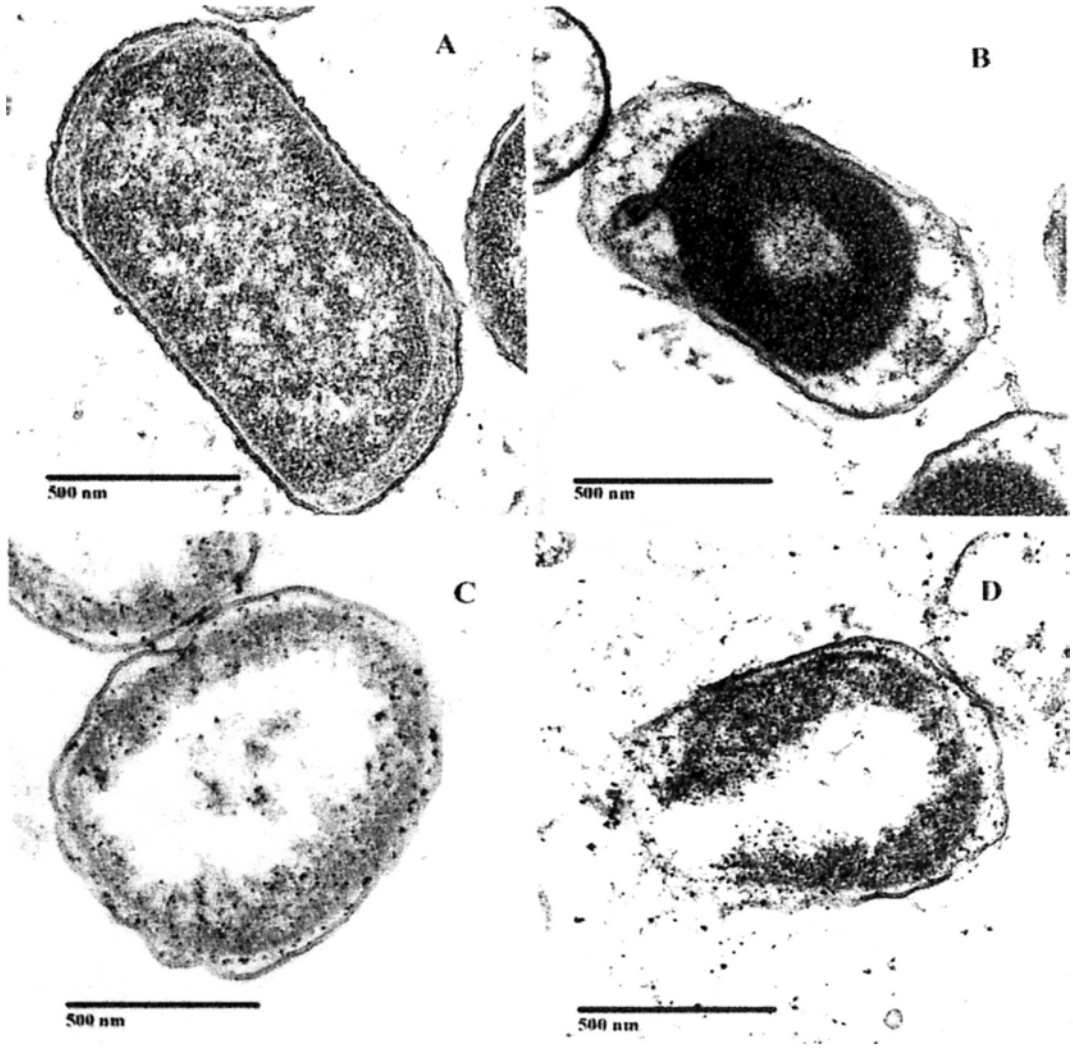

Figure 5.12 TEM images of *E. coli* photocatalytically treated with NS under FTs irradiation. (A) 0 h, (B) 6 h, (C) 12 h, and (D) 30 h. Experimental conditions: NS concentration = 1 g/L; Bacterial cell concentration = 1.5×10^8 cfu/mL.

For *M. barkeri*, the disinfection process was different from that for *E. coli* (Figure 5.13). Before photocatalytic disinfection, *M. barkeri* exhibited a well-defined cell

structure with a clear cell wall (Figure 5.13A). After 10 h irradiation treatment (Figure 5.13B), the central portion of the cell was still intact but part of the cell wall structure appeared damaged. With prolonged irradiation time of 30 h (Figure 5.13C), increasingly more of the cell wall structure disappeared and a small part of the interior components of the bacterial cells became translucent. Although the cell wall was greatly ruptured after 50 h of irradiation treatment (Figure 5.13D), the morphology of the cell did not change too much and intracellular components of the cell were still present. The TEM results suggest that the destruction process of *M. barkeri* starts from the outer cell wall.

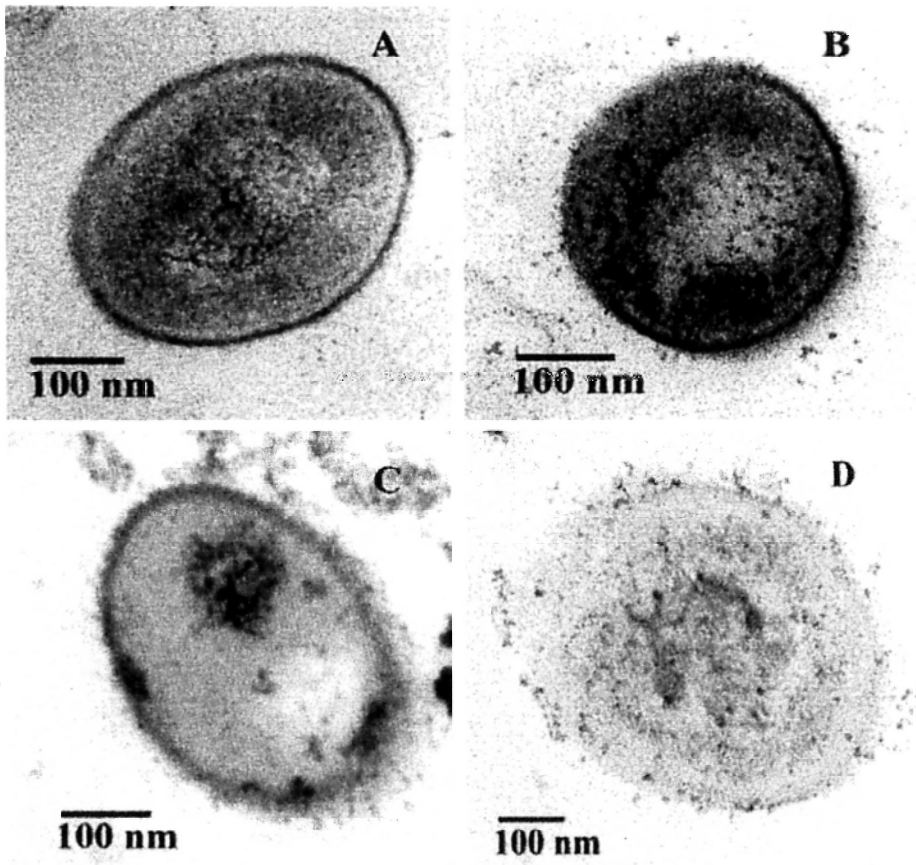

Figure 5.13 TEM images of *M. barkeri* photocatalytically treated with NS under FTs irradiation. (A) 0 h, (B) 10 h, (C) 30 h, and (D) 50 h. Experimental conditions: NS concentration = 1 g/L; Bacterial cell concentration = 1.5×10^7 cfu/mL.

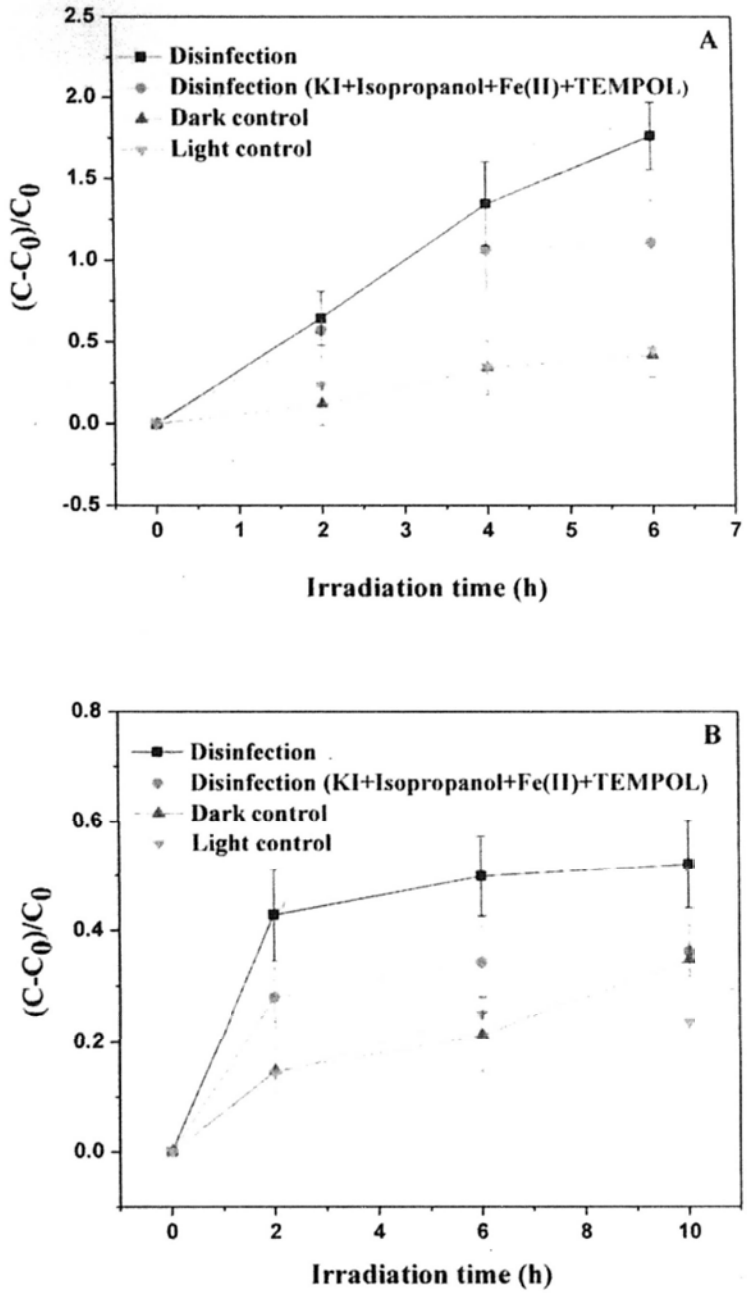

Figure 5.14 The change of K^+ leakage from (A) *E. coli* and (B) *M. barkeri* under different conditions (Disinfection: NS suspension with FTs irradiation; Disinfection (KI+isopropanol+Fe(II)+TEMPOL): the addition of quadruple scavengers at the same time in the photocatalytic disinfection; Dark control: only NS suspension; Light control: only FTs irradiation.

To confirm the destruction of intracellular cell membrane by e^-, K^+ leakage measurements were obtained (Figure 5.14). It was observed that *E. coli* rapidly accumulated K^+ in solution compared to the two sets of control experiments (dark and light controls) (Figure 5.14A). When adding KI, isopropanol, Fe(II), and TEMPOL at the same time to remove all other reactive species, with only e^- left in the disinfection system, *E. coli* also showed an immediate increase in K^+ (Figure 5.14A).

For *M. barkeri*, within a 10 h irradiation treatment, there was a little increase in K^+ compared with the dark and light controls (Figure 5.14B). This increase was likely due to the destruction of H_2O_2. Interestingly, with the addition of quadruple scavengers (KI, isopropanol, Fe(II) and TEMPOL) to study the role of e^-, the K^+ leakage was similar to the two control experiments (Figure 5.14B).

5.4 Discussion

5.4.1 Photocatalytic disinfection performance

The photocatalytic disinfection results (Figures 5.4 and 5.5) show that for both Gram –ve bacterium, *E. coli*, and Gram +ve bacterium, *M. barkeri*, more alkaline condition results in higher inactivation efficiency. This result can be explained by two aspects. On one hand, it is probably due to the strong adsorption between NS and bacterial cells at more alkaline pH. On the other hand, it is likely to produce more amounts of reactive species, such as H_2O_2, to attack bacterial cells as a function of pH.

To explain the reason why the disinfection efficiency is higher at higher pH value for both wastewater bacteria, the electrostatic interaction between the photocatalyst and bacteria is investigated. The zeta potential is widely used for the quantification of the magnitude of the electrical charge of the suspensions, indicating the net electrical charge on the surface of the suspensions. The PZC describes the condition when the electrical charge density on a surface is zero. For example, the PZC of NS is 3.5 (Figure 5.6), suggesting that at pH 3.5, NS submerged in 0.1 M NaCl solution exhibits zero net electrical charge on the surface. In the range of pH 3.5-10, all the surface of NS, the surfaces of *E. coli* and *M. barkeri* are negatively charged and the net electrical charges of all at different pHs are not significant different. As is known to all, like charges repel each other, but opposite charges attract and attraction capacity is based on the amount of electrical charge. The similar electrical charges of two subtracts at different pH indicate similar electrostatic attraction of them. These results suggest that in the range of pH 5-10, the role of electrostatic attraction between the bacterial cells and NS does not play an important role in the photocatalytic inactivation. Hence, the different photocatalytic disinfection efficiencies in the range of pH 5-10 are not due to the electrostatic interaction between bacterial cells and NS.

To investigate the amount of H_2O_2 produced by NS under FTs irradiation at different pH, H_2O_2 is analyzed photometrically by the DPD/POD method. The results show that more H_2O_2 was produced at more alkaline pH than neutral pH (Figure 5.7). Thus, it is probable that the higher disinfection efficiency at alkaline pH is due to the higher

amounts of H_2O_2 produced by NS.

At neutral pH, NS could complete disinfect a 7 log *E. coli* within 6 h and a 5 log *M. barkeri* within a 10 h treatment (Figure 5.8). Most importantly, NS has an outstanding advantage as a large amount can be obtained from mining sites at comparatively low costs. Hence, NS shows high VLD photocatalytic disinfection efficiencies to different wastewater bacteria and it can be used economically in the wastewater treatment.

5.4.2 Photocatalytic disinfection mechanism

5.4.2.1 Reactive species analysis

The experiments of Chapter 3 (Figure 3.13) have indicated that both H_2O_2 and e^- are involved in the photocatalytic disinfection of *E. coli* K-12 by NS under FTs irradiation. In this chapter, we compare Gram –ve bacterium, *E. coli*, and Gram +ve bacterium, *M. barkeri*, to investigate whether there are some differences between different structures of bacterial cells in photocatalytic disinfection. The experiment of scavenger effect on *E. coli* is repeated and further finish the reactive species analysis on *M. barkeri* to find out what is the difference on the role of reactive species between *E. coli* and *M. barkeri*.

The results of *E. coli* (Figure 5.9) were similar to Section 3.3.3. The addition of isopropanol ($^{\bullet}OH_{free}$ scavenger), KI (h^+ and $^{\bullet}OH_{ads}$ scavenger) and TEMPOL ($^{\bullet}O_2^-$ scavenger) did not influence the photocatalytic disinfection efficiency compared with

no scavenger added (Figure 5.9A). These results indicate that the very short life-time reactive species are not strongly involved in the inactivation. When Fe(II) (H_2O_2 scavenger) and Cr(VI) (e^- scavenger) were added, the photocatalytic disinfection strongly inhibited, indicating that H_2O_2 and e^- play important roles in the disinfection. When addition of multiple scavengers together, only e^- alone also strongly decreased the cell density, which further prove that the e^- plays an important role to disinfect *E. coli*.

For *M. barkeri*, the results of in the presence of KI, isopropanol, TEMPOL and Cr(VI) suggest that h^+, $^{\bullet}OH$, $^{\bullet}O_2^-$ and e^- are not involved in the photocatalytic disinfection (Figure 5.10A). Only after adding of Fe(II), the photocatalytic disinfection strongly inhibited, indicating that H_2O_2 plays an important role in the disinfection. Surprisingly, these results suggest that not e^- but H_2O_2 is involved in the photocatalytic disinfection of *M. barkeri*. The quadruple scavengers study further clarified e^- did not show any bactericidal effect on *M. barkeri*.

The results of scavenger study prove that H_2O_2 is the major reactive species involved in the photocatalytic disinfection of *E. coli* and *M. barkeri*, so CAT activity is investigated to further clarify the role of H_2O_2. As CAT is an enzyme in the bacterial defense system that protects bacterial cells from H_2O_2, a higher CAT activity implies that bacterial cells are encountering a more significant H_2O_2 attack, and can better defend against H_2O_2 attack from photocatalytic disinfection. CAT result (Figure 5.11)

indirectly supports that H_2O_2 is produced by NS under irradiation of FTs to attack the bacterial defense system. And it also suggests that *M. barkeri* has a stronger system to defend against H_2O_2 attack than *E. coli*. Hence, *M. barkeri* is more resistant to H_2O_2 than *E. coli*, which means that NS exhibits greater activity in disinfecting *E. coli* than *M. barkeri*.

5.4.2.2 Destruction process of wastewater bacteria

The scavenger study shows that in the NS-FTs system, both H_2O_2 and e^- are the major reactive species to inactivate *E. coli* (Figure 5.9A), while only H_2O_2 plays an important role in the disinfection of *M. barkeri* (Figure 5.10A). The difference between the two bacteria is that e^- is not involved in the disinfection of *M. barkeri*. The TEM results suggest that the intracellular cell membrane is the first attack site for *E. coli* (Figure 5.12), while the outer cell wall is the first attack site for *M. barkeri* (Figure 5.13). This infers that without e^-, the intracellular cell membrane is not easily destroyed and the e^- destruction process starts from the intracellular cell membrane.

The Gram +ve bacterium, *M. Barkeri*, has a thicker cell wall than the Gram –ve bacterium, *E. coli*, (Slonczewski and Foster, 2011). The above study proposes the following mechanism for the bactericidal effect of e^- produced by NS. The conduction band of NS is positioned at a much more negative potential (-1.4 V vs. SCE) (Zang *et al.*, 1995) so that e^- can inactivate the bacterial cells. The initial attack site is the intracellular cell membrane, and e^- shall pass through the outer cell wall to contact the

cell membrane, after which damage to the intracellular cell membrane occurs. The intracellular cell membrane and the outer cell wall are subsequently decomposed by e^-, causing cell death. Due to the short lifetime of e^-, it can only pass through bacteria with thin cell walls such as *E. coli*. For thick cell wall bacteria such as *M. barkeri*, e^- does not make contact with the intracellular cell membrane and cannot inactivate *M. barkeri* directly.

To prove e^- does not damage the cell membrane of *M. barkeri* but that of *E. coli*, permeability change of cell membrane is studied. K^+ actually exists in bacterial cells and is involved in the regulation of polysome content and protein synthesis (Hu *et al.*, 2006; Ren *et al.*, 2009). Any damage in the cell membrane structure during the photocatalytic disinfection will cause the leakage of K^+ because of the permeability change in the cell membrane and the loss of cell viability. It was observed that for *E. coli,* no matter adding scavenger or not, the leakage of K^+ for photocatalytic disinfection was more than dark and light controls (Figure 5.14A), which suggests that e^- alone directly attacks the intracellular cell membrane of *E. coli*. However, H_2O_2 can also destroy the cell membrane, and thus the increase of leaked K^+ caused by e^- alone is a little lower than that caused by H_2O_2 and e^-. While for *M. barkeri*, only in the condition of photocatalytic disinfection without any scavenger, the leakage of K^+ was a little more than two control experiments (Figure 5.14B), which is probably the attack of H_2O_2. After adding quadruple scavengers, e^- alone did not influence the leakage of K^+, suggesting that there is no damage of cell membrane of *M. barkeri*.

This observation well matches the previous observation that e^- cannot attack the intracellular cell membrane of *M. barkeri* and is not involved in the disinfection of *M. barkeri*.

5.5 Conclusions

A new photocatalyst, NS, shows high photocatalytic activity to disinfect wastewater bacteria such as *E. coli* and *M. barkeri* under FTs irradiation. The photocatalytic disinfection efficiencies at different pH are strongly influenced by the amount of ROSs. Moreover, the results of scavenger studies reveal that both e^- and H_2O_2 are involved in the photocatalytic disinfection of the Gram –ve bacterium, *E. coli,* while only H_2O_2 plays an important role in the photocatalytic disinfection of the Gram +ve bacterium, *M. barkeri*. The mechanism proposed to disinfect bacterial cells is that e^- can pass through the thin cell wall and damage the intracellular cell membrane. Thus, NS easily obtained from the earth's surface can be used cost-effectively for the large-scale photocatalytic disinfection of wastewater bacteria.

6. General conclusions

Most of the photocatalysts can only be excited by UV irradiation, which is only 4% of the sunlight. It is necessary to develop new photocatalysts, which have high photocatalytic activity under VL to degrade the pollutants and disinfect bacterial cells. Actually, there are large quantities of semiconducting minerals on the surface of the earth. They are in good coherence with the modified synthetic photocatalysts. Therefore, it is important to evaluate the photocatalytic disinfection efficiency of bacterial cells by the natural photocatalyst and investigate its mechanism. The disinfection capability of a natural semiconducting mineral, NS, is studied for the first time.

In Chapter 3, NS can completely inactivate 1.5×10^7 cfu/mL *E. coli* K-12 within 6 h irradiated by FTs. Moreover, the photocatalytic disinfection mechanism for NS is investigated by using multiple scavengers. It is the first time to experimentally prove that e^- plays an important role in the bacterial disinfection of *E. coli* K-12. In addition, H_2O_2 is also involved in the photocatalytic disinfection, which is proven by using a partition system combined with different scavengers. Furthermore, the photocatalytic destruction of the bacterial cells is observed in TEM analysis. NS is very stable and can be reuse.

In Chapter 4, to explore what parameters influence the disinfection efficiency of NS under VL irradiation, the photocatalytic disinfection efficiencies of *E. coli* K-12 under

different spectra of light sources (FTs, Xenon lamp and LED lamps), different wavelengths of LED lamps, and different intensities of VL irradiation are studied. NS can completely inactivate 1.5×10^7 cfu/mL *E. coli* K-12 within 8 h irradiated by white LED lamps at pH 8. No bacterial colony can be detected in a 96 h bacterial regrowth test, which reveals that the VL-photocatalytic disinfection leads to an irreversible damage to the bacterial cells. In addition, the spectrum effect of VL indicates that the "discreted peak spectrum" is more effective than "continuous spectrum" to inactivate bacterial cells. Furthermore, the blue, green, yellow, red and white LED lamps are chosen to study the wavelength effect of VL. The results show that the most effective range of VL for photocatalytic disinfection by NS is the wavelengths of 440-490 and 570-620 nm. The disinfection efficiency increases as a function of VL intensity increasing.

In Chapter 5, the photocatalytic disinfection another Gram positive wastewater bacterium is also investigated. NS shows high disinfection efficiency in disinfecting 1.5×10^5 cfu/mL of *M. barkeri* within 10 h at neutral pH. In addition, the pH effect on the photocatalytic bacterial disinfection is studied. The results suggest that the amount of H_2O_2 is crucial to high bactericidal efficiency. Moreover, the photocatalytic disinfection mechanisms to *E. coli* K-12 and *M. barkeri* for NS are investigated by using multiple scavengers. The results of CAT activity reveal *M. barkeri* is more resistance than *E. coli*. The photocatalytic destruction of the cell wall and cell membrane is directly observed by TEM and further confirms by the leakage of K^+

before and after photocatalytic inactivation. A possible cell damage mechanism by the photogenerated e^- produced by NS is tentatively proposed.

Therefore, this work does not only report a new natural semiconductor to photocatalytic disinfection of wastewater bacteria, but also provides some insight into the photocatalytic mechanism of the natural photocatalyst irradiated by VL. It is concluded that NS shows a high VLD photocatalytic disinfection efficiency under VL irradiation. Natural photocatalyst is abundant and easy to obtain, and possesses excellent VL photocatalytic activity. These superior properties make it a promising solar-driven photocatalyst for large-scale cost-effective wastewater treatment.

7. References

Amezaga-Madrid, P., Silveyra-Morales, R., Cordoba-Fierro, L., Nevarez-Moorillon, G.V., Miki-Yoshida, M., Orrantia-Borunda, E. and Solis, F.J. 2003. TEM evidence of ultrastructural alteration on *Pseudomonas aeruginosa* by photocatalytic TiO_2 thin films. *Journal of Photochemistry and Photobiology B: Biology* 70: 45-50.

Asahi, R., Morikawa, T., Ohwaki, T., Aoki, K. and Taga, Y. 2001. Visible-light photocatalysis in nitrogen-doped titanium oxides. *Science* 293: 269-271.

Ayliffe, G.A.J., Collins, B.J. and Deverill, E.A. 1974. Tests of disinfection by heat in a bedpan washing machine. *Journal of Clinical Pathology* 27: 760-763.

Backhaus, K., Marugan, J., van Grieken, R. and Sordo, C. 2010. Photocatalytic inactivation of *E. faecalis* in secondary wastewater plant effluents. *Water Science and Technology* 61: 2355-2361.

Bader, H., Sturzeneger, V. and Hoigne, J. 1988. Photometric method for the determination of low concentrations of H_2O_2 by the peroxidase catalyzed oxidation of N,N-Diethyl-*p*-Phenylenediamine (DPD). *Water Research* 22: 1109-1115.

Baker, J.C. 1926. Chlorine in sewage and waste disposal. *Water & Sewage* 50: 127-128.

Bancroft, K., Chrostowski, P., Wright, R.L. and Suffet, I.H. 1984. Relationship to disinfection and microorganisms regrowth. *Water Research* 18: 473-478.

Benabbou, A.K., Derriche, Z., Felix, C., Lejeune, P. and Guillard, C. 2007.

Photocatalytic inactivation of *Escherichia coli*: Effect of concentration of TiO_2 and microorganism, nature, and intensity of UV irradiation. *Applied Catalysis B: Environmental* 76: 257-263.

Blake, D.M., Maness, P.C., Huang, Z., Wolfrum, E.J., Jacoby, W.A. and Huang, J. 1999. Application of the photocatalytic chemistry of titanium dioxide to disinfection and the killing of cancer cells. *Separation and Purification Methods* 28: 1-50.

Bors, W., Michel, C. and Saran, M. 1979. On the nature of biochemically generated hydroxyl radicals. *European Journal of Biochemistry* 95: 621-627.

Carp, O., Huisman, C.L. and Reller, A. 2004. Photoinduced reactivity of titanium dioxide. *Progress in Solid State Chemistry* 32: 33-177.

Cayman Chemical Company. 2009. *Protocol for Catalase Assay*, Ann Arbor, MI, USA.

Centers for Disease Control and Prevention. 2005. *Preventing Bacterial Waterborne Diseases Division of Bacterial Diseases.* National Center for Immunization and Respiratory Diseases, Atlanta, USA.

Chen, F.N., Yang, X.D. and Wu, Q. 2009. Photocatalytic oxidation of *Escherischia coli*, *Aspergillus niger*, and formaldehyde under different ultraviolet irradiation conditions. *Environmental Science & Technology* 43: 4606-4611.

Chen, Y.X., Yang, S.Y., Wang, K. and Lou, L.P. 2005. Role of primary active species and TiO_2 surface characteristic in UV-illuminated photodegradation of Acid Orange 7. *Journal of Photochemistry and Photobiology A: Chemistry* 172:

47-54.

Cheng, Y.W., Chan, C.Y. and Wong, P.K. 2007. Disinfection of *Legionella pneumophila* by photocatalytic oxidation. *Water Research* 41: 842-852.

Cho, M., Chung, H. and Yoon, J. 2003. Quantitative evaluation of the synergistic sequential inactivation of *Bacillus subtilis* spores with ozone followed by chlorine. *Environmental Science & Technology* 37: 2134-2138.

Cho, M., Chung, H., Choi, W. and Yoon, J. 2004. Linear correlation between inactivation of *E. coli* and OH radical concentration in TiO_2 photocatalytic disinfection. *Water Research* 38: 1069-1077.

Cho, M., Chung, H., Choi, W. and Yoon, J. 2005. Different inactivation behaviors of MS-2 phage and *Escherichia coli* in TiO_2 photocatalytic disinfection. *Applied and Environmental Microbiology* 71: 270-275.

Čík, G., Priesolová, S., Bujdáková, H., Šeršeň, F., Potheöová, T. and Krištín, J. 2006. Inactivation of bacteria G^+-*S. aureus* and G^--*E. coli* by phototoxic polythiophene incorporated in ZSM-5 zeolite. *Chemosphere* 63: 1419-1426.

Claxton, L.D., Pegram, R., Schenck, K.M., Simmons, J.E. and Warren, S.H. 2008. Integrated disinfection by-products research: *Salmonella* mutagenicity of water concentrates disinfected by chlorination and ozonation/postchlorination. *Journal of Toxicology and Environmental Health, Part A: Current Issues* 71: 1187-1194.

Collins, M.D., Jones, D., Keddie, R.M., Kroppenstedt, R.M. and Schleifer, K.M. 1983. Classification of some coryneform bacteria in a new genus *Aureobacterium*. *Systematic and Applied Microbiology* 4: 236-252.

Davies, C.M., Roser, D.J., Feitz, A.J. and Ashbolt, N.J. 2009. Solar radiation disinfection of drinking water at temperate latitudes: Inactivation rates for an optimized reactor configuration. *Water Research* 43: 643-652.

Dehghani, M.H. 2005. Effectiveness of ultrasound on the destruction of *E. coli*. *American Journal of Environmental Sciences* 1: 187-189.

Depero, L.E. 1993. Coordination geometry and catalytic activity of vanadium on TiO_2 surfaces. *Jouranl of Solid State Chemistry* 103: 528-532.

Docampo, R. 1995. *Antioxidant Mechanisms.* In J. Marr and M. Müller, (Eds.). Biochemistry and Molecular Biology of Parasites. London: Academic Press. pp. 147-160.

Doroszkiewicz, W., Sikorska, I. and Jankowski, S. 1994. Studies on the influence of ozone on complement-mediated killing of bacteria. *FEMS Immunology and Medical Microbiology* 9: 281-285.

Dunlop, P.S.M., Byrne, J.A., Manga, N. and Eggins, B.R. 2002. The photocatalytic removal of bacterial pollutants from drinking water. *Journal of Photochemistry and Photobiology A: Chemistry* 148: 355-363.

Dunstan, D.E., Hagfeldt, A., Almgren, M., Siegbahm, H.O.G. and Mukhtar, E. 1990. Importance of surface reactions in the photochemistry of zinc sulfide colloids. *The Journal of Physical Chemistry* 94: 6797-6804.

Excelitas Technologies' Cermax®, Xenon lamps, Modules and Power Supplies, Excelitas Technologies, Fremont, USA.

Fu, H.B., Pan, C.S., Yao, W.Q. and Zhu, Y.F. 2005. Visible-light-induced degradation of Rhodamine B by nanosized Bi_2WO_6. *The Journal of Physical Chemistry B* 109: 22432-22439.

Fujishima, A., Rao, T.N. and Tryk, D.A. 2000. Titanium dioxide photocatalysis. *Journal of Photochemistry and Photobiology C: Photochemistry* 1: 1-21.

Haag, W.R. and Hoigne, J. 1983. Ozonation of bromide-containing water: Kinetics of formation of hypobromous acid and bromated. *Environmental Science & Technology* 17: 261-267.

Hancock, G.G. and Davis, E.M. 1999. Regrowth potential of coliforms after UV disinfection of municipal wastewater. *Journal of Environmental Science and Health, Part A* 34: 1737-1743.

Hara, M., Kondo, T., Komoda, M., Ikeda, S., Shinohara, K., Tanaka, A., Kondo, J.N. and Domen, K. 1998. Cu_2O as a photocatalyst for overall water splitting under visible light irradiation. *Chemical Communications* 357: 357-358.

Hashimoto, K., Irie, H. and Fujishima, A. 2007. TiO_2 photocatalysis: A historical overview and future prospects. *Association of Asia Pacific Physical Societies Bulletin* 17: 12-28.

Hass, C.N. and Engelbrecht, R.S. 1980. Chlorine dynamics during inactivation of coliforms, acid-fast bacteria and yeasts. *Water Research* 14: 1749-1757.

Hayat, M.A. 1985. *Basic Techniques for Transmission Electron Microscopy.* Academic Press, Orlando, USA. pp.127-150.

He, Z., Lin, L., Song, S., Xia, M., Xu, L., Ying, H. and Chen, J. 2008. Mineralization

of C.I. Reactive Blue 19 by ozonation combined with sonolysis: Performance optimization and degradation mechanism. *Separation and Purification Technology* 62: 376-381.

Hoffmann, M.R., Martin, S.T., Choi, W. and Bahnemann, D.W. 1995. Environmental applications of semiconductor photocatalysis. *Chemical Reviews* 95: 69-96.

Honda, H., Ishizaki, A., Soma, R., Hashimoto, K. and Fujishima, A. 1998. Application of photocatalytic reactions caused by TiO_2 film to improve the maintenance factor of lighting systems. *Journal of the Illuminating Engineering Society* 27: 42-49.

Hu, C., Lan, Y.Q., Qu, J.H., Hu, X.X. and Wang, A.M. 2006. Ag/AgBr/TiO_2 visible light photocatalyst for destruction of azo dyes and bacteria. *The Journal of Physical Chemistry B* 110: 4066-4072.

Hu, C., Wang, Y.Z. and Tang, H.X. 2001. Preparation and characterization of surface bond-conjugated TiO_2/SiO_2 and photocatalysis for azo dyes. *Applied Catalysis B: Environmental* 30: 277-285.

Hua, G. and Reckhowa, D.A. 2007. Comparison of disinfection byproduct formation from chlorine and alternative disinfectants. *Water Research* 41: 1667-1678.

Huang, J., Tan, Y., Wang, L., Yang, S., Wan, L. and Shi, B. 2003. Influence of the mixed disinfectant of ClO_2 and Cl_2 on formation of chloroform. *Chinese Journal of Environmental Science* 24: 102-107.

Huang, W.J., Fang, G.C. and Wang, C.C. 2005. The determination and fate of disinfection by-products from ozonation of polluted raw water. *Science of the*

Total Environment 345: 261-272.

Huang, Z., Maness, P.C., Blake, D.M., Wolfrum, E.J., Smolinski, S.L. and Jacoby, W.A. 2000. Bactericidal mode of titanium dioxide photocatalysis. *Journal of Photochemistry and Photobiology A: Chemistry* 130: 163-170.

Ishibashi, K., Fujishima, A., Watanabe, T. and Hashimoto, K. 2000. Detection of active oxidative species in TiO_2 photocatalysis using the fluorescence technique. *Electrochemistry Communications* 2: 207-210.

Jacoby, W.A., Maness, P.C., Wolfrum, E.J., Blake, D.M. and Fennell, J.A. 1998. Mineralization of bacterial cell mass on a photocatalytic surface in air. *Environmental Science & Technology* 32: 2650-2653.

Jagger, J. 1967. *Introduction to Research in Ultraviolet Photobiology*. Prentice-Hall Inc., Englewood Cliffs, New Jersey. USA, pp. 13-28.

Kambala, V.S.R. and Naidu, R. 2009. Disinfection studies on TiO_2 thin films prepared by a sol-gel method. *Journal of Biomedical Nanotechnology* 5: 121-129.

Kawahara, T., Yamada, K.I. and Tada, H. 2006. Visible light photocatalytic decomposition of 2-naphthol by anodic-biased alpha-Fe_2O_3 film. *Journal of Colloid and Interface Science* 294: 504-507.

Khodja, A.A., Boulkamh, A. and Richard, C. 2005. Phototransformation of metobromuron in the presence of TiO_2. *Applied Catalysis B: Environmental* 59: 147-154.

Kikuchi, Y., Sunada, K., Iyoda, T., Hashimoto, K. and Fujishima, A. 1997. Photocatalytic bactericidal effect of TiO_2 thin films: Dynamic view of the active

oxygen species responsible for the effect. *Journal of Photochemistry and Photobiology A: Chemistry* 106: 51-56.

Kim, B., Kim, D., Cho, D. and Cho, S. 2003. Bactericidal effect of TiO_2 photocatalyst on selected food-borne pathogenic bacteria. *Chemosphere* 52, 277-281.

Knox, W.E., Stumpf, P.K., Green, D.E. and Auerbach, V.H. 1948. The inhibition of sulfhydryl enzymes as the basis of the bacterial action of chlorine. *Journal of Bacteriology* 55: 451-458.

Koizumi, Y., Yamada, R., Nishioka, M., Matsumura, Y., Tsuchido, T. and Taya, M. 2002. Deactivation kinetics of *Escherichia coli* cells correlated with intracellular superoxide dismutase activity in photoreaction with titanium dioxide particles. *Journal of Chemical Technology and Biotechnology* 77: 671-677.

Kubin, M., Sedlácková, J. and Vacek, K. 1982. Ionizing radiation in the disinfection of water contaminated with potentially pathogenic mycrobacteria. *Journal of Hygiene, Epidemiology, Microbiology and Immunology* 26: 31-36.

Kubitschek, H.E. 1990. Cell volume increase in *Escherichia coli* after shifts to richer media. *Journal of Bacteriology* 172: 94-101.

Kudo, A., Omori, K. and Kato, H. 1999. A novel aqueous process for preparation of crystal form-controlled and highly crystalline $BiVO_4$ powder from layered vanadates at room temperature and its photocatalytic and photophysical properties. *Journal of the American Chemical Society* 121: 11459-11467.

Kudo, A., Sayama, K., Tanaka, A., Asakura, K., Domen, K., Maruya, K. and Onishi, T. 1989. Nickel-loaded $K_4Nb_6O_{17}$ photocatalyst in the decomposition of H_2O into

H_2 and O_2: Structure and reaction mechanism. *Journal of Catalysis* 120: 337-352.

Kühn, K.P., Chaberny, I.F., Massholder, K., Stickler, M., Benz, V.W., Sonntag, H.G. and Erdinger, L. 2003. Disinfection of surfaces by photocatalytic oxidation with titanium dioxide and UVA light. *Chemosphere* 53: 71-77.

LeChevallier, M.W. and Au, K.K. 2004. *Water Treatment and Pathogen Control: Process Efficiency in Achieving Safe Drinking Water.* World Health Organization, London, UK.

Lejeune, D., Hasanuzzaman, M., Pitcock, A., Francis, J. and Sehgal, I. 2006. The superoxide scavenger TEMPOL induces urokinase receptor (μPAR) expression in human prostate cancer cells. *Molecular Cancer* 5: 21-26.

Leung, T.Y., Chan, C.Y., Hu, C., Yu, J.C. and Wong, P.K. 2008. Photocatalytic disinfection of marine bacteria using fluorescent light. *Water Research* 42: 4827-4837.

Li, G.S., Zhang, D.Q. and Yu, J.C. 2009. A new visible-light photocatalyst: CdS quantum dots embedded mesoporous TiO_2. *Environmental Science & Technology* 43: 7079-7085.

Li, Y., Lu, A.H. and Wang, C.Q. 2006. Photocatalytic reduction of Cr(VI) by natural sphalerite suspensions under visible light irradiation. *Acta Geologica Sinica* 80: 267-272.

Li, Y., Lu, A.H. and Wang, C.Q. 2009a. Semiconducting mineralogical characteristics of natural sphalerite gestating visible-light photocatalysis. *Acta Geologica Sinica*

83: 633-639.

Li, Y., Lu, A.H., Jin, S. and Wang, C.Q. 2009b. Photo-reductive decolorization of an azo dye by natural sphalerite: Case study of a new type of visible light-sensitized photocatalyst. *Journal of Hazardous Materials* 170: 479-486.

Li, Y., Lu, A.H., Wang, C.Q. and Wu, X.L. 2008. Characterization of natural sphalerite as a novel visible-light-driven photocatalyst. *Solar Energy Materials & Solar Cells* 92: 953-959.

Lisle, J.T., Broadaway, S.C., Prescott, A.M., Pyle, B.H., Fricker, C. and MaFeters, G.A. 1998. Effects of starvation on physiological activity and chlorine disinfection resistance in *Escherichia coli* O157:H7. *Applied and Environmental Microbiology* 64: 4658-4662.

Lu, A.H., Guo, Y.J., Liu, J., Liu, F., Wang, C.Q., Li, N. and Li, Q.R. 2004a. Photocatalytic effect of nature and modified V-bearing rutile. *Chinese Science Bulletin* 49: 2284-2287.

Lu, A.H., Li, Y., Lv, M., Wang, C.Q., Yang, L., Liu, J., Wang, Y.H., Wong, K.H. and Wong, P.K. 2007. Photocatalytic oxidation of methyl orange by natural V-bearing rutile under visible light. *Solar Energy Materials and Solar Cells* 91: 1849-1855.

Lu, A.H., Liu, J., Zhao, D.G., Guo, Y.J., Li, Q.R. and Li, N. 2004b. Photocatalysis of V-bearing rutile on degradation of halohydrocarbons. *Catalysis Today* 90: 337-342.

Ma, J., Wang, Y.H., Ji, F., Yu, X.H. and Ma, H.L. 2005. UV-violet photoluminescence emitted from SnO_2: Sb thin films at different temperature. *Materials Letters* 59:

2142-2145.

Ma, J., Wei, Y., Liu, W.X. and Cao, W.B. 2009. Preparation of nanocrystalline Fe-doped TiO_2 powders as a visible-light-responsive photocatalyst. *Research on Chemical Intermediates* 35: 329-336.

Maness, P.C., Smolinski, S., Blake, D.M., Huang, Z., Wolfrum, E.J. and Jacoby, W.A. 1999. Bactericidal activity of photocatalytic TiO_2 reaction: Toward an understanding of its killing mechanism. *Applied and Environmental Microbiology* 65: 4094-4098.

Marazza, V. 1960. Is the resistance of muscle-Trichinella lowered to freezing during prophylactic disinfection treatment of meat? *World Wide Abstract General Medicine* 6: 311-312.

Matsunaga, T., Tomade, R., Nakajima, T. and Wake, H. 1985. Photoelectrochemical sterilization of microbial cells by semiconductor powders. *FEMS Microbiology Letter* 29: 211-214.

Matsunaga, T., Tomoda, R., Nakajima, T., Nakajima, N. and Komine, T. 1988. Continuous sterilization system that uses photosemiconductor powders. *Applied and Environmental Microbiology* 54: 1330-1333.

McDonnell, G.E. 2007. *Antisepsis, Disinfection, and Sterilization: Types, Action, and Resistance*. American Society for Microbiology, USA.

Metcalf, E. 2005. *Wastewater Engineering Treatment and Reuse*. Tata McGraw-Hill Publishing Company Limited, New Delhi, India.

Muszkat, L., Halman, M. and Raucher, D. 1992. Solar photodegradation of xenobiotic

contaminants in polluted well water. *Journal of Photochemistry and Photobiology A: Chemistry* 65: 409-417.

Ollis, D.F. 1985. Contaminant degradation in water. *Environmental Science & Technology* 19: 80-484.

Pal, A., Pehkonen, S.O., Yu, L.E. and Ray, M.B. 2007. Photocatalytic inactivation of Gram-positive and Gram-negative bacteria using fluorescent light. *Journal of Photochemistry and Photobiology A: Chemistry* 186: 335-341.

Parsons, S. 2004. *Advanced Oxidation Process for Water and Wastewater Treatment*. CRC Press, London, UK.

Patton, W., Bacon, V., Duffield, A.M., Halpern, B., Hoyano, Y., Pereira, W. and Lederberg, J. 1972. Chlorine studies 1. The reaction of hypochlorous acid with cytosine. *Biochemical and Biophysical Research Communications* 48: 880-884.

Pichat, P., Guillard, C., Laurence, A., Renard, A.C. and Plaidy, O. 1995. Assessment of the importance of the role of H_2O_2 and O_2^{0-} in the photocatalytic degradation of 1,2-dimethoxybenzene. *Solar Energy Materials and Solar Cells* 38: 391-399.

Plewa, M.J., Wagner, E.D., Richardson, S.D., Thruston Jr., A.D., Woo, Y.T. and Mckague, A.B. 2004. Chemical and biological characterization of newly discovered iodoacid drinking water disinfection byproducts. *Environmental Science & Technology* 38: 4713-4722.

Rakness, K.L. 2005. *Ozone in Drinking Water Treatment: Process Design, Operation, and Optimization*. American Water Works Association, USA.

Ranieri, E. and Świetlik, J. 2010. DBPs control in European drinking water treatment

plants using chlorine dioxide: Two case studies. *Journal of Environmental Engineering and Landscape Management* 18: 85-91.

Reddy, M.P., Phil, H.H. and Subrahmanyam, M. 2008. Photocatalytic disinfection of *Escherichia coli* over titanium (IV) oxide supported on Hβ zeolite. *Catalysis Letters* 123: 56-64.

Ren, C., Wang, W.Z., Zhang, L., Chang, J. and Sheng, H. 2009. Photocatalytic inactivation of bacteria by photocatalyst Bi_2WO_6 under visible light. *Catalysis Communication* 10: 1940-1943.

Rice-Evans, C.A. and Gopinathan, V. 1995. Oxygen toxicity, free radicals and antioxidants in human disease: Biochemical implications in atherosclerosis and the problems of premature neonates. *Essays in Biochemistry* 29: 39-63.

Richardson, S.D., Simmons, J.E. and Rice, G. 2002. Phylogenetic characterization of microbial communities that reductively dechlorinate TCE based upon a combination of molecular techniques. *Environmental Science & Technology* 36: 2652-2662.

Richardson, S.D., Thruston Jr., A.D., Rav-Acha, C., Groisman, L., Popilevsky, I., Juraev, O., Glezer, V., McKague, A.B., Plewa, M.J. and Wagner, E.D. 2003. Tribromopyrrole, brominated acids, and other disinfection byproducts produced by disinfection of drinking water rich in bromide. *Environmental Science & Technology* 37: 3782-3793.

Richardsons, S.D., Thruston Jr., A.D., Caughran, T.V., Chen, P.H., Collette, T.W.,

Floyd, T.L., Schenck, K.M. and Lykins Jr., B.W. 1999. Identification of new ozone disinfection byproducts in drinking water. *Environmental Science & Technology* 33: 3368-3377.

Rincón, A.G. and Pulgarin, C. 2003. Photocatalytical inactivation of *E. coli*: Effect of (continuous-intermittent) light intensity and of (suspended-fixed) TiO_2 concentration. *Applied Catalysis B: Environmental* 44: 263-284.

Rincón, A.G. and Pulgarin, C. 2004. Effect of pH, inorganic ions, organic matter and H_2O_2 on *E. coli* K12 photocatalytic inactivation by TiO_2: Implications in solar water disinfection. *Applied Catalysis B: Enviromental* 51: 283-302.

Rincón, A.G. and Pulgarin, C., 2005. Use of coaxial photocatalytic reactor (CAPHORE) in the TiO_2 photo-assisted treatment of mixed *E. coli* and *Bacillus sp* and bacterial community present in wastewater. *Catalysis Today* 101: 331-344.

Saito, T., Iwase, T. and Morioka, T. 1992. Mode of photocatalytic bactericidal action of powdered semiconductor TiO_2 on mutants streptococci. *Journal of Photochemistry and Photobiology B: Biology* 14: 369-379.

Sakthivel, S. and Kisch, H. 2003. Daylight photocatalysis by carbon-modified titanium dioxide. *Angewandte Chemie International Edition* 42: 4908-4911.

Scheutz, F. and Strockbine, N.A. 2005. In: Brenner, D.J., Krieg, N.R. and Staley, J.T. (ed.). *Bergey's Manual® of Systematic Bacteriology, Volume Two, Part B*. New York, USA, pp. 607-624.

Selma, M.V., Allende, D.A. and Mlgil, E.V. 2007. Elimination by ozone of *Shigella*

sonnei in shredded lettuce and water. *Food Microbiology* 24: 492-499.

Senthilnanthan, M., Ho, D.P., Vigneswaran, S., Ngo, H.H. and Shon, H.K. 2010. Visible light responsive ruthenium-doped titanium dioxide for the removal of metsulfuron-methyl herbicide in aqueous phase. *Separation and Purification Technology* 75: 415-419.

Shangguan, W.F. and Yoshida, A. 2002. Photocatalytic hydrogen evolution from water on nanocomposites incorporating cadmium sulfide into the interlayer. *Journal of Physical Chemistry B* 106: 12227-12230.

Shannon, M.A., Bohn, P.W., Elimelech, M., Georgiadis, J.G., Mariñas, B.J. and Mayes, A.M. 2008. Science and technology for water purification in the coming decades. *Nature* 452: 301-310.

Sichel, C., Blanco, J., Malato, S. and Fernández-Ibáñez, P. 2007. Effects of experimental condition on *E. coli* survival during solar photocatalytic water disinfection. *Journal of Photochemistry and Photobiology A: Chemistry* 189: 239-246.

Sies, H. 1985. *Oxidative Stress: Introductory Remarks.* In H. Sies, (Ed.). Oxidative Stress. Academic Press, London, UK. pp. 1-7.

Slonczewski, J.L. and Foster, J.W. 2011. *Microbiology: An Evolving Science.* W.W. Norton & Company, Inc., New York, USA.

Snider, K.E., Darby, J.L. and Chobanoglous, G. 1991. *Evaluation of Ultraviolet Disinfection for Wastewater Reuse Applications in California.* University of

California, Davis, California, USA.

Sobotka, J. 1993. The efficiency of water treatment and disinfection by means of ultraviolet radiation. *Water Science and Technology* 27: 343-346.

Sökmen, M., Candan, F. and Sümer, Z. 2001. Disinfection of *E. coli* by the Ag-TiO_2/UV system: Lipidperoxidation. *Journal of Photochemistry and Photobiology A: Chemistry* 143: 241-244.

Strul, G., Frimer, A.A. and Weiner, L. 1993. Spin-trapping study of free radical penetration into liposomal membranes. *Journal of Chemical Society Perkin Transactions* 2: 2057-2059.

Subrahmanyam, M., Boule, P., Kumari, V.D., Kumar, D.N., Sancelme, M. and Rachel, A. 2008. Pumice stone supported titanium dioxide for removal of pathogen in drinking water and recalcitrant in wastewater. *Solar Energy* 82: 1099-1106.

Sunada, K., Kikuchi, Y., Hashimoto, K. and Fujishima, A. 1998. Bactericidal and detoxification effects of TiO_2 thin film photocatalysts. *Environmental Science & Technology* 32: 726-728.

Sunada, K., Watanabe, T. and Hashimoto, K. 2003. Studies on photokilling of bacteria on TiO_2 thin film. *Journal of Photochemistry and Photobiology A: Chemistry* 156: 227-233.

Tang, W.Z. and Huang, C.P. 1995. Inhibitory effect of thioacetamide on CdS dissolution during photocatalytic oxidation of 2,4-dichlorophenol. *Chemosphere* 30: 1385-1399.

United States Environmental Protection Agency. 1991. *Guidance Manual for*

Compliance with the Filtration and Disinfection Requirements for Public Water Systems using Surface Water Sources. Office of Drinking Water, United States Environmental Protection Agency. Washington, D.C., USA.

United States Environmental Protection Agency. 1999a. *Combined Sewer Overflow Technology Fact Sheet Chlorine Disinfection.* Office of Water, United States Environmental Protection Agency. Washington, D.C., USA.

United States Environmental Protection Agency. 1999b. *Alternative Disinfectants and Oxidants Guidance Manual.* EPA 815-R-99-014. Office of Drinking Water, United States Environmental Protection Agency. Washington, D.C., USA.

United States Environmental Protection Agency. 1999c. *Wastewater Technology Fact Sheet Ozone Disinfection.* Office of Water, United States Environmental Protection Agency. Washington, D.C., USA.

United States Environmental Protection Agency. 1999d. *Wastewater Technology Fact Sheet Ultraviolet Disinfection.* Office of Water, United States Environmental Protection Agency. Washington, D.C., USA.

United States Environmental Protection Agency. 2001. *Toxicological Review of Bromate in Support of Integrated Risk Information System (IRIS).* Office of Research and Development, United States Environmental Protection Agency. Washington, D.C., USA.

United States Environmental Protection Agency. 2003. *Long Term 2 Enhanced Surface Water Treatment Rule Toolbox Guidance Manual (DRAFT).* EPA 815-D-03-009. Office of Drinking Water, United States Environmental

Protection Agency. Washington, D.C., USA.

United States Environmental Protection Agency. 2009. *Drinking Water Pathogens and Their Indicators: A Reference Resource.* Office of Drinking Water, United States Environmental Protection Agency. Washington, D.C., USA.

van Grieken, R., Marugan, J., Pablos, C., Furones, L. and Lopez, A. 2010. Comparison between the photocatalytic inactivation of Gram-positive *E. faecalis* and Gram-negative *E. coli* faecal contamination indicator microorganisms. *Applied Catalysis B: Environmental* 100: 212-220.

Venkobachar, C., Iyengar, L. and Rao, A.V.S.P. 1977. Mechanism of disinfection: Effect of chlorine on a cell membrane functions. *Water Research* 11: 727-729.

Wang, D., Oppenländer, T., El-Din, M.G. and Bolton, J.R. 2010. Comparison of the disinfection effects of vacuum-UV (VUV) and UV light on Bacillus subtilis spores in aqueous suspensions at 172, 222 and 254 nm. *Photochemistry and Photobiology* 86: 176-181.

Watanabe, T., Hashimoto, K. and Fujishima, A. 1992. Proceedings of the 1st International Conference on TiO_2 Photocatalyst, edited by Al-Ekabi, H. London, UK.

Watt, R.J., Kong, S.H., Orr, M.P., Miller, G.C. and Herny, B.E. 1995. Photocatalytic inactivation of coliform bacteria and virused in secondary wastewater effluent. *Water Research* 29: 95-100.

Wert, E.C., Rosario-Ortiza, F.L., Druryb, D.D. and Snyder, S.A. 2007. Formation of oxidation byproducts from ozonation of wastewater. *Water Research* 41:

1481-1490.

Whang, T.J., Huang, H.Y., Hsieh, M.T. and Chen, J.J. 2009. Laser-induced silver nanoparticles on titanium oxide for photocatalytic degradation of methylene blue. *International Journal of Molecular Sciences* 10: 4707-4718.

White, G.C. 1992. *Handbook of Chlorination and Alternative Disinfectants.* John Wiley and Sons, Inc., van Nostrand Reinhold, New York, USA. pp. 1430-1465.

Wolfe, R.L. 1990. Ultraviolet disinfection of potable water. *Environmental Science & Technology* 24: 768-773.

Wolfrum, E.J. and Ollis, D.F. 1994. *Hydrogen Peroxide in Heterogeneous Photocatalyis* In: G.R. Helz, R.G. Zepp, D.G. Crosby (Eds.), Aquatic and Surface Photochemistry, Lewis, Boca Raton, USA. pp. 451-465.

World Health Organization/United Nations Children's Fund/Joint Monitoring Programme for Water Supply and Sanitation. 2005. *Water for Life: Making It Happen.* World Health Organization, Geneva, Switzerland.

World Health Organization. 2003. *Emerging Issues in Water and Infectious Disease.* World Health Organization, Geneva, Switzerland.

World Health Organization. 2004. *Guidelines for Drinking-Water Quality: Microbial Aspect.* World Health Organization, Geneva, Switzerland.

Xu, X., Stewart, P.S. and Chen, X. 1996. Transport limitation of chlorine disinfection of *Pseudomonas aeruginosa* entrapped in alginate beads. *Biotechnology and Bioengineering* 49: 93-100.

Yamagiwa, K., Tsujikawa, M., Yoshida, M. and Ohkawa, A. 2002. Disinfection

kinetics of *Legionella pneumophila* by ultraviolet irradiation. *Water Science and Technology* 46: 311-317.

Yin, H., Wada, Y., Kitamura, T. and Yanagida, S. 2001. Photoreductive dehalogenation of halogenated benzene derivatives using ZnS or CdS nanocrystallites as photocatalysts. *Environmental Science & Technology* 35: 227-231.

Young, S.B. and Setlow, P. 2004. Mechanisms of *Bacillus subtilis* spore resistance to and killing by aqueous ozone. *Journal of Applied Microbiology* 96: 1133-1142.

Yu, J.C., Ho, W.K., Yu, J.G., Yip, H.Y., Wong, P.K. and Zhao, J.C. 2005. Efficient visible-light-induced photocatalytic disinfection on sulfur-doped nanocrystalline titania. *Environmental Science & Technology* 39: 1175-1179.

Yu, X.X., Yu, J.G., Cheng, B. and Huang, B.B. 2009. One-pot template-free synthesis of monodisperse zinc sulfide hollow spheres and their photocatalytic properties. *Chemistry: A European Journal* 15: 6731-6739.

Zang, L., Liu, C.Y. and Ren, X.M. 1995. Photochemistry of semiconductor particles. 3. Effects of surface charge on reduction rate of methyl orange photosensitized by ZnS sols. *Journal of Photochemistry and Photobiology A: Chemistry* 85: 239-245.

Zhang, L.S., Wong, K.H., Chen, Z.G., Yu, J.C., Zhan, J.C., Hu, C., Chan, C.Y. and Wong, P.K. 2009a. AgBr-Ag-Bi_2WO_6 nanojunction system: A novel and efficient photocatalyst with double visible-light active components. *Applied Catalysis A: General* 363: 221-229.

Zhang, L.S., Wong, K.H., Yip, H.Y., Hu, C., Yu, J.C., Chan, C.Y. and Wong, P.K. 2010.

Effective photocatalytic disinfection of *E. coli* K-12 using AgBr-Ag-Bi_2WO_6 nanojunction system irradiated by visible light: The role of diffusing hydroxyl radicals. *Environmental Science & Technology* 44: 1392-1398.

Zhang, L.S., Wong, K.H., Zhang, D.Q., Hu, C., Yu, J.C., Chan, C.Y. and Wong, P.K. 2009b. Zn:$In(OH)_yS_z$ solid solution nanoplates: Synthesis, characterization, and photocatalytic mechanism. *Environmental Science & Technology* 43: 7883-7888.

Zhang, L.Z., Yu, J.C., Yip, H.Y., Li, Q., Kwong, K.W., Xu, A.W. and Wong, P.K. 2003. Ambient light reduction strategy to synthesize silver nanoparticles and silver-coated TiO_2 with enhanced photocatalytic and bactericidal activities. *Langmuir* 19: 10372-10380.

Zou, Z.G., Ye, J.H., Sayama, K. and Arakawa, H. 2001. Direct splitting of water under visible light irradiation with an oxide semiconductor photocatalyst. *Nature* 414: 625-627.

Zuma, F., Lin, J. and Jonnalagadda, S.B. 2009. Ozone-initiated disinfection kinetics of *Escherichia coli* in water. *Journal of Environmental Science and Health, Part A* 44: 48-56.